Plate 1
Utah Geological Survey Map 284DM
Geologic Map of the Tooele 30' x 60' Quadrangle

UTAH GEOLOGICAL SURVEY
a division of
Utah Department of Natural Resources

GEOLOGIC MAP OF THE TOOELE 30' X 60' QUADRANGLE, TOOELE, SALT LAKE, AND DAVIS COUNTIES, UTAH

by

Donald L. Clark[1], Charles G. Oviatt[2], and David A. Dinter[3]

2020

[1]Utah Geological Survey, Salt Lake City, Utah
[2]Emeritus, Department of Geology, Kansas State University, Manhattan, Kansas
[3]Department of Geology & Geophysics, University of Utah, Salt Lake City, Utah

SCALE 1:62,500

1 0.5 0 1 2 3 MILES
1 0.5 0 1 2 3 4 5 KILOMETERS

CONTOUR INTERVAL 20 METERS

GREAT SALT LAKE BATHYMETRIC CONTOUR INTERVAL 1 FOOT

Great Salt Lake shoreline elevation of 4200 feet (1280 m) from Baskin and Allen (2005)

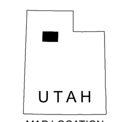

MAP LOCATION

APPROXIMATE MEAN DECLINATION, 2020

Disclaimer

Although this product represents the work of professional scientists, the Utah Department of Natural Resources, Utah Geological Survey, makes no warranty, expressed or implied, regarding its suitability for a particular use. The Utah Department of Natural Resources, Utah Geological Survey, shall not be liable under any circumstances for any direct, indirect, special, incidental, or consequential damages with respect to claims by users of this product. Geology intended for use at 1:62,500 scale.

This geologic map was funded by the Utah Geological Survey and the U.S. Geological Survey, National Cooperative Geologic Mapping Program through USGS STATEMAP award numbers G13AC00169 (2013–14), G14AC00214 (2014–15), G15AC00249 (2015–16), and G16AC00191 (2016–17). The views and conclusions contained in this document are those of the authors and should not be interpreted as necessarily representing the official policies, either expressed or implied, of the U.S. Government. This map and explanatory information is submitted for publication with the understanding that the U.S. Government is authorized to reproduce and distribute reprints for governmental use.

This map was created from geographic information system (GIS) files. Persons or agencies using these data specifically agree not to misrepresent the data, nor to imply that changes they made were approved by the Utah Geological Survey, and should indicate the data source and any modifications they make on plots, digital copies, derivative products, and in metadata.

Base from USGS Tooele 30' x 60' Quadrangle (1980)
Shaded relief derived from USGS 10-meter NED
Projection: UTM Zone 12
Datum: NAD 1927
Spheroid: Clarke 1866

Mapping by authors: 2013-2017, 2020
Project Manager: Robert F. Biek
Program Manager: Grant C. Willis
GIS and Cartography: Basia Matyjasik and Donald L. Clark

Utah Geological Survey
1594 West North Temple, Suite 3110
Salt Lake City, UT 84116
(801) 537-3300
geology.utah.gov
https://doi.org/10.34191/M-284DM

CORRELATION OF QUATERNARY-LATE TERTIARY (NEOGENE) GEOLOGIC UNITS

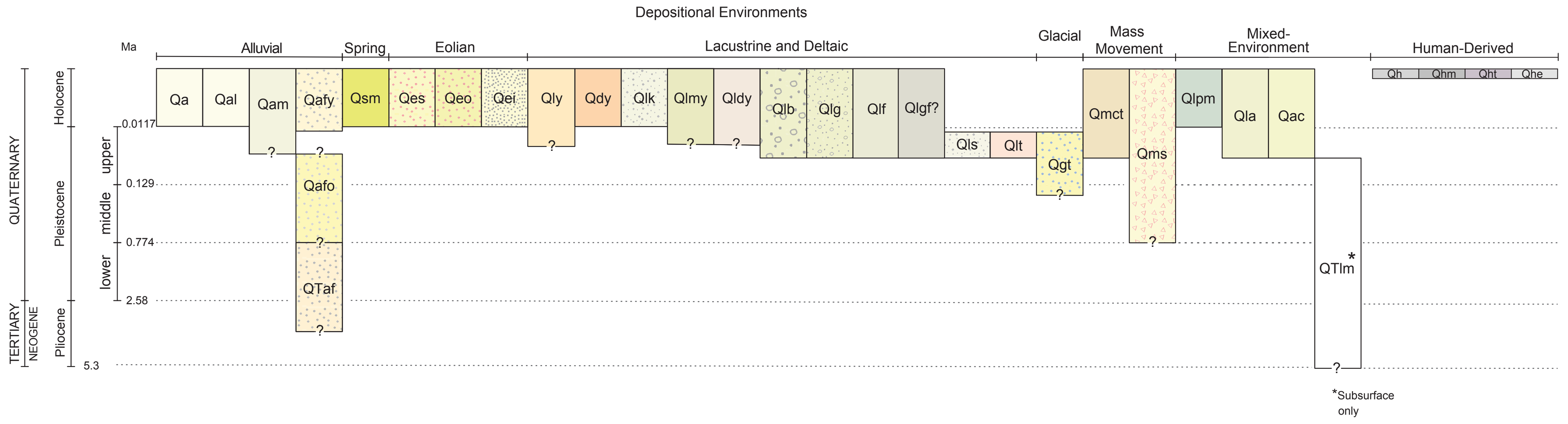

CORRELATION OF TERTIARY (NEOGENE-PALEOGENE) GEOLOGIC UNITS

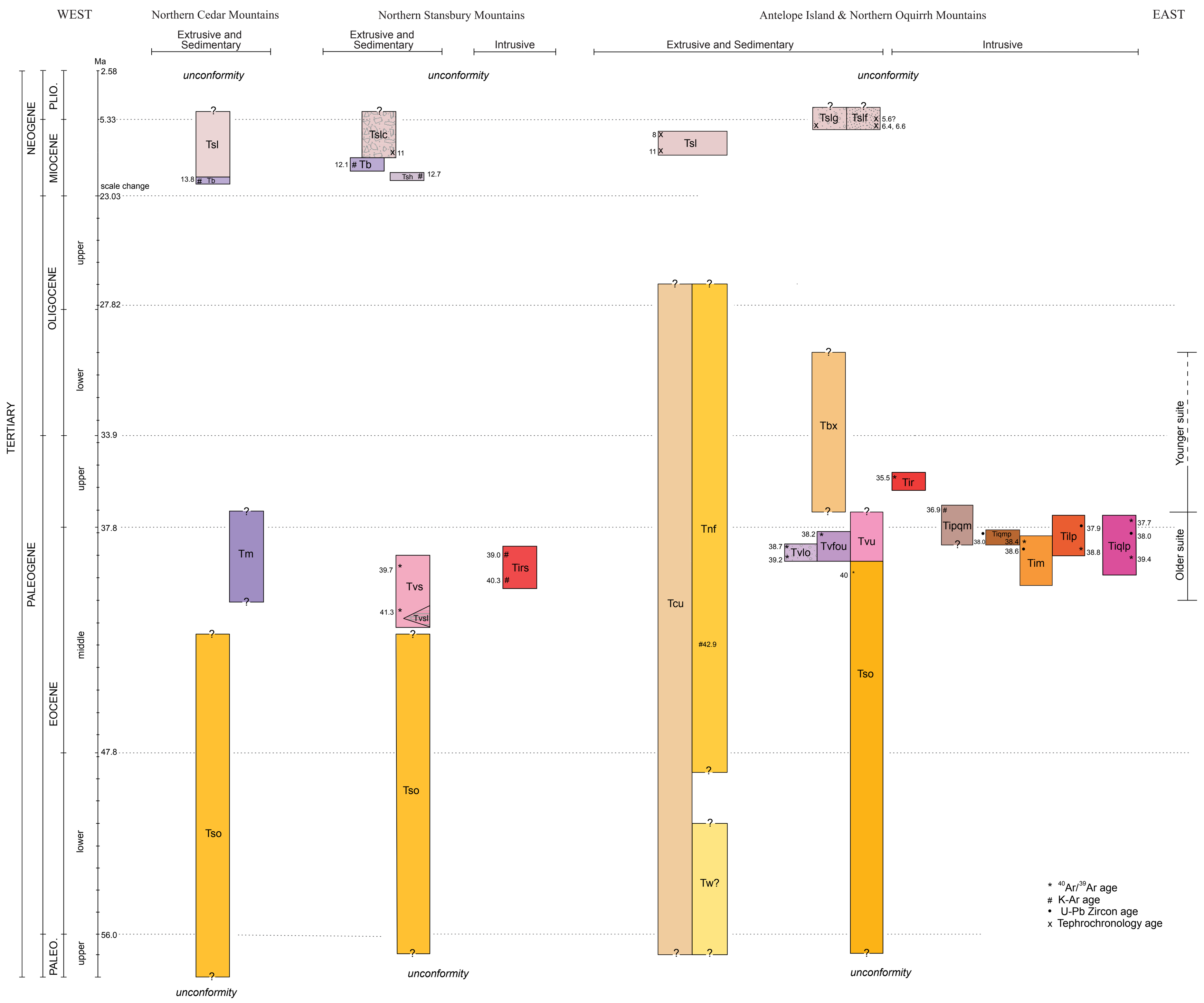

CORRELATION OF MESOZOIC, PALEOZOIC, AND PRECAMBRIAN GEOLOGIC UNITS

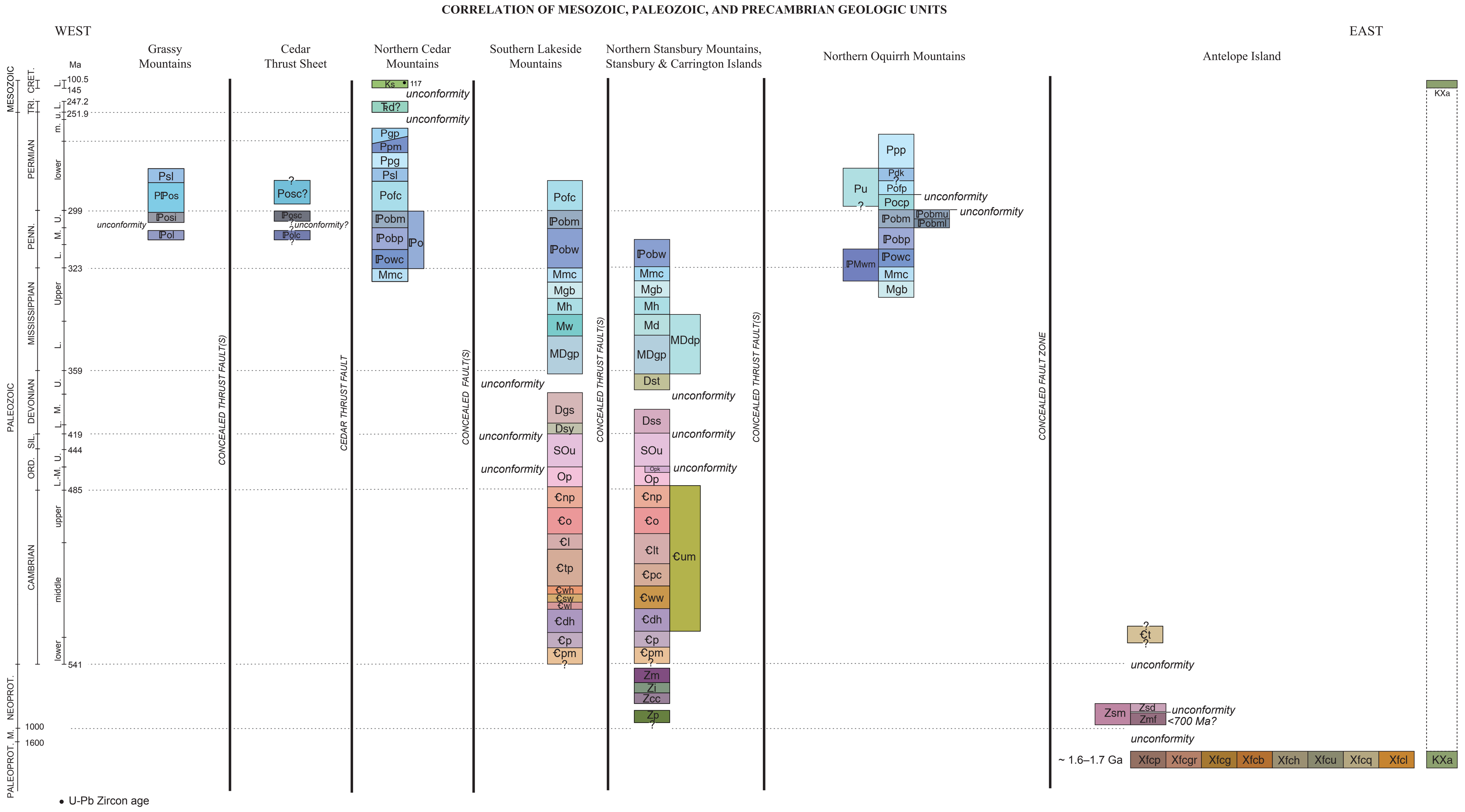

Boundary ages from International Chronostratigraphic Chart v2020/01

GEOLOGIC SYMBOLS

- Contact
- High-angle normal fault – Dashed where approximately located, dotted where concealed; dotted and queried where existence and location inferred; bar and ball on downthrown side
- Normal fault, geophysical, seismic – Located from shallow seismic reflection data for Great Salt Lake fault zone; heavier line for main faults and lighter line for subsidiary faults; dotted where concealed; bar and ball on downthrown side; colors indicate relative age of youngest sediments affected by faulting: red for lake bottom displacement, green for Holocene, blue for pre-Holocene
- Normal fault, geophysical, gravity – Located from gravity data, concealed and very approximately located; bar and ball on downthrown side
- Strike-slip or oblique-slip fault – Dashed where approximately located, dotted where concealed; arrows and bar and ball indicate relative displacement
- Fault with unknown geometry and offset – Dashed where approximately located, dotted where concealed, dotted and queried where existence and location inferred
- Fault movement on cross section - toward (dot), away (cross)
- Thrust fault – Dashed where approximately located, dotted where concealed; dotted and queried where existence and location inferred; teeth on hanging wall; bar and ball where later normal movement
- Reverse fault – Dashed where approximately located; teeth on hanging wall
- Attenuation fault – Dotted where concealed; boxes on hanging wall
- Low-angle normal fault – Dotted where concealed; boxes on hanging wall
- Lineament – From aerial photo interpretation
- Quartz vein
- Igneous dike or sill
- Axial trace of anticline – Dashed where approximately located, dotted where concealed; arrow shows plunge
- Axial trace of overturned anticline – Dashed where approximately located, dotted where concealed; arrow shows plunge
- Axial trace of syncline – Dashed where approximately located, dotted where concealed; arrow shows plunge
- Axial trace of overturned syncline – Dashed where approximately located, dotted where concealed; arrow shows plunge
- Lake Bonneville shorelines (see Currey, 1982; Chen and Maloof, 2017) – Dashed where approximately located
  - B — Bonneville shoreline 5110–5327 ft (1558–1624 m)
  - P — Provo shoreline 4812–4920 ft (1467–1500 m)
  - S — Stansbury shoreline 4420–4540 ft (1348–1384 m)
- GSL — Great Salt Lake shoreline (historical average 4200 ft [1280 m])
- Glacial cirque headwall
- Nivation hollow headwall and adjacent ridge crests
- Scarp (landslide or undefined) – Hachures on down-dropped or lower side
- Pit/Open pit mine extent – SE Antelope Island gravel pit, Bingham, Barneys Canyon, Melco mines
- Unconformity (on cross sections)
- Sedimentary bedding attitude –
  - 20 Inclined
  - Inclined approximate
  - Vertical
  - 50 Overturned
- Volcanic and metamorphic foliation attitude –
  - 45 Inclined
  - Vertical
- Spring
- Mine or quarry (active and inactive)
- Adit (active and inactive)
- Shaft (active and inactive)
- Sand and gravel pit (active and inactive)
- Sediment core – Great Salt Lake and vicinity (see table 1)
- Drill hole – Oil/Gas exploration (see table 2)
- Groundwater well/monitoring well (see table 2)
- Tephrochronology sample (see table 4)
- Radiometric geochronology sample (see table 5)
- U-Pb zircon geochronology sample (see table 6)
- Geochemical sample (see table 7)
- Fossil sample (see table 8)
- Qes/Qlg — Stacked unit — Indicates thin cover of the first unit overlying the second unit
- Paleoseismic trench, approximate length
- Shear zone on Antelope Island
- Areas of mine waste rock (2011)
- Ditches and disturbed areas in lake bed below Great Salt Lake shoreline (4200 ft)
- A — A' Line of cross section
- Gravity data (see GIS data) —
  - Point
  - -170 Contour line (mGal)
- Seismic data (see GIS data) —
  - Seismic reflection trackline

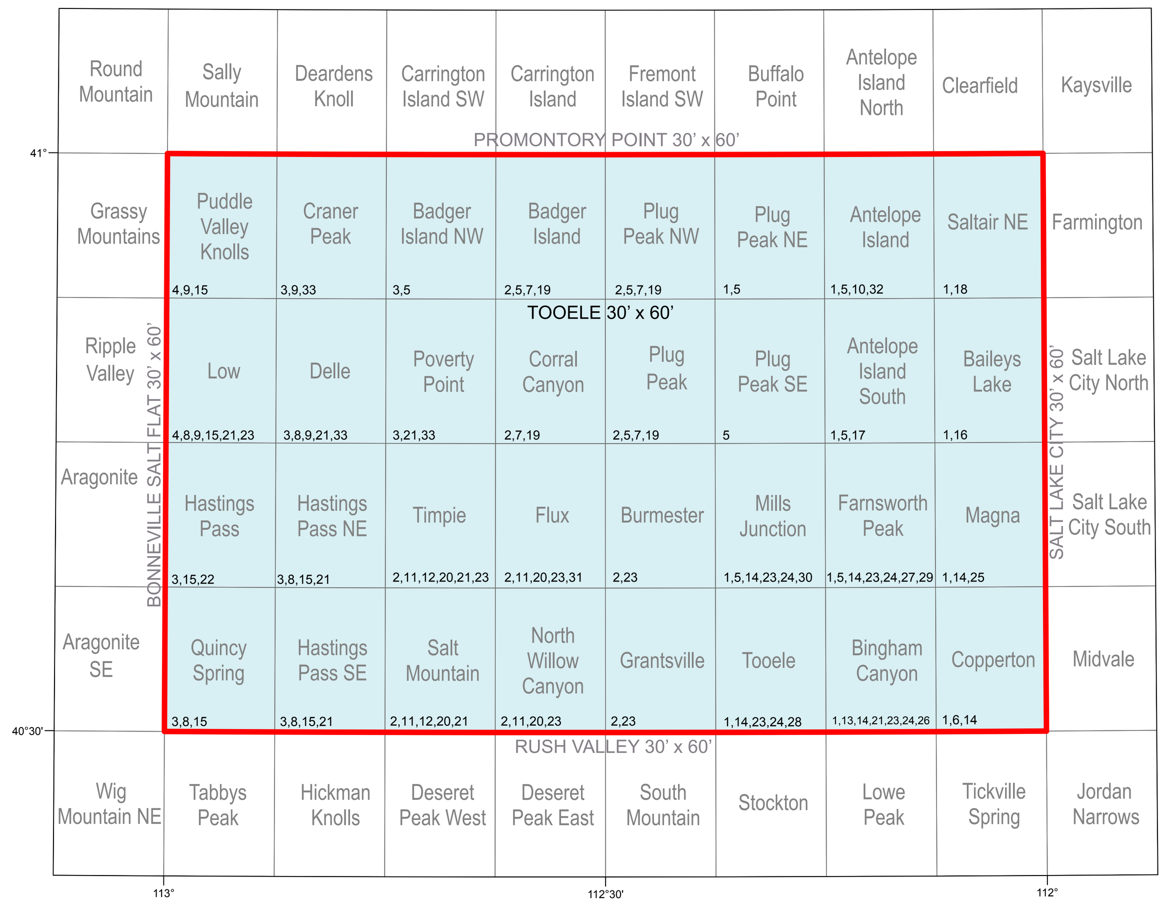

PRIMARY SOURCES OF GEOLOGIC MAPPING

1. Clark, D.L. (UGS) and Oviatt, C.G. (KSU), 2013-2014 (year 1 of 4), photogeologic and limited field mapping
2. Clark, D.L. (UGS) and Oviatt, C.G. (KSU), 2014-2015 (year 2 of 4), photogeologic and limited field mapping
3. Clark, D.L. (UGS), 2015-2016 (year 3 of 4), photogeologic and limited field mapping
4. Clark, D.L. (UGS), 2016-2017 (year 4 of 4), photogeologic and limited field mapping
5. Dinter, D.A. (UU), unpublished work, data collected 1998, 2003, 2006, Great Salt Lake fault zone mapping
6. Biek and others (2007)
7. Chapusa (1969)
8. Dames & Moore and others (1987)
9. Doelling (1964)
10. Doelling and others (1990)
11. Foose (1989)
12. Helm (1994)
13. KUCC (2009)
14. Laes and others (1997)
15. Maurer (1970)
16. McKean and Hylland (2019)
17. McKean and others (2019)
18. McKean (2019)
19. Palmer (1970)
20. Rigby (1958)
21. Sack (1993)
22. Schurer (1979a)
23. Solomon (1993)
24. Solomon (1996)
25. Solomon and others (2007)
26. Swenson and Kennecott staff (1991)
27. Thomas (1957)
28. Tooker (1980)
29. Tooker and Roberts (1971a)
30. Tooker and Roberts (1971b)
31. Trexler (1992)
32. Yonkee and others (2000a)
33. Young (1953)

GEOLOGIC UNITS

Qa	Alluvium, undivided
Qal	Stream alluvium
Qam	Alluvial mud
Qafy	Younger fan alluvium, post-Lake Bonneville
Qafo	Older fan alluvium, pre-Lake Bonneville
QTaf	Oldest fan alluvium
Qsm	Spring and marsh deposits
Qes	Eolian sand
Qeo	Eolian oolitic sand
Qei	Eolian silt
Qly	Younger lacustrine deposits, Great Salt Lake
Qdy	Younger deltaic deposits, Great Salt Lake
Qlk	Younger lacustrine carbonate-chip sand and gravel, Great Salt Lake
Qlmy	Younger lacustrine mud, Great Salt Lake
Qldy	Younger lacustrine and deltaic deposits, Great Salt Lake
Qlb	Lacustrine boulders, Great Salt Lake and Lake Bonneville
Qlg	Lacustrine gravel, Great Salt Lake and Lake Bonneville
Qlf	Lacustrine fine-grained deposits, Great Salt Lake and Lake Bonneville
Qls	Lacustrine sand, Lake Bonneville
Qlt	Lacustrine tufa, Lake Bonneville
Qgt	Glacial till
Qmct	Colluvium and talus
Qms	Landslide deposits
Qlpm	Great Salt Lake and playa mud
Qla	Lacustrine and alluvial deposits, undivided
Qac	Alluvial and colluvial deposits
QTlm	Lacustrine mudflat and eolian deposits, undivided [subsurface only]
Qh	Human disturbance
Qhm	Mine dumps
Qht	Tailings impoundment
Qhe	Evaporation ponds
Qh/Tsl	Human disturbance over Salt Lake Formation, undivided
Qh/Tnf?	Human disturbance over Norwood Formation and Fowkes Formation, undivided?
Qh/Tw?	Human disturbance over Wasatch Formation?
Qei/Qlgf?	Eolian silt over lacustrine gravel to fine-grained deposits
Qes/Qafy	Eolian sand over younger fan alluvium
Qes/Qla	Eolian sand over lacustrine and alluvial deposits, undivided
Qes/Qlg	Eolian sand over lacustrine gravel
Qes/Qls	Eolian sand over lacustrine sand
Qes/Qlf	Eolian sand over lacustrine fine-grained deposits
Qes/Qafo	Eolian sheet sand deposits over older fan alluvium
Qes/Ks	Eolian sand over Cretaceous strata
Qlf/Posc?	Lacustrine fine-grained deposits over Oquirrh Group, sandstone and limestone unit (Cedar thrust sheet?)
QTaf/Tslc	Oldest fan alluvium over Salt Lake Formation, conglomerate lithosome
Tsl	Salt Lake Formation
Tslc	Salt Lake Formation, conglomerate lithosome
Tslf	Salt Lake Formation, fine-grained lithosome
Tslg	Salt Lake Formation, gravel lithosome
Tcu	Tertiary conglomerate, undivided
Tnf?	Norwood and Fowkes Formation, undivided?
Tw?	Wasatch Formation?
Tso	Older Tertiary strata, undivided
Tb	Trachybasalt and basalt
Tsh	Shoshonite
Tm	Olivine melanephelinite
Tvs	Rhyolitic to andesitic volcanic rocks of Stansbury Mountains
Tvsl	Rhyolitic to andesitic volcanic rocks of Stansbury Mountains, lacustrine limestone
Tirs	Rhyolite and trachydacite porphyry intrusions of Stansbury Mountains
Tbx	Breccia pipes and bodies
Tvu	Volcanic rocks, undivided
Tir	Rhyolitic intrusion
Tvfou	Older intermediate lava flows
Tvlo	Older lahars and debris avalanches
Tipqm	Porphyritic quartz monzonite intrusions
Tiqmp	Quartz monzonite porphyry intrusion
Tim	Monzonite intrusions
Tilp	Latite to dacite porphyry sills and dikes
Tiqlp	Quartz latite porphyry dikes and sills
Ks	Cretaceous strata
Ŧd?	Dinwoody Formation?
Pgp	Gerster Formation and Plympton Formation, undivided
Ppp	Park City Formation and Phosphoria Formation, undivided
Ppm	Phosphoria Formation, Meade Peak Member
Ppg	Park City Formation, Grandeur Member
Psl	Permian sandstone, limestone and dolomite
Pu	Permian strata, undivided
Pdk	Diamond Creek Sandstone and Kirkman Formation, undivided
PIPos	Oquirrh Group, sandstone and limestone unit (Grassy Mountains)
IPosi	Oquirrh Group, sandstone and siltstone unit (Grassy Mountains)
IPol	Oquirrh Group, limestone unit (Grassy Mountains)
Posc?	Oquirrh Group, sandstone and limestone unit (Cedar thrust sheet?)
IPosc	Oquirrh Group, sandstone and siltstone unit (Cedar thrust sheet)
IPolc	Oquirrh Group, limestone unit (Cedar thrust sheet)
Pofc	Oquirrh Group, Freeman Peak Formation and Curry Peak Formation, undivided
Pofp	Oquirrh Group, Freeman Peak Formation
Pocp	Oquirrh Group, Curry Peak Formation
IPo	Oquirrh Group, Pennsylvanian formations, undivided
IPobm	Oquirrh Group, Bingham Mine Formation
IPobmu	Oquirrh Group, Bingham Mine Formation, upper member
IPobml	Oquirrh Group, Bingham Mine Formation, lower member
IPobw	Oquirrh Group, Butterfield Peaks Formation and West Canyon Limestone, undivided
IPobp	Oquirrh Group, Butterfield Peaks Formation
IPMwm	Oquirrh Group, West Canyon Limestone and Manning Canyon Formation, undivided
IPowc	Oquirrh Group, West Canyon Limestone
Mmc	Manning Canyon Formation
Mgb	Great Blue Limestone
Mh	Humbug Formation
MDdp	Deseret Limestone, Gardison Limestone, Fitchville Formation, Pinyon Peak Limestone, undivided
Md	Deseret Limestone
Mw	Woodman Formation
MDgp	Gardison Limestone, Fitchville Formation, Pinyon Peak Limestone, undivided
Dst	Stansbury Formation
Dst(SOu)	Stansbury Formation, slide blocks of Laketown and Ely Springs Dolomite
Dgs	Guilmette Formation and Simonson Dolomite, undivided
Dss	Simonson Dolomite and Sevy Dolomite, undivided
Dsy	Sevy Dolomite
SOu	Laketown Dolomite, Ely Springs Dolomite, Eureka Quartzite, undivided
Op	Pogonip Group, undivided
Opk	Pogonip Group, Kanosh Shale
Ꞓum	Upper and Middle Cambrian strata, undivided
Ꞓnp	Notch Peak Formation
Ꞓo	Orr Formation
Ꞓlt	Lamb Dolomite and Trippe Limestone, undivided
Ꞓl	Lamb Dolomite
Ꞓtp	Trippe Limestone and Pierson Cove Formation, undivided
Ꞓpc	Pierson Cove Formation
Ꞓww	Wheeler Formation, Swasey Limestone, Whirlwind Formation, undivided
Ꞓwh	Wheeler Formation
Ꞓsw	Swasey Limestone
Ꞓwl	Whirlwind Formation
Ꞓdh	Dome Limestone, Chisholm Formation, Howell Limestone, undivided
Ꞓp	Pioche Formation
Ꞓpm	Prospect Mountain Quartzite
Zm	Mutual Formation
Zi	Inkom Formation
Zcc	Caddy Canyon Quartzite
Zp	Perry Canyon Formation
KXa	Altered and deformed rocks
Ꞓt	Tintic Quartzite
Zsm	Slate and dolomite unit and Mineral Fork Formation, undivided
Zsd	Slate and dolomite
Zmf	Mineral Fork Formation
Xfcp	Farmington Canyon Complex, granite and pegmatite
Xfcgr	Farmington Canyon Complex, granitic gneiss, red
Xfcg	Farmington Canyon Complex, granitic gneiss, migmatitic
Xfcb	Farmington Canyon Complex, banded gneiss
Xfch	Farmington Canyon Complex, hornblende-plagioclase gneiss
Xfcu	Farmington Canyon Complex, metamorphosed ultramafic rock
Xfcq	Farmington Canyon Complex, quartz-rich gneiss
Xfcl	Farmington Canyon Complex, layered gneiss
	water

Note - Duplicated queried units not included here, see Geologic Unit Descriptions.

LITHOLOGIC COLUMN

Grassy Mountains

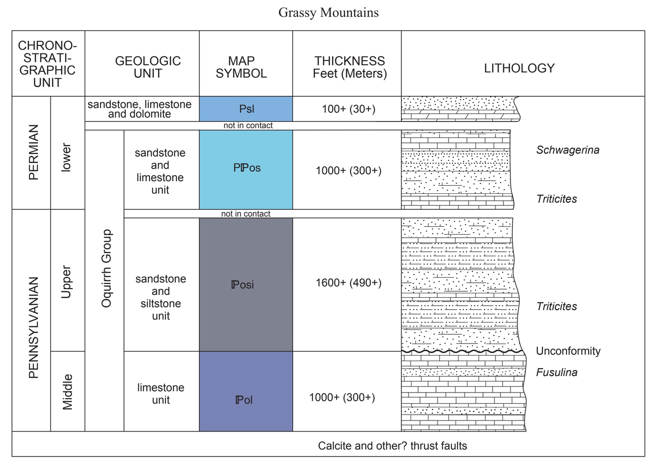

LITHOLOGIC COLUMN

Western Cedar Mountains
(Cedar thrust sheet)

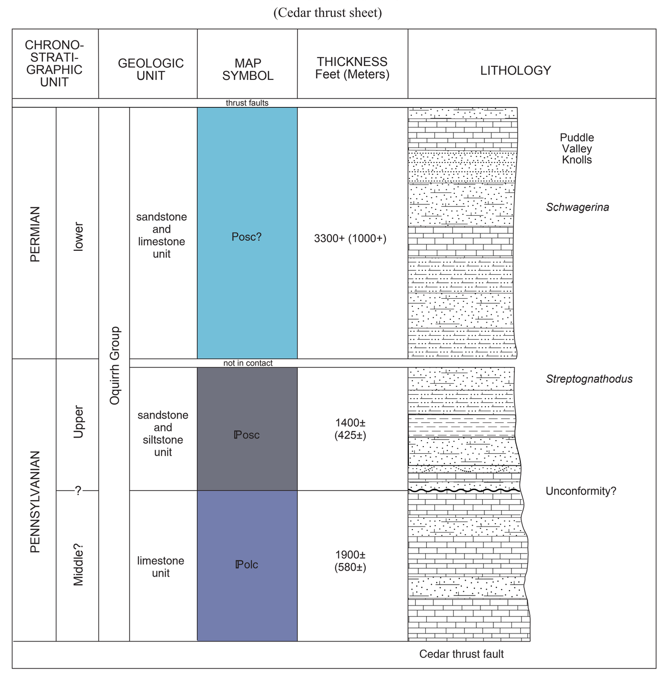

Major Facies Change in Oquirrh Group Rocks West of Central Cedar Mountains

LITHOLOGIC COLUMN

Northern Cedar Mountains

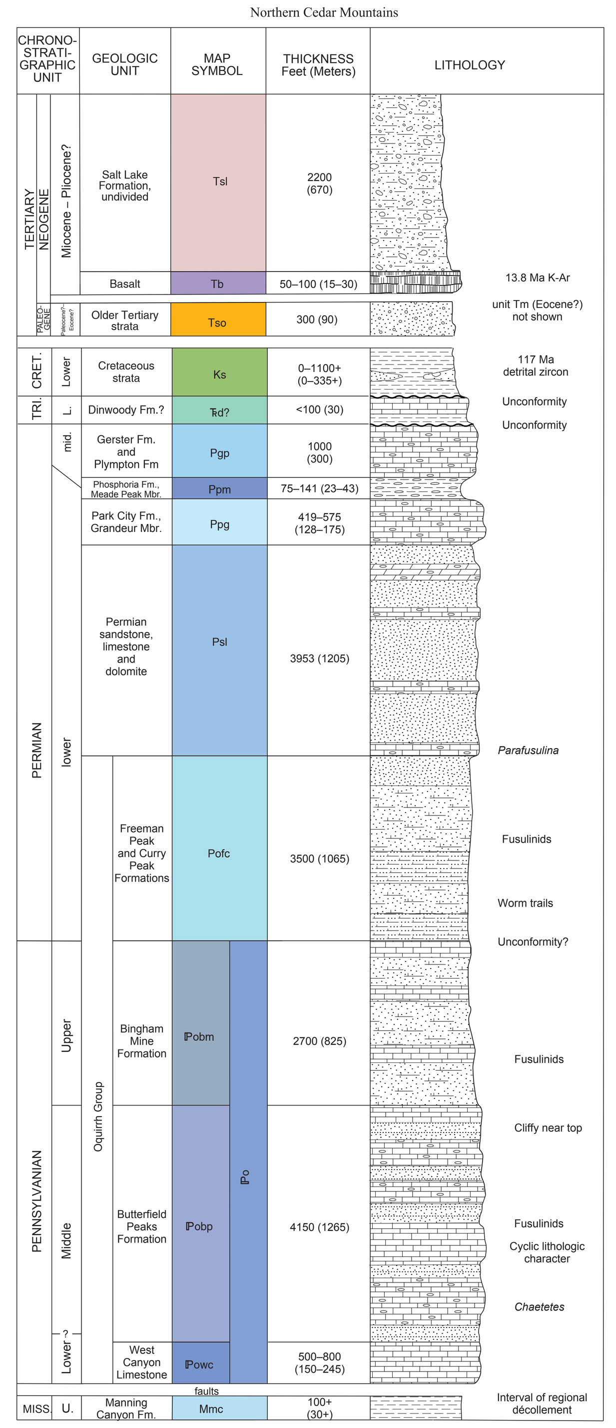

LITHOLOGIC COLUMN

Southern Lakeside Mountains

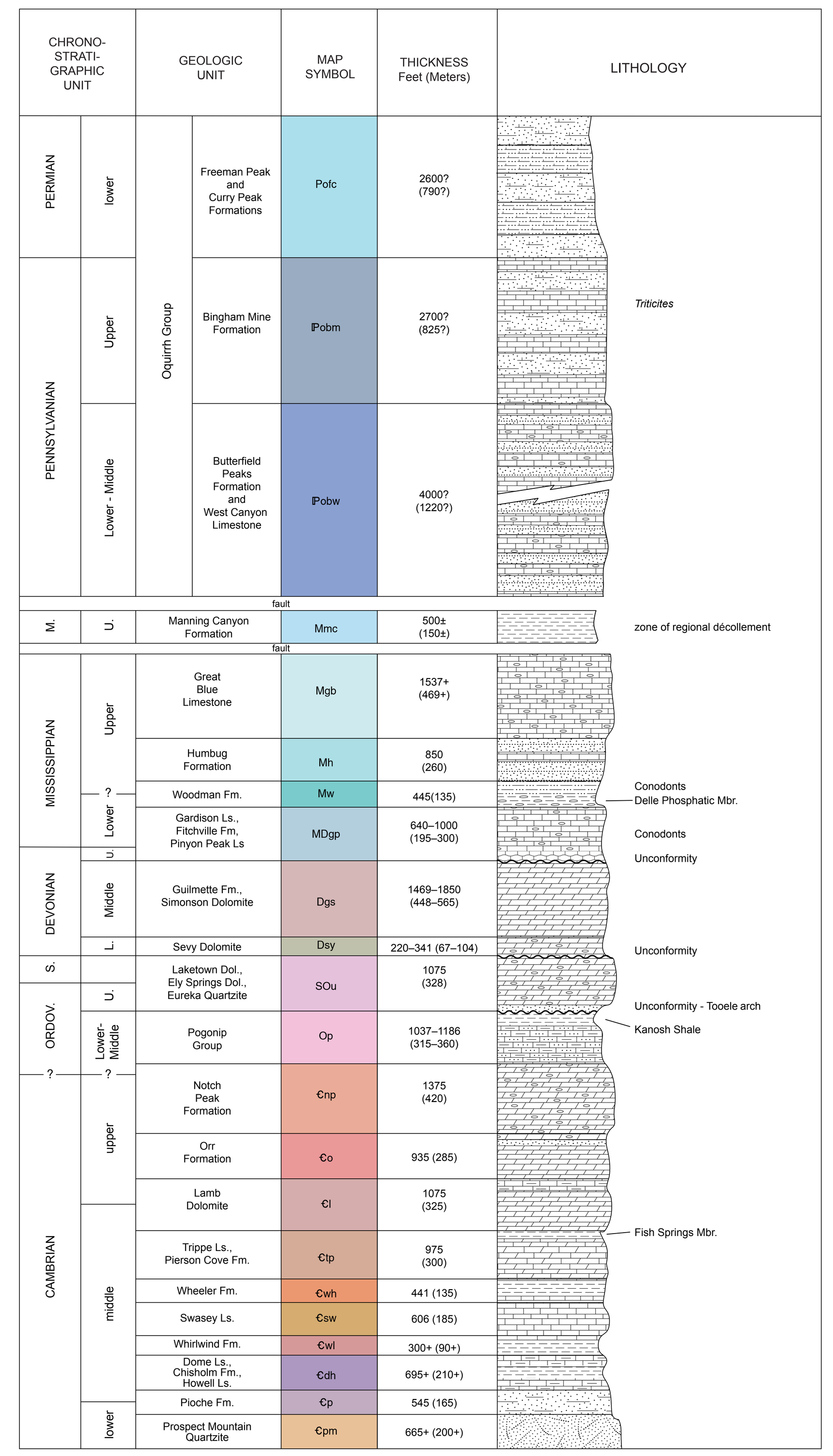

LITHOLOGIC COLUMN

Northern Stansbury Mountains,
Stansbury and Carrington Islands

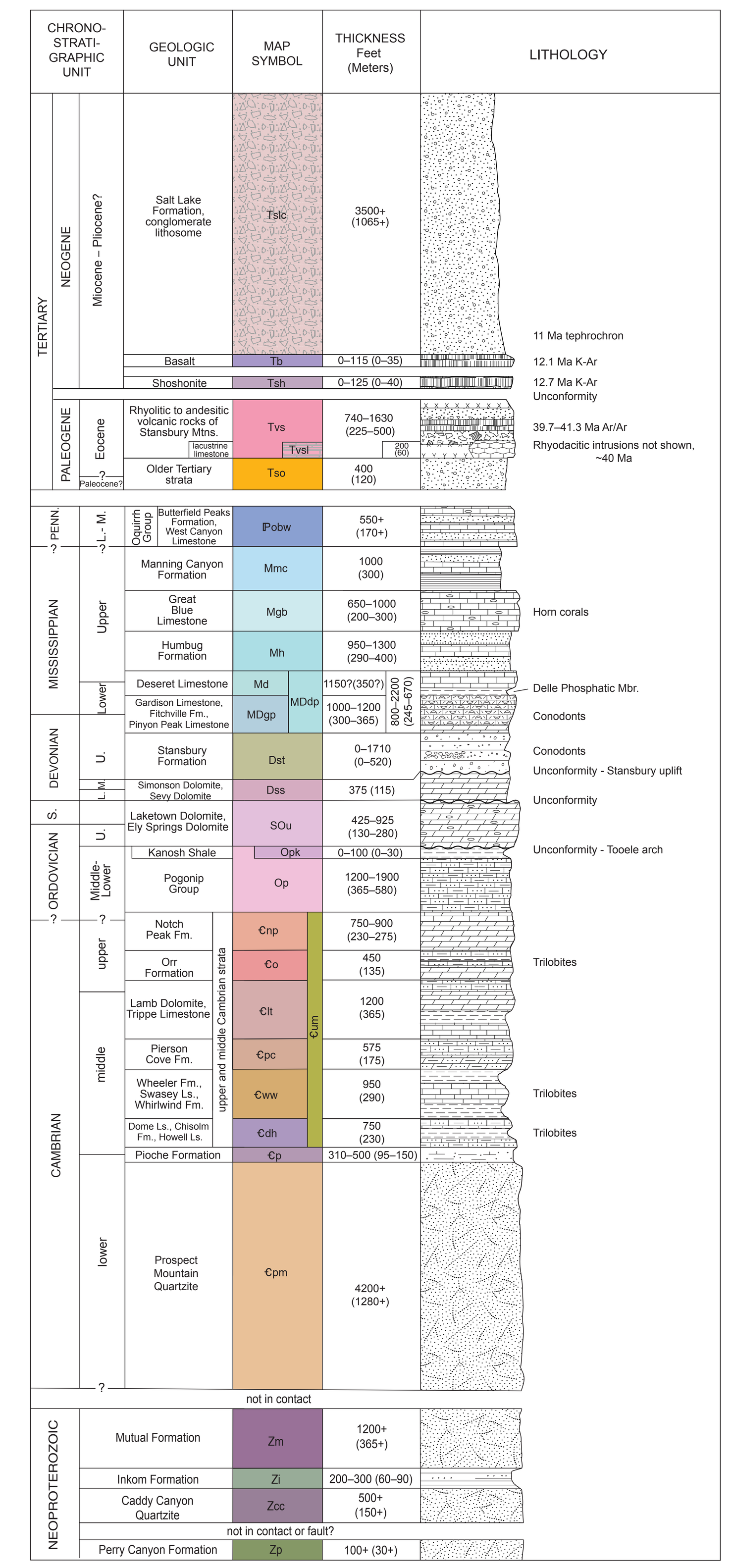

LITHOLOGIC COLUMN

Northern Oquirrh Mountains and Antelope Island

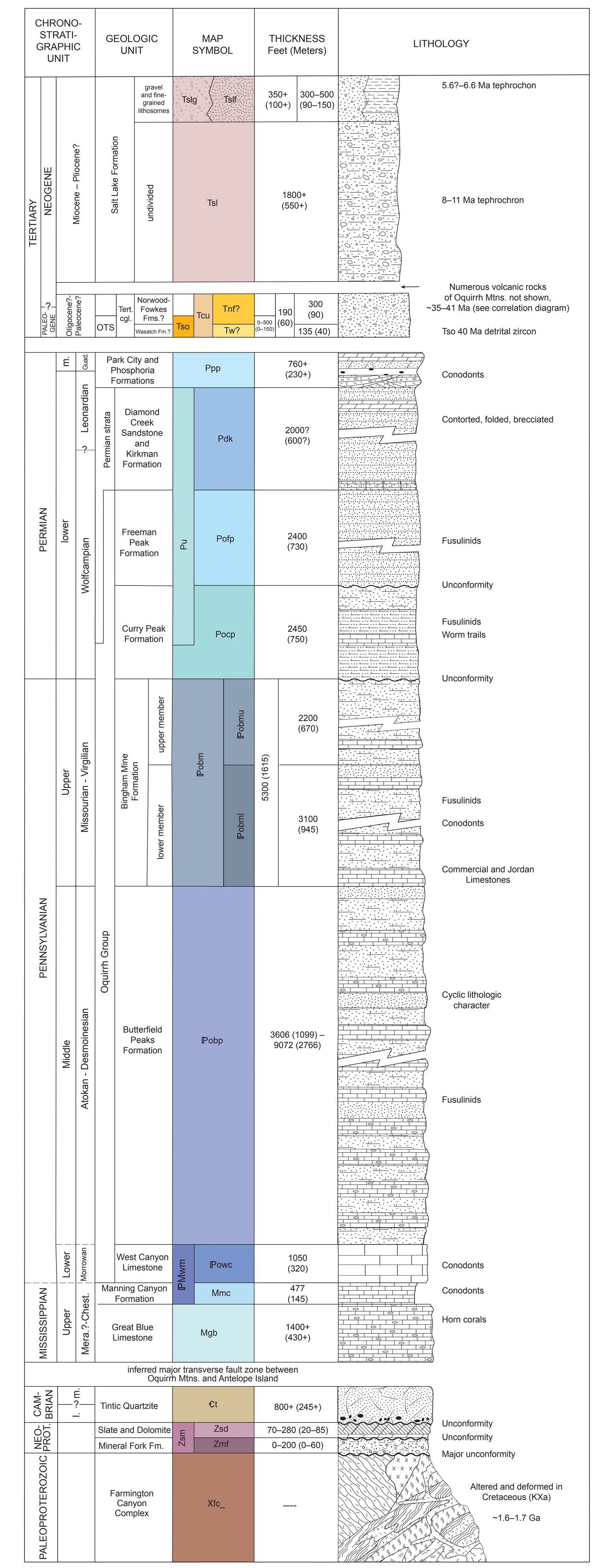

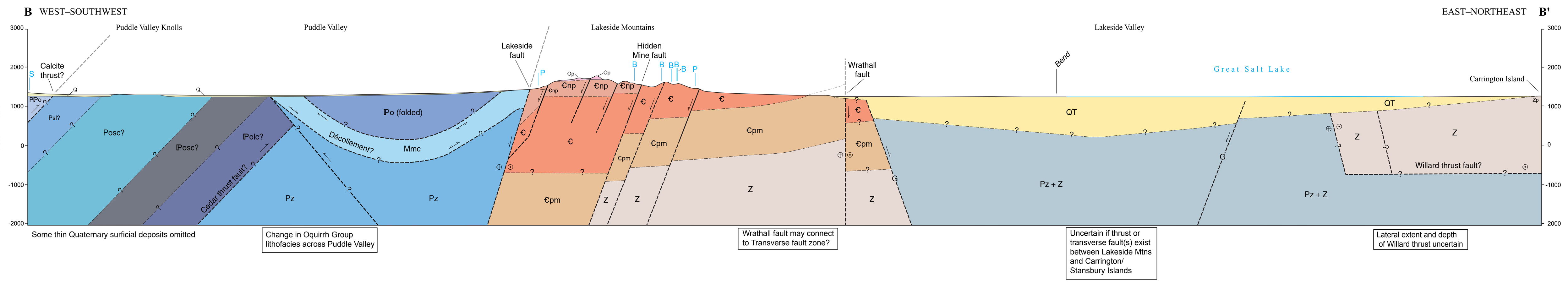

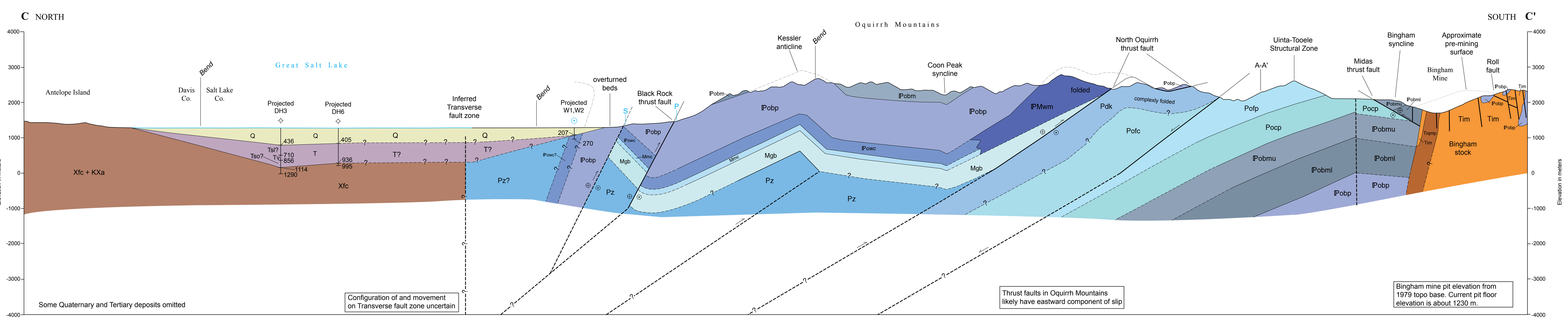

Sevier Orogenic Belt Fault Map, Northwestern Utah

Compiled and reinterpreted by D.L. Clark from numerous sources, but notably Willis (1999), Kwon and Mitra (2004), and Yonkee and Weil (2011). The Wyoming salient is located north of the Uinta-Tooele structural zone and the Provo/Charleston-Nebo salient is located south to the Leamington zone. South-central Utah part of Sevier belt is south of the Leamington zone. Geologic map base and geologic units from Hintze and others (2000). Grid is 30′ x 60′ quadrangles. SLC is Salt Lake City.

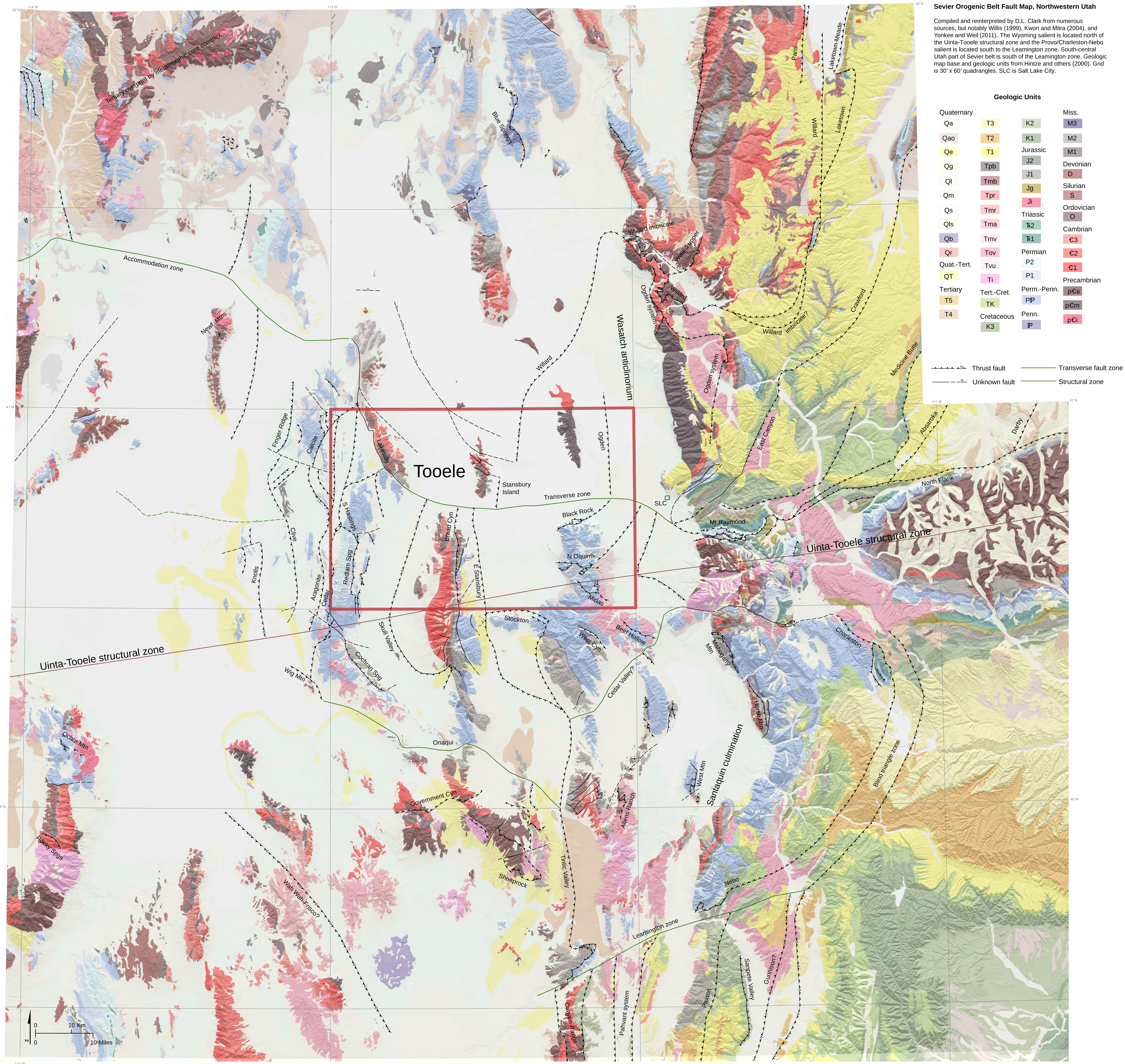

GEOLOGIC MAP OF THE TOOELE 30' X 60' QUADRANGLE, TOOELE, SALT LAKE, AND DAVIS COUNTIES, UTAH

by Donald L. Clark, Charles G. Oviatt, and David A. Dinter

MAP 284DM
UTAH GEOLOGICAL SURVEY
a division of
UTAH DEPARTMENT OF NATURAL RESOURCES
2020

Blank pages are intentional for printing purposes.

GEOLOGIC MAP OF THE TOOELE 30' X 60' QUADRANGLE, TOOELE, SALT LAKE, AND DAVIS COUNTIES, UTAH

by Donald L. Clark[1], Charles G. Oviatt[2], and David A. Dinter[3]

[1] Utah Geological Survey, Salt Lake City, Utah
[2] Emeritus, Department of Geology, Kansas State University, Manhattan, Kansas
[3] Department of Geology and Geophysics, University of Utah, Salt Lake City, Utah

Cover photo: *View to the south along the east side of the northern Cedar Mountains, Hastings Canyon area. Photo by Donald L. Clark.*

Suggested citation:

Clark, D.L., Oviatt, C.G., and Dinter, D.A., 2020, Geologic map of the Tooele 30' x 60' quadrangle, Tooele, Salt Lake, and Davis Counties, Utah: Utah Geological Survey Map 284DM, 48 p., 2 appendices, 4 plates, scale 1:62,500, https://doi.org/10.34191/M-284DM.

MAP 284DM
UTAH GEOLOGICAL SURVEY
a division of
UTAH DEPARTMENT OF NATURAL RESOURCES
2020

STATE OF UTAH
Gary R. Herbert, Governor

DEPARTMENT OF NATURAL RESOURCES
Brian Steed, Executive Director

UTAH GEOLOGICAL SURVEY
R. William Keach II, Director

PUBLICATIONS
contact
Natural Resources Map & Bookstore
1594 W. North Temple
Salt Lake City, UT 84116
telephone: 801-537-3320
toll-free: 1-888-UTAH MAP
website: mapstore.utah.com
email: geostore@utah.gov

UTAH GEOLOGICAL SURVEY
contact
1594 W. North Temple, Suite 3110
Salt Lake City, UT 84116
telephone: 801-537-3300
website: geology.utah.gov

This geologic map was funded by the Utah Geological Survey and the U.S. Geological Survey, National Cooperative Geologic Mapping Program through USGS STATEMAP award numbers G13AC00169 (2013–14), G14AC00214 (2014–15), G15AC00249 (2015–16), and G16AC00191 (2016–17). The views and conclusions contained in this document are those of the authors and should not be interpreted as necessarily representing the official policies, either expressed or implied, of the U.S. Government. This map and explanatory information is submitted for publication with the understanding that the U.S. Government is authorized to reproduce and distribute reprints for governmental use.

CONTENTS

FIGURES

PLATES

GEOLOGIC MAP OF THE TOOELE 30' X 60' QUADRANGLE, TOOELE, SALT LAKE, AND DAVIS COUNTIES, UTAH

by Donald L. Clark, Charles G. Oviatt, and David A. Dinter

ABSTRACT

The Tooele 30' x 60' quadrangle geologic map straddles the Interstate 80 corridor west of Salt Lake City. The map area includes several basement provinces associated with the east-west-oriented Uinta-Tooele structural zone, which records successive tectonic events including the Tooele arch, Stansbury uplift, Uinta arch, and aligned Tertiary igneous rocks and mineralization. Prior to Mesozoic tectonism, the area accumulated a thick sequence of Neoproterozoic and Paleozoic strata (7.8 miles, 12.5 km) on Paleoproterozoic basement. This map presents stratigraphic nomenclature that is consistent across multiple thrust sheets of the Sevier orogenic belt. The map straddles the Wyoming salient (north) and Provo salient (south), which are two main Sevier fold-thrust-belt segments in Utah. Mapped structures and syntectonic sediments reveal new insights into the architecture and timing of thrusting at this latitude in the Sevier orogenic belt. Following Sevier deformation, calc-alkaline volcanism occurred from Paleogene volcanic centers (41 to 35 Ma) in the Oquirrh and Stansbury Mountains. This volcanism produced a world class porphyry copper deposit at Bingham Canyon and smaller gold deposits at Barneys Canyon and Melco in the Oquirrh Mountains. Extensional tectonism created the distinctive basin and range topography from about 17 Ma to the present. Early extensional basin fill includes Miocene-Pliocene sedimentary and volcanic rocks overlain by Pliocene-Pleistocene-Holocene surficial deposits. Most of the map area was covered by late Pleistocene Lake Bonneville and now a smaller successor, Great Salt Lake. Lake Bonneville deposits are associated with three levels of regional shorelines. Quaternary fault zones include those of Puddle Valley, Stansbury, Great Salt Lake, Oquirrh, and West Valley, while other Quaternary normal faults lacking scarps are inferred. The 2020 M_W 5.7 Magna earthquake is interpreted to have been caused by slip on the Wasatch fault zone in the area of the Saltair graben. This map also includes information on subsurface materials and gravity, geochronologic, paleontologic, and geochemical data.

INTRODUCTION

The introductory text is intended to provide context for the geologic mapping and highlights on key issues of the quadrangle (see Notes sections on deposits, rocks, stratigraphy, structure, resources and waste management). Additional details are beyond the scope of this project.

Location and Setting

The Tooele 30' x 60' quadrangle straddles urban and rural areas west of Salt Lake City in Tooele, Salt Lake, and Davis Counties, northwest Utah. The map area is in the eastern Basin and Range Province and includes several north-south-trending mountain ranges and intervening valleys, and the southern part of Great Salt Lake (plate 1, figure 1). The map area includes populated and rapidly growing suburban areas in western Salt Lake and Tooele Valleys. Land use is mixed between private, public, and military. The eastern half of the quadrangle is primarily private land with some public land (Antelope Island and Great Salt Lake State Parks, new State prison site, western Oquirrh Mountains, Stansbury Peninsula/Island area), and also military land of the Tooele Army Depot in Tooele Valley. The western half of the map area is primarily public land with some smaller areas of private land. The public land is administered by the U.S. Bureau of Land Management (including Cedar Mountains Wilderness), the U.S. Forest Service (Uinta-Wasatch-Cache National Forest including part of the Deseret Peak Wilderness), and the State of Utah (SITLA–School and Institutional Trust Lands Administration). The bed of Great Salt Lake is sovereign land managed by the State of Utah (Division of Forestry, Fire, and State Lands).

Purpose

This geologic map is part of an ongoing effort by the Utah Geological Survey (UGS) to map the geology of the state of Utah at an intermediate scale (Clark, 2017; Willis, 2017). Demand for this map is high considering the proximity to the Salt Lake City metropolitan area and the Interstate Highway 80 (I-80) corridor. The map will be useful in land use planning, as well as protecting and developing resources, namely water, metals, industrial minerals, oil and gas, and recreation. In addition, our mapping connects recent and ongoing intermediate-scale mapping projects in the northern part of the state (Clark and others, 2012, 2021; Clark and others, 2016; Clark and others, 2020; Constenius and others, 2011, in preparation; Coogan and King, 2016; Miller and others, 2020, in preparation; Miller, Felger and Langenheim, 2020, in preparation).

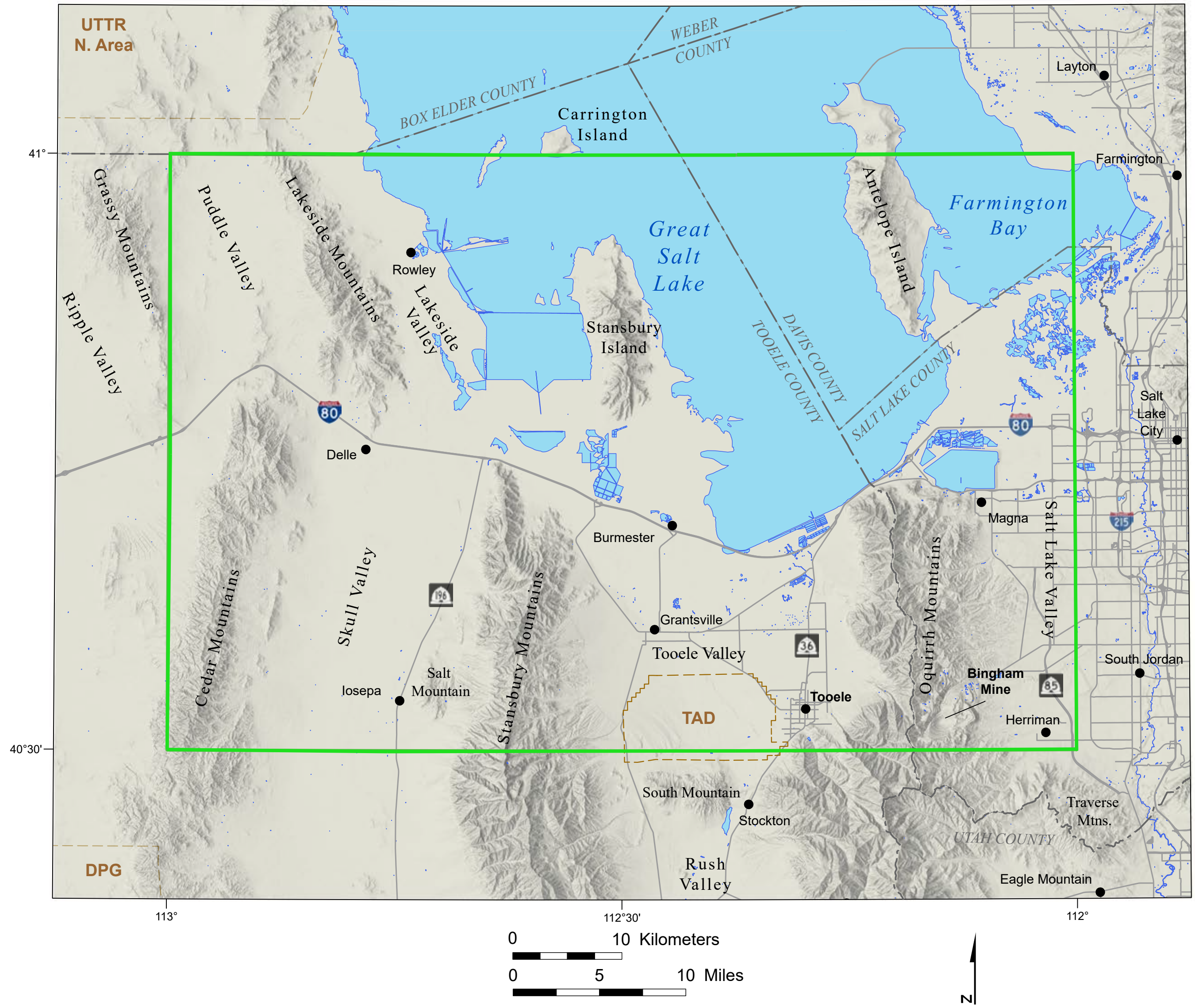

Figure 1. Primary geographic features in the Tooele 30' x 60' quadrangle (green rectangle). TAD is Tooele Army Depot. DPG is Dugway Proving Ground (U.S. Army). UTTR is Utah Test and Training Range (U.S. Air Force).

This map updates prior regional-scale (1:250,000) geologic maps by Stokes (1963) and Moore and Sorensen (1979).

Methods

The mapping was accomplished through compilation of geologic mapping data, where possible, and revising and remapping other areas using existing source maps and through aerial photograph interpretation and field mapping (see the Primary Sources of Geologic Mapping on plate 2). Clark compiled, revised, and mapped the bedrock and surficial deposit geology; Oviatt revised part of the Quaternary-Tertiary geology; and Dinter provided prior mapping of the Great Salt Lake fault zone and the Carrington fault (discussed later in the Quaternary normal faults section). In addition, we used selected exploration drill hole, water well, and available geophysical data from several sources. Clark and Oviatt mapped on stereo aerial photographs (2009 U.S. Department of Agriculture, National Agriculture Imagery Program, color, approximately 1:30,000 scale) from the UGS statewide set of imagery. Field mapping data were collected using a recreational-grade Global Positioning System (GPS) and Brunton compass. Geology was compiled in ArcGIS using digital basemaps including 7.5' orthophoto maps and imagery (commonly 2011 USDA NAIP and Google) and 7.5' topographic maps (USGS and US Topo). UGS did not use recent lidar datasets in this mapping project. Complete lidar data for the entire map area are not yet available. Basia Matyjasik (UGS) managed the GIS data and cartography. The mapping was conducted over four years (2013–14, 2014–15, 2015–16, 2016–17), and interim geologic maps of the progress were prepared each year (UGS Open-File Reports 633, 644, 656, and 669). We conducted a field review of the quadrangle mapping on May 9–10, 2017, and we presented posters at the Geological Society of America regional meeting in May 2018 (Clark and others, 2018a) and the

UGS-sponsored Lake Bonneville Geologic Conference and Short Course in October 2018 (Clark and others, 2018b). We subsequently prepared the final map and GIS data (this publication), which supersedes the open-file reports and poster presentations. The geology is intended for use at 1:62,500 scale.

GEOLOGIC OVERVIEW

The quadrangle contains exposed rocks from Precambrian (Paleoproterozoic) to Tertiary (Miocene) age that are mantled by late Tertiary and Quaternary surficial deposits. The Paleoproterozoic basement rocks (~1.6–1.7 Ga) are exposed only at Antelope Island. Basement rocks of the Mojave and Yavapai provinces were accreted onto the older continental core consisting of the Grouse Creek block, Farmington zone, and Wyoming province, presumably along an east-west-trending suture zone near the latitude of Salt Lake City (Presnell, 1997; Vogel and others, 2001), although it may lay farther north (Nelson and others, 2011).

Sedimentary cover rocks from Neoproterozoic through Cretaceous age crop out in the ranges and cumulatively are roughly 41,000 feet (7.8 mi, 12.5 km) thick. These rocks were deposited over a span of about 585 million years (~700 to 117 Ma), initially in basins and rifting environments (Neoproterozoic to Early Cambrian) and followed by largely marine environments along a subsiding passive margin (miogeocline) west of the Wasatch hingeline (Stokes, 1986; Hintze and Kowallis, 2009; Yonkee and Weil, 2011). Paleozoic strata were subsequently affected by structural features coincident with reactivation of the Uinta-Tooele structural zone (Presnell, 1997; Tooker, 1999; Clark, 2020) including the Ordovician Tooele arch (Webb, 1958; Hintze, 1959) and the Devonian Stansbury uplift (Rigby, 1959). Mississippian to Permian strata were deposited in the Oquirrh basin located between the Antler orogenic belt on the west and Ancestral Rocky Mountains on the east (Jordan and Douglass, 1980; Hintze and Kowallis, 2009).

Utah lies within the Cordilleran orogenic belt of North America (DeCelles, 2004; Yonkee and Weil, 2011). Northern Utah contained a hinterland metamorphic belt on the west, an eastern transitional zone (Jurassic and Cretaceous), and a frontal thrust belt to the east (Early Cretaceous to Eocene, about 145 to 50 Ma) (Miller and others, 1992; DeCelles, 2004; DeCelles and Coogan, 2006; Yonkee and Weil, 2011). The map area straddles the Wyoming and Provo salients of the Sevier fold-thrust belt (DeCelles, 2004). We attribute discordant lithofacies in Paleozoic rocks across Tooele Valley and southernmost Great Salt Lake to the western and eastern thrust systems, each carrying distinctive rock packages on different thrust sheets (see Yonkee and others, 2014).

The few low-angle normal faults are likely related to post-compressional collapse or relaxation of the Sevier orogenic belt (Constenius, 1996; Constenius and others, 2003). The local basins collected sediment, and drainages developed in other areas that deposited various sediments in alluvial, floodplain, and lacustrine environments in the Eocene and possibly from the Paleocene to Oligocene.

Cenozoic volcanism swept from north to south across the western U.S. related to the change in subduction regime (see for example, Lipman and others, 1972; Christiansen and Lipman, 1972; Best and Christiansen, 1991). Older Tertiary volcanic rocks and intrusions at Bingham and the Stansbury Mountains are Eocene in age (41 to 35 Ma). Geochemical data indicate these rock units are largely intermediate to silicic in composition, although a few mafic units occur.

Basin and Range extension began about 20 to 17 Ma (Miocene) and continues to the present; it is characterized by distinctive topography (north-trending ranges and basins) and bimodal volcanism (see for example, Christiansen and McKee, 1978; Zoback, 1983). Numerous normal faults in the ranges and exposed and inferred along the valley margins are related to this Neogene extension. The basins in northwest Utah preserve sedimentary and volcanic rocks of the Miocene Salt Lake Formation (at least 13 to 5.6 Ma), which is present at Antelope Island, western Salt Lake Valley, and the Stansbury and Cedar Mountains.

Extensive late Tertiary to Quaternary surficial deposits blanket the area. Pliocene and Pleistocene deposits are related to lacustrine, mudflat, eolian, and alluvial environments, but are generally not well understood since they are commonly in the subsurface of basins. Alluvial fans also developed along the basin margins as regional extension continued. Two levels of alluvial fans are considered to pre-date Lake Bonneville because they were higher than, or eroded by, the lake.

Late Pleistocene Lake Bonneville was the youngest and deepest of several large pluvial lakes in northern Utah (Oviatt and others, 1992, 1999; Oviatt, 2015). Figure 2 depicts a hydrograph and chronology of the lake. Threshold control was maintained at Red Rock Pass, Idaho. The lake generally increased in size (transgressive phase) from about 30,000 to 18,000 cal yr B.P. The Stansbury shoreline and shoreline zone were formed during lake oscillations around 25,000 cal yr B.P. Subsequently, after transgressing to its highest level, the lake quickly fell (Bonneville flood) from its greatest extent (Bonneville shoreline) to establish the Provo shoreline (18,000 to 15,000 cal yr B.P.), and then continued to regress (regressive phase) until about 13,000 cal yr B.P. (Oviatt and others, 1992; Godsey and others, 2011; Oviatt, 2015). Evidence of Lake Bonneville is recorded in the lake deposits (mud, marl, sand, and gravel) and shoreline remnants, including the Stansbury, Bonneville, and Provo shorelines. The deepest part of Lake Bonneville, and the center of post-Bonneville isostatic rebound, was near the northwest corner of the map area (Crittenden, 1963; Currey, 1982; Adams and Bills, 2016; Chen and Maloof, 2017).

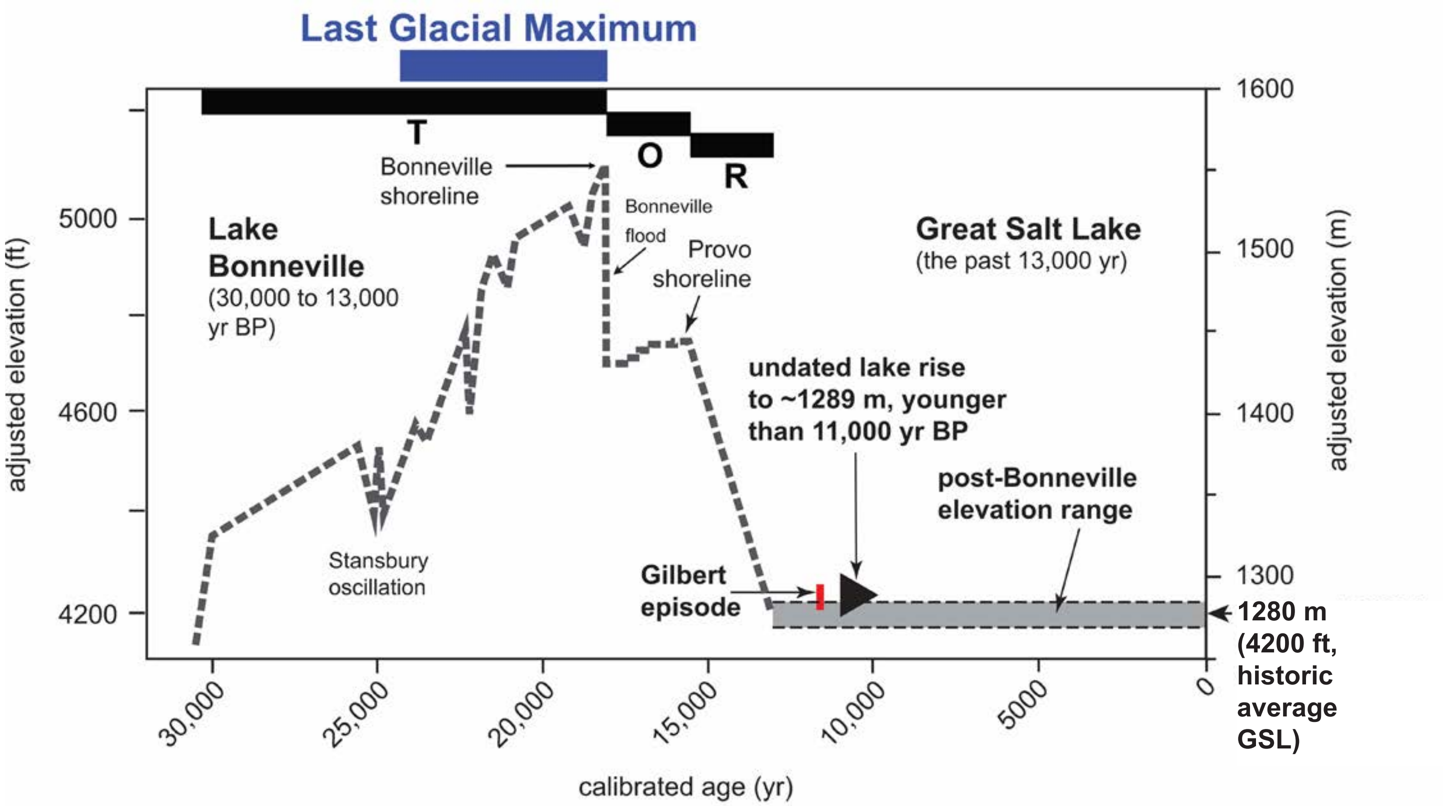

Figure 2. *Simplified Lake Bonneville hydrograph and chronology (based on Oviatt, 2015). Elevation adjusted for isostatic rebound. GSL is Great Salt Lake.*

Coeval with Lake Bonneville, small alpine glaciers occupied cirque basins and valleys in the higher elevations of the Stansbury and Oquirrh Mountains during the Last Glacial Maximum at 21 ± 2 ka (Laabs and Monroe, 2016). These Pleistocene glacial deposits are primarily of Angel Lake or Pinedale age (~24 to 12 ka), but limited older deposits are probably Lamoille or Bull Lake in age (Marine Oxygen Isotope Stage 6, ~190 to 130 ka) (Laabs and Carson, 2005; Laabs and Monroe, 2016; Pierce and others, 2018).

After about 13,000 years B.P. the level of Great Salt Lake averaged close to the modern elevation (4200 feet, 1280 m), and the Gilbert episode lake peaked at about 11,500 cal yr B.P. (Oviatt, 2014, 2015). After 11,500 cal yr B.P., Great Salt Lake remained at altitudes similar to those of the modern average lake, with minor rises during wet intervals. Lacustrine and deltaic deposits of Great Salt Lake occur below the level of the Gilbert-episode lake (4250 feet, 1295 m) (Murchison, 1989; Oviatt, 2014).

Holocene deposition included sediments of alluvial and eolian environments. Younger alluvial fans continued to develop. Eolian silt and sand deposits throughout the western part of the map area likely emanated from the Great Salt Lake Desert. Sediments from spring, colluvial, mass movement and mixed depositional environments also occur.

Some Basin and Range faults have developed Quaternary scarps along the margins of several major valleys; these faults have associated seismic risk. Water levels of Great Salt Lake continue to rise and fall, as anticipated with a terminal lake. Substantial areas of the quadrangle have undergone human disturbance.

NOTES ON QUATERNARY-TERTIARY SURFICIAL DEPOSITS

Subsurface Data

Subsurface data in the quadrangle includes sediment cores and drill holes (see tables A1 and A2). Major Neogene to Recent basins include Skull Valley, Lakeside Valley, northern Tooele Valley, south arm of Great Salt Lake, southeast Antelope Island, and Salt Lake Valley. Subsurface data are available from several basins.

Several sediment cores were collected from the map area in the vicinity of Great Salt Lake (table A1) including three "Eardley" cores (S28, Saltair, Burmester), four "Spencer" cores (A, C, G, H), an unpublished USGS core (95-2), and two Global Lakes Drilling Program (GLAD) cores at site 3. Associated radiocarbon ages and tephrochronologic data are summarized in tables A3 and A4. These cores encountered Quaternary and Neogene deposits and provide a record of sedimentation during and prior to Great Salt Lake and Lake Bonneville. The deepest core (Burmester) was initially interpreted by Eardley and others (1973), but later reinterpreted by Williams (1994) and Oviatt and others (1999).

Amoco advanced deep drill holes in Great Salt Lake with some cores resulting in published scientific studies. Two of the drill holes (Antelope Island and Sandbar) are in the quadrangle (table A2) and others are located to the north. Bortz and others (1985) and Bortz (2002) reported that Pleistocene, Pliocene, and Miocene deposits were encountered based on palynology data. Other studies on the Amoco cores were by Moutoux (1995), Davis (1998), and Kowalewska and Cohen (1998). Other drill holes were advanced in Skull, Tooele, and Salt Lake Valleys.

Lake Bonneville

Lake Bonneville was the largest late Pleistocene pluvial lake in the Great Basin, and encompassed parts of Utah, Wyoming, Idaho, and Nevada. Studies began with G.K. Gilbert (1890) and have continued, leading to a recent compilation on the science by coauthor C.G. (Jack) Oviatt (see Oviatt and Shroder, 2016); several book chapters include data and features from the map area. Some key Lake Bonneville issues and features from the quadrangle are discussed as follows.

Stansbury Shoreline

The Stansbury shoreline of Lake Bonneville is more of a shoreline zone. The shoreline is not well expressed everywhere, so we typically mapped the shoreline where tufa-cemented gravel, plastered on the bedrock, is easily observed. In places more than one gravel barrier, at multiple elevations within a vertical zone of about 150 feet (45 m), are present within the Stansbury shoreline zone.

Exposures of deposits and geomorphic features related to the Stansbury shoreline are present at Stansbury Gulch on Stansbury Island, as reported on by Currey and others (1983), Green and Currey (1988), and Oviatt and Miller (1997). Results document the transgression of Lake Bonneville during an oscillation in lake level due to climatic effects (see Oviatt and others, 1990).

Provo Shoreline Complex

Burr and Currey (1988) reported on the Provo shoreline complex at Tooele Army Depot in southern Tooele Valley. They reported that the complex consists of several shorelines and discussed the relationship of the enormous ramp of prograding and aggrading beach ridges north of Stockton Bar to the threshold control at Red Rock Pass. Godsey and others (2005) obtained radiocarbon ages and elevation data at this location to further constrain the chronology and morphology of the Provo shoreline complex. Miller (2016) synthesized the current state of the science regarding the Provo shoreline.

Puddle Valley Lake

Sack (1995) described a lake separate from Lake Bonneville in Puddle Valley, called Lake Puddle by Currey (1980). Sack (1995) interpreted that Puddle Valley experienced catastrophic inflow from the main lake, which produced the gravel inflow bar feature at the north end during the regressive phase of Lake Bonneville. In contrast, Oviatt (Oviatt and Miller, 1997) observed that the Bonneville marl overlies the inflow feature and therefore considered it formed before the Stansbury level or is Stansbury in age (having formed during the transgressive phase of Lake Bonneville). Sack (1995) noted the presence of three Puddle Valley shorelines (PVA, PVB, and PVC). Sack's (1995) interpretation was that the PVB and PVC shorelines were formed during the transgressive phase of Lake Bonneville; she interpreted the PVC shoreline as part of the Stansbury shoreline complex. In Sack's (1995) interpretation, the PVB shoreline marks the first shoreline to form in Puddle Valley, and is about 10 feet (3 m) below the Puddle Valley threshold elevation (~4470 feet, ~1362 m). Sack (1995) thought the threshold may have been filled in by that amount by lacustrine and subaerial deposits. We mapped PVC as the Stansbury shoreline zone at an elevation of 4524 feet (1379 m). The PVA shoreline is marked by barriers at an elevation of ~4390 feet (~1338 m), composed of sand and carbonate chips, which we included in unit Qls.

Gilbert Shoreline and Pilot Valley Shoreline

Some prior geologic mapping in the quadrangle included the Gilbert shoreline as part of the Bonneville lake cycle (see Currey, 1982). Oviatt (2014) investigated the Gilbert shoreline issue and pointed out that the Gilbert-episode lake occupied a closed basin with no threshold control; thus the Gilbert-episode lake was probably caused by a shift in water balance and the lake did not maintain a constant elevation for long. Apparently, Currey (1982) connected a series of lacustrine barriers with a line on a map and called the line the "Gilbert shoreline." However, because the separate shoreline segments are not dated, and because a mappable shoreline produced by the Gilbert-episode lake has not been found, we consider the Gilbert shoreline of Currey (1982) to be an incorrect interpretation. Oviatt (2014) suggested that the Gilbert-episode lake did not reach elevations higher than 4250 feet (1295 m), and that most or all of the isostatic rebound in response to the Lake Bonneville water load was complete prior to the Gilbert episode.

Some gravel exposures in the southern Lakeside Mountains, eastern Cedar Mountains, and Antelope Island (near an elevation of 4280 to 4290 feet [1305–1308 m]) could be considered as representative of the Pilot Valley shoreline (see Miller and Phelps, 2016). However, we did not map this shoreline on the Tooele 30' x 60' quadrangle.

Great Salt Lake

The map area contains the southern half of the south arm of GSL, the largest salt water lake in the Western Hemisphere.

Gwynn (1980, 2002) provided compilations of scientific data. The chronology and hydrograph of Holocene Great Salt Lake are not as well understood as Lake Bonneville because of lack of data and other complications (see for example, Oviatt and others, in preparation). Atwood (2006) reported on shoreline superelevation, evidence of coastal processes of Great Salt Lake. Baskin and Allen (2005) provided bathymetry data.

NOTES ON TERTIARY SEDIMENTARY AND VOLCANIC ROCKS

Miocene Rocks

In the map area, extensional basins collected Miocene sedimentary and basaltic volcanic rocks in the Cedar, Stansbury, and Oquirrh Mountains, and south arm of Great Salt Lake (table A2). These rocks are likely present in deeper, unexplored parts of Neogene to Recent basins. We updated the tephrochronology in the eastern Oquirrh Mountains (table A3; UGS and others, 2015). We attempted to obtain new radiometric ages on basaltic rocks in the Stansbury and Cedar Mountains, but the Nevada Isotope Geochronology Laboratory (NIGL) reported they were too altered for reliable results.

Eocene Rocks

Older Tertiary volcanic rocks in the map area are associated with Eocene volcanic centers in the Oquirrh (Bingham mining district) and Stansbury Mountains, and have been encountered in the subsurface (table A2). The Bingham area has been the subject of extensive geologic study over several decades (see below); accordingly, mapping data were compiled there with few revisions. In the Stansbury Mountains, the UGS obtained new radiometric ages (Utah Geological Survey and Nevada Isotope Geochronology Laboratory, 2017) and geochemical data. A summary of radiometric age data is provided in tables A5 and A6. New and unpublished whole-rock geochemical data are presented in table A7; we did not compile the voluminous geochemical data from the Bingham area (references in next section), or older data from the Stansbury Mountains (Hogg, 1972).

Volcanic Rocks of the Northern and Central Oquirrh Mountains

Volcanic rocks in the Bingham mining district were divided into four informal compositional suites by Waite (1996) and Waite and others (1997): (1) younger volcanic suite, (2) older volcanic suite, (3) nepheline minette-shoshonite suite (within the older volcanic suite), and (4) Bingham intrusive suite. Biek and others (2005) and Biek (2006a) informally referred to the younger suite as the "volcanic and intrusive rocks of the west Traverse Mountains," and combined the latter three suites as the "volcanic and intrusive rocks of the Bingham Canyon suite." Clark (this map) also grouped the igneous rocks into younger and older suites, and further separated the suites into extrusive and sedimentary rocks, and intrusive rocks. The terminology of intrusive rocks of the Bingham mining district (after Lanier and others, 1978) is based on historical usage in the district (for the purpose of separating similar rock units); it is entrenched and does not necessarily reflect geochemical composition and newer geochemistry-based rock classifications. Information on Bingham area geology and ore genesis is provided in numerous publications, including Moore (1973), Bray and Wilson (1975), Economic Geology (1978), Black and Babcock (1991), Chesley and Ruiz (1997), John and Ballantyne (1997), Gruen and others (2010), Kloppenburg and others (2010), Landtwing and others (2010), Redmond and Einaudi (2010), Porter and others (2012), and Pankow and others (2014). For geochemical and age data see Moore and others (1968), Moore and Lanphere (1971), Moore (1973), Warnaars and others (1978), Moore and McKee (1983), Waite (1996), Deino and Keith (1997), Waite and others (1997), Pulsifer (2000), Maughan (2001), Maughan and others (2002), Parry and others (2001), Biek and others (2005), Biek (2006b), New Mexico Geochronology Research Laboratory and Utah Geological Survey (2006), von Quadt and others (2011), and Clark and Biek (2017). Key geologic maps are indicated in the mapping sources shown on plate 2.

Younger Volcanic and Intrusive Suite (early Oligocene to late Eocene, ~30–37 Ma): Younger volcanic and intrusive rocks are widely exposed in the western Traverse Mountains just south of the quadrangle. Part of one intrusion extends into the map area (Biek and others, 2005; Clark and others, 2012, 2021).

Older Volcanic and Intrusive Suite (upper to middle Eocene, ~37–41 Ma): Older suite rocks are largely comagmatic with the Bingham intrusive complex (Waite and others, 1997) and contain significantly higher chromium and barium concentrations and more magnetic minerals than the younger suite (Pulsifer, 2000).

In the northern Cedar Mountains, a few exposures of an ultrabasic rock (olivine melanephelinite, unit Tm) were discovered. Rocks of similar composition occur at Bingham, south of the map area (Waite and others, 1997; Clark and others, 2012, 2021).

Older Tertiary sedimentary rocks, mostly conglomerate, occur at Antelope Island and in the Oquirrh, Stansbury and Cedar Mountains. A new Eocene detrital zircon age was obtained from the Oquirrh Mountains (table A6; Utah Geological Survey and O'Sullivan, 2017).

NOTES ON STRATIGRAPHY

The Mesozoic, Paleozoic, and Proterozoic bedrock stratigraphic nomenclature were updated for consistency across the map area. Stratigraphic evaluation was aided by drill hole/well data (table A2) and fossil data (table A8). Tables A9 and A10 list various prior map units and stratigraphic designations to show how the nomenclature has evolved over time. Previous workers applied a complicated mixture of Paleozoic and Proterozoic stratigraphic nomenclature drawn from western, northern, and central Utah in the map area. This nomenclature was used without complete consideration of the many structural features. All nomenclatural issues have not been resolved, but Clark typically applied western Utah nomenclature (like that used by Hintze and Davis, 2003) to rocks of the western thrust system (bounded on the east by the Willard and East Stansbury thrust faults). The western thrust system carries thicker, deeper water, passive-margin facies rocks (table A9). Nomenclature of northern and central Utah was applied to rocks of the eastern thrust system (Antelope Island and Oquirrh Mountains) (table A10). The eastern thrust system carries correlative, thinner, cratonic facies rocks.

Mesozoic Rocks

A section of red beds in the western Cedar Mountains was previously mapped as the North Horn? Formation (Maurer, 1970). Because of the structural position of these strata, in the footwall of the Cedar thrust sheet, the UGS obtained a detrital zircon sample that yielded an Early Cretaceous age (table A6; Utah Geological Survey and O'Sullivan, 2017). Clark (2019) further described these red beds.

A few small outcrops of the Triassic Dinwoody Formation? were mapped in the Cedar Mountains. These rocks were not previously noted.

Paleozoic Rocks

One of the most challenging aspects of this mapping project was the Oquirrh Group and associated rocks. In the Oquirrh Mountains, Tooker and Roberts (1970) divided Permian, Pennsylvanian, and Mississippian rocks into three sequences (from north to south: Rogers Canyon, Curry Peak, and Bingham, each interpreted to belong to a separate thrust sheet), for which Tooker and Roberts (1998) and Tooker (1999) provided different formation nomenclature per thrust nappe. Conversely, Welsh (1976, 1983, 1998) and Welsh and James (1998) argued that there were no major lithologic facies changes between structural blocks of the Oquirrh Mountains, and applied Bingham-area stratigraphic nomenclature to the northern Oquirrh Mountains (Rogers Canyon sequence). Bingham nomenclature was modified by Kennecott geologists to include Lower Permian formations (Swensen, 1975; Swensen and others, 1991; Laes and others, 1997). Clark applied these revised Oquirrh Group and associated formation names from Bingham across a larger area (and across thrust sheets) based on similar lithofacies and age relations throughout this part of Utah (figure 3; tables A9 and A10; see also Constenius and others, 2011; Clark and others, 2012, 2016, 2021). Clark and others (2016) revised the Oquirrh Group stratigraphy in the Cedar Mountains from that of Maurer (1970). Oquirrh Group lithofacies and nomenclature change from the Cedar Mountains to the Grassy Mountains across thrust sheets of the Sevier orogenic belt (figure 3; table A9).

The name Kessler Canyon Formation is not used on this map. The Kessler Canyon Formation was included as the upper part of the Oquirrh Group of the Rogers Canyon sequence of Tooker and Roberts (1970) in the northern Oquirrh Mountains. However, Swensen (1975) and Welsh (1998) noted that east of the Garfield fault (located near Kessler Canyon) this unit is roughly equivalent to several formations (Diamond Creek-Kirkman, Freeman Peak, and Curry Peak?) and therefore omitted it from the Oquirrh Group. Clark herein reassigned strata formerly mapped as the Kessler Canyon Formation south of the Arthur fault (located near Little Valley Wash) to undivided Permian strata (unit Pu), whereas west of the Garfield fault and north of the Arthur fault he reinterpreted most of the Kessler Canyon Formation as the Oquirrh Group, Bingham Mine Formation.

Tooker and Roberts (1970) divided the Bingham Mine Formation into the Markham Peak and Clipper Ridge Members, and later Kennecott maps (Swensen and others, 1991; Laes and others, 1997; KUCC, 2009) also used the names Markham and Clipper Members. However, Clark followed Swensen (1975), who reported the type section of Tooker and Roberts (1970) is faulted (and therefore invalid), and used informal upper and lower members. The informal members were not mapped outside of the Bingham district due to map scale considerations.

The type section for the Mississippian Delle Phosphatic Member (a member of several formations across Utah) occurs in the southern Lakeside Mountains (Sandberg and Gutschick, 1984). Sandberg and Gutschick (1984) and Silberling and Nichols (1992b) conducted stratigraphic studies on the Delle and associated units. For other Mississippian and Upper Devonian rocks, there are different stratigraphic interpretations and nomenclature in the Stansbury Mountains and Island to Lakeside Mountains area by Sandberg and Gutschick (1979), Poole and Sandberg (1991), Nichols and others (1992), and Trexler (1992); maybe further studies can shed light on these issues, as Clark could not quickly resolve them. Trexler (1992) conducted an updated evaluation of the Devonian Stansbury Formation in the northern Stansbury Mountains and Stansbury Island.

For Ordovician rocks, Clark departed from using different nomenclature south and north of the Tooele arch (see Hintze, 1959, 1988). Instead it is postulated that thrust sheets of western Utah carry Ordovician rocks with similar lithologies and therefore should have similar nomenclature. Rock unit

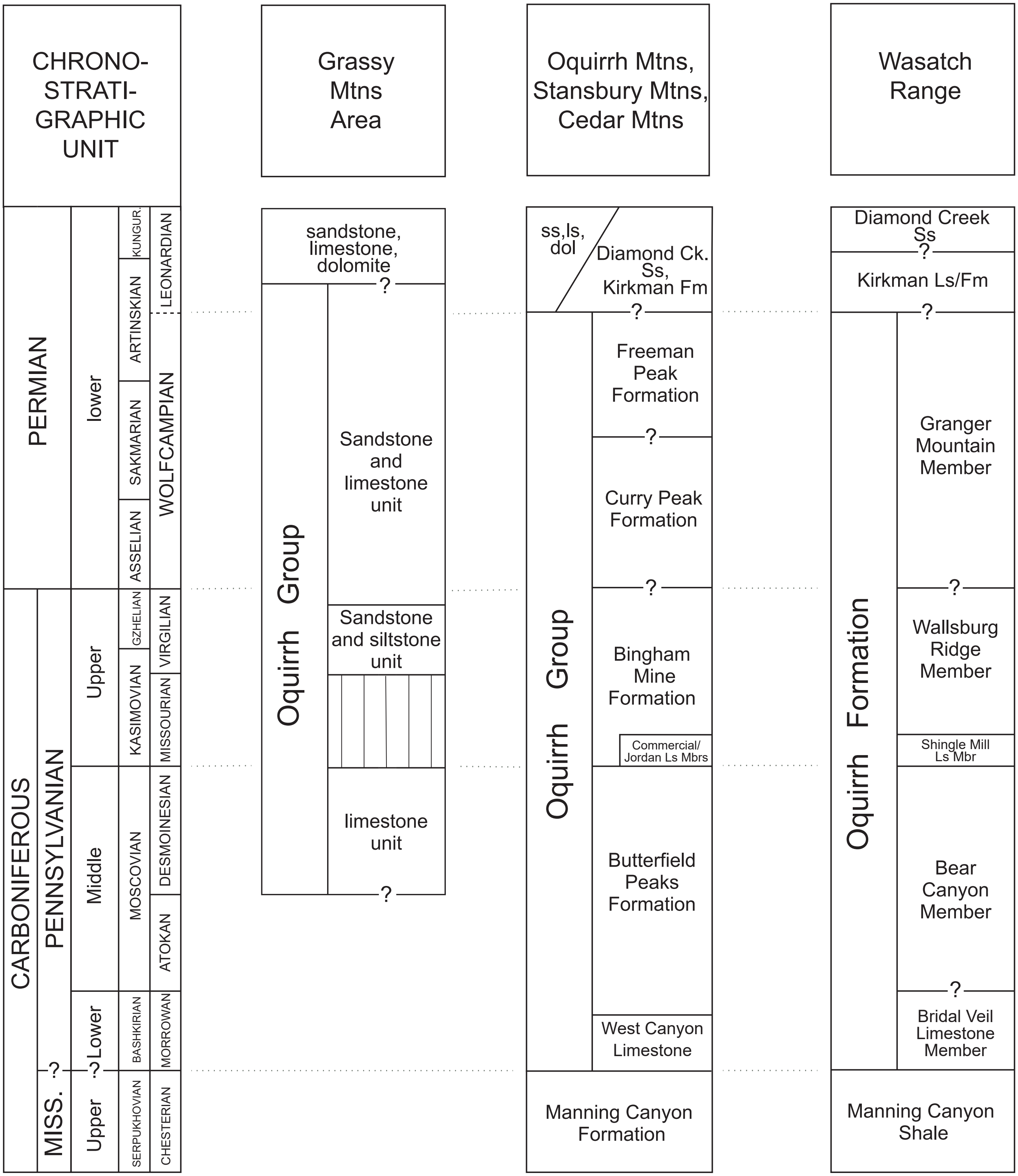

Figure 3. *Comparison of Permian-Pennsylvanian nomenclature of the Oquirrh Group/Formation and other units used on this map and adjacent areas. Grassy Mountains after Clark and others (2020) modified from Doelling (1964) and Jordan (1979a, 1979b). Oquirrh, Stansbury, and Cedar Mountains from this study. See Constenius and others (2011) for the Wasatch Range.*

names from the Willard thrust sheet are not used in western Utah (J.K. King, UGS, verbal communication to D.L. Clark, September 22, 2010).

Cambrian stratigraphic nomenclature for the Stansbury Mountains was revised by Clark and Kirby (2009) from that of Rigby (1958) and Teichert (1959). These strata correspond to the thicker, deeper water, passive-margin facies (western Utah nomenclature), rather than the correlative thinner, eastern, cratonic facies (East Tintic nomenclature). Due to the map scale, some formations were combined, similar to the map units in Millard County (see Hintze and Davis, 2003). This Cambrian nomenclature also appears to be applicable at the southern Lakeside Mountains (see revisions to Young, 1953, 1955; Doelling, 1964). Clark used the western Utah nomenclature on Stansbury Island, but further work is needed (see description for map unit Ꞓum).

Neoproterozoic Rocks

Northern Stansbury Island was previously mapped as the Big Cottonwood series and Formation (Chapusa, 1969; Palmer, 1970). Clark remapped this section of rock (descending) as the Mutual Formation, Inkom Formation, and Caddy Canyon Quartzite, which are faulted against Cambrian rocks. To the north, Carrington Island is composed of the Perry Canyon Formation (Yonkee and others, in preparation).

NOTES ON STRUCTURE

There are several structural features in the quadrangle that warrant further discussion. Due to complex structures and limited exposures, subsurface geology requires substantial interpretation (see table A2; cross sections, plate 3). Further detailed structural analysis is advisable to clarify the structural relations.

Uinta-Tooele Structural Zone

An important structural zone and associated igneous/mineral belt crosses the quadrangle and adjacent areas (see Clark, 2020). This zone has been called the Cortez-Uinta axis (Roberts and others, 1965), Uinta-Gold Hill trend (Erickson, 1974), Uinta arch (Crittenden, 1976), Uinta trend (Moore and McKee, 1983; Tooker, 1999), Uinta axis (Presnell, 1997), and numerous other names (see for example, Rowley, 1998). Lines of evidence presented for its existence include (1) a suture in Precambrian basement (see, for example, Houston, 1993; Yonkee and others, 2014), (2) a zone of Tertiary igneous rocks extending west from Park City, (3) Tertiary (Eocene) uplift in the Bingham area, (4) irregular, local uplifts during the Paleozoic, and (5) geophysical evidence in the Tooele 1° x 2° quadrangle (Erickson, 1974; Moore and McKee, 1983; Tooker, 1999). This structural zone appears to have been intermittently active as a tectonic uplift as the Ordovician Tooele arch (Webb, 1958; Hintze, 1959) and later as the Devonian Stansbury uplift (Rigby, 1959). There is also evidence (bending and rotation) that some of the eastward-directed thrust sheets of the Sevier fold-thrust belt impinged upon the Uinta arch and Uinta zone (Tooker, 1983; 1999; Bradley and Bruhn, 1988; Cashman, 1992; Paulsen and Marshak, 1999; Kwon and Mitra, 2004; Yonkee and Weil, 2011).

Sevier Fold-Thrust Belt

The map area straddles the boundary between the Wyoming and Provo (Charleston-Nebo) salients of the Sevier fold-thrust belt (see for example, Coogan and Constenius, 2003; DeCelles, 2004). Clark prepared an updated Sevier belt tectonic map for northern Utah (plate 4) that reinterprets a map by Tooker (1983), and covers both the Wyoming and Provo salients, previously addressed separately (Kwon and Mitra, 2004; Yonkee and Weil, 2011). Several major faults and folds (both named and unnamed) are indicated on the geologic map and plate 4; some of these are inferred.

The Willard thrust fault is thought to extend between Stansbury Island and Antelope Island based on lithofacies relations, but the extent and depth of the Willard thrust sheet to the south and west is uncertain. The western edge of the Willard sheet may extend northwestward toward Gunnison Island (plate 4). The Wasatch anticlinorium lies between Antelope Island and the Wasatch Range (Eardley, 1939; DeCelles, 2004; Yonkee and Weil, 2011). The Willard and East Stansbury thrust faults demark the line between the western and eastern thrust systems (Yonkee and others, 2014); however, linkage is uncertain as their hanging-wall and footwall relations are considerably different across the Transverse fault zone. The structure at the north end of the Oquirrh Mountains may represent a lateral ramp.

More recent structural interpretations in the map area include those by Cashman, Foose, and Clark. Cashman's (1992) study on the northern Stansbury Mountains showed the structure is dominated by Mesozoic folding and thrusting overprinted on a cryptic Devonian deformation event. Foose (1989) reported the unconformity associated with the Stansbury uplift appears to be faulted and sheared, which could represent Sevier reactivation. Clark (this study) observed small-scale, west-vergent folds in the hanging wall of the Redlam Spring fault, consistent with backthrusting.

Thrust timing in northern Utah is from about 145 to 50 Ma (Kwon and Mitra, 2004; Yonkee and Weil, 2011; Eleogram, 2014; Geunthner and others, 2015). In the map area, the age of synorogenic Cretaceous strata (117 Ma) in the footwall of the Cedar thrust may indicate timing of thrust emplacement (Utah Geological Survey and O'Sullivan, 2017; this study). In addition, some out-of-sequence thrusting is probable, considering the presence of backthrusts, and possibly the timing of the Cedar thrust.

Manning Canyon Décollement

In outcrop, the Manning Canyon Formation generally appears to be a highly deformed unit. This unit has acted as a décollement associated with both compressional and extensional deformation. In the northern Stansbury and southern Lakeside Mountains, the rocks above the Manning Canyon appear to be more tightly folded than the rocks below.

Chaos Zone

In the northern Oquirrh Mountains, a highly deformed interval is associated with Diamond Creek and Kirkman rocks and called "the chaos" (Welsh and James, 1961; Swensen, 1975; Schurer, 1979a, 1979b; Gunter, 1991; Gunter and Austin, 1997). This zone is reportedly related to both soft-sediment and tectonic deformation. Tectonic deformation involved compression associated with the North Oquirrh thrust and other faults impinging on the Uinta-Tooele structural zone and subsequent relaxation.

Oquirrh Basin

The thick package of rocks in the map area of Mississippian, Pennsylvanian, and Permian age was deposited in the Oquirrh basin (Chamberlin and Clark, 1973; Welsh and Bissell, 1979; Jordan and Douglass, 1980). The basin was northwest trending, presumably fault bounded, and probably subdivided by the Uinta-Tooele zone or another structural feature considering the differing lithofacies sequences to the north and south (Roberts and others, 1965; Jordan and Douglass, 1980; Erskine, 1997). Oquirrh basin rocks were translated eastward during Sevier thrusting; the southeast edge of the basin now coincides with the Charleston-Nebo thrust (Kwon and Mitra, 2004; Erskine, 1997).

Fault Zones and Faults

Transverse Fault Zone

Evidence indicates that a major transverse fault zone exists near the southern margin of Great Salt Lake in the map area (plate 1, plate 4). Prior workers suggested or indicated this feature, including Young (1953), Mabey and others (1963), Cashman (1992), Doelling and others (1994), and Lawton and others (1994). The location of the transverse fault zone is not well constrained, but Clark shows it as a queried fault zone between the Oquirrh Mountains and Antelope Island based on bedrock drill hole and gravity data (plate 3, cross section C-C'). The zone likely extends to the west between Stansbury Island and the Stansbury Mountains. It may merge with the Lakeside fault, Wrathall fault, or head northward up Lakeside Valley toward Strongs Knob. The transverse zone may also extend through the northern part of Stansbury Island or south of Carrington Island. Another option is that the fault zone may extend westward between the Cedar Mountains and Skunk Ridge, crosses Grassy Ridge (a more difficult connection), and could possibly connect to an east-west gravity lineament near the southern Grayback Hills and northern part of the Knolls (Clark and others, 2020). To the east, the structural zone presumably extends across Salt Lake Valley and links to the Mt. Raymond thrust duplex on the north side of the Uinta arch. Because the zone appears to separate major Neogene-Recent basins, it may have helped accommodate extension in the Cenozoic.

Low-angle Normal Faults

A few low-angle normal faults (exhibiting younger-over-older relations) in the quadrangle may be related to collapse of the Sevier belt or subsequent extension. In the Oquirrh Mountains, the fault that cuts through the Melco mine area and the Roll fault in Bingham mine could be examples of such faults.

Unknown Faults

Several faults on the map may have had two or more episodes of slip of differing geometry to account for large displacements. It is uncertain if some steeply dipping faults are related to Sevier-age structure, later basin and range extension, or both. Named examples of faults in this category include the Garfield and Arthur faults (northern Oquirrh Mountains) and Grassy Pass fault and German Valley fault (Grassy Mountains) (see Clark and others, 2020). Some substantial and inferred unknown faults are in and near Stansbury Island.

Oblique-slip and Strike-slip Faults

The Wrathall fault and Lakeside fault are mapped as oblique-slip faults. Slickenlines indicate the Lakeside fault had oblique-slip movement, but it may link with the transverse fault zone and could have had a more complicated history. There is no evidence that the Lakeside fault cuts Quaternary deposits. Some faults in Stansbury Island appear to be oblique-slip and strike-slip faults based on map relations.

High-angle Normal Faults

Several high-angle normal faults bound and cut the ranges of the map area. Displacements are small to large (up to several hundreds or thousands of feet and meters). These faults generally trend north-south, northwest-southeast, and northeast-southwest. Most are not named, but named faults include Elephant Head, Stringham Peak, and Mormon Rocks faults (Antelope Island), Harkers fault and Occidental fault (northern Oquirrh Mountains), Timpie Ridge fault (northern Stansbury Mountains), Hastings Canyon fault and Straight Canyon fault (northern Cedar Mountains), and Hidden Mine fault (southern Lakeside Mountains). The Harkers fault was previously shown on the UGS Quaternary fault database, but we see no evidence that it cuts Quaternary deposits (including pre-Lake Bonneville alluvial fans).

We used geologic and geomorphic evidence, gravity and seismic data, available subsurface data, and fault scarp mapping to map normal faults at the margins of the major valleys. Sources of gravity data include Arnow and Mattick (1968), Zoback (1983), Cook and others (1989), Radkin and others (1989), Smith and others (2011), and Pan-American Center for Earth and Environmental Studies (2012) and updated complete Bouguer gravity anomaly data for parts of the map area (western ¼ and Saltair graben areas) (UGS, unpublished data). Linear, steep gravity gradients can represent faults or fault zones (Zoback, 1983; Saltus and Blakely, 2011). Concealed basin-bounding normal faults were mapped using this method, although there are limitations, and fault existence and location would benefit from additional interpretive tools. Smaller valleys may be fault bounded, but have no substantial gravity signature. Because of considerable uncertainty of subsurface structure, these faults are queried or not mapped. Sources of seismic data include Lambert and West (1988), Radkin and others (1989), and McNeil and Smith (1992). Bortz and others (1985) and Bortz (2002) presented an interpreted seismic section across the basin under Great Salt Lake and west of Antelope Island. The section showed a faulted basin containing about 10,000 feet (3000 m) of Quaternary and Tertiary deposits and rocks underlain by pre-Tertiary and Precambrian rocks. Substantial basins (gravity lows) are located in Skull Valley, Lakeside Valley, northern Tooele Valley, south arm of Great Salt Lake, southeastern Antelope Island, and parts of western Salt Lake Valley. Some major thrust faults (East Stansbury, Broad Canyon, and Ogden, for example) may have had later normal movement, considering their proximity to these Neogene-Recent basins.

Quaternary Normal Faults

Several high-angle normal faults and fault zones in the map area exhibit fault scarps that cut Quaternary deposits, including the West Valley fault zone, Great Salt Lake-Oquirrh fault zone, Carrington fault, Stansbury fault zone, Puddle Valley fault zone, and a newly mapped fault of the west Cedar Mountains. These mapped faults have known seismic risk (see Working Group on Utah Earthquake Probabilities, Wong and others, 2016). Other normal faults with Quaternary movement, though lacking fault scarps, are inferred to exist based on topography and geophysical studies. These faults also pose seismic risk yet to be quantified.

Normal faults with scarps: Part of the West Valley fault zone is within the map area. The fault zone was mapped by Personius and Scott (1992) and has undergone paleoseismic evaluations (Keaton and others, 1987; Keaton and Currey, 1989; Hylland and others, 2014).

Coauthor Dinter contributed prior mapping of part of the Great Salt Lake fault zone and Carrington fault (see Colman and others, 2002; Dinter and Pechmann, 2014; Dinter and Pechmann, 2015). This mapping was conducted over several years using seismic reflection methods by boat. Boat tracklines were made to collect seismic reflection profiles. Dinter compared the data to the bathymetry data of Baskin and Allen (2005), which we also include on our map. Three sets of faults are indicated by age. The youngest faults cut the lakebed, the other two sets are concealed and are younger or older than a prominent reflector (H_0). Janecke and Evans (2017) also recently conducted mapping of the Great Salt Lake fault and other faults to the north. Their mapping used Google Earth imagery through lake water for the Great Salt Lake fault area and addressed only the main fault scarp cutting the lakebed. Their mapping is in general agreement with Dinter's mapping, but has some differences in detail. Dinter has reservations about this mapping method in a subaqueous environment considering the lake bottom topography could be altered by processes not related to faulting. Future mapping will involve evaluation of Great Salt Lake fault data.

The north Oquirrh fault zone was mapped by Barnhard and Dodge (1988) and Solomon (1993, 1996) with slight modifications by Clark (this study), and a paleoseismic study was conducted by Olig and others (1996). Bunds (Utah Valley University, 2017, 2018, Utah Quaternary Fault Parameters Working Group Meetings, unpublished data) recently conducted some additional work.

The Stansbury fault zone was mapped by Barnhard and Dodge (1988), Sack (1993), and Helm (1994, 1995) with slight modifications by Clark (this study). Swan and others (2005) conducted a paleoseismic investigation of the Stansbury and Skull Valley (mid-valley) faults. The northern part of the Stansbury fault zone near Burnt Spring and Muskrat Canyon consists of several west-facing scarps that are enigmatic as to origin (tectonic versus lacustrine) (Oviatt and several others, verbal communications, May 10, 2017). The features were previously reported to be fault scarps (Barnhard, 1988; Sack, 1993; Helm, 1994), and scarp profile data were provided by Barnhard and Dodge (1988) and Helm (1994, 1995). UGS measured several scarp profiles using survey-grade GPS equipment on June 8, 2017, to gather additional data. Unfortunately, there remains no consensus on the origin of these features.

In northern Skull Valley, the Springline fault (Rigby, 1958) and additional northwest-trending splay (Skull Valley mid-valley faults in the UGS Quaternary fault database) are shown as queried due to inconclusive evidence. No scarps were noted and there is no substantial gravity signature. The alignment of springs could be related to permeability differences in the surficial deposits. Faults along the northeast flank of the Cedar Mountains are not evident, and one lineament is shown there.

The Puddle Valley fault zone was mapped by Barnhard and Dodge (1988) and shown on the USGS Quaternary fault map. Clark slightly modified the fault mapping using more recent imagery.

A new Quaternary fault was mapped on the west side of the Cedar Mountains (sections 16 and 21, T. 2 S., R. 10 W.). The fault cuts pre-Bonneville alluvial-fan deposits mantled by eolian sand. A lineament was noted on trend about 2 miles (3 km) north that may be related. The fault is shown as approximately located because it is somewhat obscured due to the eolian cover.

Normal faults lacking scarps: We used gravity and other geophysical data to map several normal faults with probable Quaternary movement but no obvious scarps. These faults are located west of the Cedar Mountains, Skull Valley, Lakeside Valley, Tooele Valley, southern Great Salt Lake, and Salt Lake Valley.

Of particular note are normal faults in northwest Salt Lake Valley. On March 18, 2020, a M_w 5.7 earthquake occurred in northwest Salt Lake Valley, with an epicenter 3.7 miles (6 km) north-northeast of Magna and a focal depth of 7.4 miles (11.9 km) (Pang and others, 2020). Numerous aftershocks occurred in the subsequent days and weeks. A prior M_L 5.2 earthquake occurred in this area in 1962 (Kleber and others, 2020; Pang and others, 2020). Pang and others (2020) and Kleber and others (2020) worked to obtain more information about the seismologic and geologic features that contributed to the 2020 earthquake. Kleber and others (2020) reevaluated the mapping of faults in the area using recently collected complete Bouguer gravity anomaly data. Wong and others (1995) identified a structure in this area that they called the Saltair structure and which, using the updated gravity data, Kleber and others (2020) interpreted to be a graben. Our geologic map (plate 1) reflects the revised fault configuration. The northwest-trending Saltair graben is thought be bounded by the reactivated Ogden thrust fault (northeast side) and a northwest-trending fault (southwest side of graben) that may be linked to the Harkers fault to the south; the structure is probably bisected by the inferred east-west-trending transverse fault zone. The Saltair graben may be bounded below by the relatively shallowly west-dipping Wasatch fault zone. The source of the 2020 Magna earthquake is interpreted to be from slip on the Wasatch fault zone in the area of the Saltair graben (Kleber and others, 2020; Pang and others, 2020).

Aeromagnetic Data

Available aeromagnetic data from Stein and others (1989), Raines and others (1996), and Langenheim (2016) show magnetic lows across the quadrangle except for areas near Bingham, Antelope Island, and Stansbury Island. The Last Chance stock at Bingham has a magnetic anomaly (Stein and others, 1989). Magnetic highs associated with the Antelope Island area correspond to Farmington Canyon Complex basement rocks, whereas the Stansbury Island anomaly indicates a concealed source within the crystalline basement (Stein and others, 1989; Langenheim, 2016).

NOTES ON RESOURCES AND WASTE MANAGEMENT

Resources

Water

Water is an important resource in this arid, rapidly developing area. Some of the key studies on water resources and hydrogeology in this part of the Great Basin include those in Skull Valley (Hood and Waddell, 1968), Tooele Valley (Lowe and Wallace, 1999; Lowe and others, 2004; Kenney and others, 2006; Brooks, 2006; Stolp and Brooks, 2009), and Salt Lake Valley (Lambert, 1995; Thiros, 1995). Blackett and Wakefield (2004) summarized geothermal resources in Utah. Thermal springs and wells (> 20°C, > 68°F) are present around the perimeter of the northern Stansbury Mountains, in Skull and Tooele Valleys, and in the Cedar and Oquirrh Mountains.

Minerals

Known and potential mineral resources are described by Stein and others (1989) and Tripp and others (1989). Industrial minerals are key resources in the map area. These minerals include salt (sodium chloride and magnesium chloride), limestone, dolomite, aragonite, travertine, silica, and sand and gravel; refer to a summary by Tripp and others (1989) and the Utah Division of Oil, Gas and Mining mineral mines database. Metallic minerals exist in several districts including Bingham (Oquirrh Mountains), Free Coinage and Third Term (Stansbury Mountains), and Lakeside. The largest and most notable is the Bingham district located 22 miles (35 km) southwest of Salt Lake City.

Bingham district: Bingham (West Mountain) is the oldest (1863) and largest mining district in Utah and hosts a giant porphyry Cu-Au-Mo deposit. The Bingham Canyon (Utah Copper) open pit mine is the largest producing mine in the U.S. and the district is the largest Cu, Mo, Au, Ag, Pb, and Zn producing district in Utah.

The Bingham district lies on the Bingham-Park City mineral belt and is centered on a giant, high-K, calc-alkaline, porphyry copper deposit. This deposit is associated with a small, composite monzonite stock dated at about 38 Ma that intrudes a thick, intercalated sequence of Pennsylvanian-Permian marine quartz sandstones and limestones. A 400- to 1000-foot-wide (120–300 m) quartz monzonite porphyry dike and a swarm of narrower, east-northeast-trending dikes cut the north flank of the early monzonite stock. The hypogene porphyry mineralization is concentrically zoned around the quartz monzonite porphyry dike from a deep, inner, low-sulfide core through progressively overlapping hypogene molybdenite, bornite-chalcocite, chalcopyrite, and pyrite zones. The inverted cup-shaped

Cu shell is largely coincident with potassic alteration and garnet Cu-Au skarns. The surrounding pyrite halo is spatially associated with propylitically-altered rocks. Each of three major phases of porphyry intrusions was followed by cycles of fracturing, alteration, veining, and metal introduction. This cyclic vein formation resulted in complex vein relationships partly constrained by isotopic ages and cross-cutting relationships. The quartz monzonite porphyry dike and younger dikes are spatially coincident with the highest grades of copper and gold in the ore body (Porter and others, 2012). The exposed quartz monzonite porphyry stock is too small to have provided the fluids and metals for the district, signifying a connection to a larger magma chamber at depth.

The outermost fringe of the pyrite halo is overprinted by the inner margin of a 3000-foot-wide (910 m), intermediate-sulfidation, sphalerite-galena ± tetrahedrite manto-vein zone where alteration is largely confined to the immediate vein walls. The outer perimeter of the Pb-Zn veins locally contains rhodochrosite and/or barite. The Barneys Canyon and Melco distal disseminated gold deposits lie 4 miles (6 km) north-northeast of the center of the district and outside Bingham's megascopically recognizable sulfide and alteration system, but on the outer fringe of a weak arsenic-gold geochemical halo (Babcock and others, 1995).

Other Resources

There is some potential for hydrocarbon resources. The Rozel heavy oil reservoir is located under the north arm of Great Salt Lake, and two wells (Antelope Island and Sandbar) from the Amoco exploration program in the map area (south arm) revealed shows of oil and gas (Bortz and others, 1985; Bortz, 2002).

Exceptional outdoor recreational resources exist on the varied topography and geology of the quadrangle on state and federal lands. These include Antelope Island and Great Salt Lake State Parks, Great Salt Lake, and U.S. Forest Service, Wilderness, Bureau of Land Management, and county lands. Interpretive scientific information is available at the state parks and the northern Stansbury Island County Park.

Waste Management

Several areas are used to manage waste materials in the map area. Western Salt Lake Valley has several solid and municipal waste sites. Kennecott/Rio Tinto maintains a large mine tailings impoundment at the north end of the Oquirrh Mountains, and waste rock dumps surround and cover parts of the Bingham mine. A Class V landfill is located on the east side of the Lakeside Mountains. A hazardous waste incinerator is located west of the Cedar Mountains at Aragonite.

GEOLOGIC UNIT DESCRIPTIONS

QUATERNARY-TERTIARY SURFICIAL DEPOSITS

Q **Quaternary surficial deposits, undivided** – Cross section only.

QT **Quaternary-Tertiary surficial deposits and rocks, undivided** – Cross section only.

Alluvial deposits

Qa **Alluvium, undivided** (Holocene) – Primarily clay, silt, and sand deposited in a broad, flat area in northern Tooele Valley; sediment reflects local sources; locally merges with alluvial-fan deposits and playa mud, and locally includes lacustrine and eolian deposits; thickness generally less than about 20 feet (6 m).

Qal **Stream alluvium** (Holocene) – Primarily clay, silt, and sand with some gravel lenses deposited by streams in channels and broad drainages, but in mountain valleys deposits are coarser grained and associated with more colluvium; locally merges with alluvial-fan deposits; locally includes alluvial-fan, colluvial, low-level terrace, lacustrine, and eolian deposits; thickness generally less than about 20 feet (6 m).

Qam **Alluvial mud** (Holocene to upper Pleistocene?) – Silt, clay, some sand, and minor gravel deposited by streams and sheetwash in depressions that were lagoons behind gravel barriers deposited during the Bonneville lake cycle (some low-elevation lagoon depressions may be related to Great Salt Lake rather than Lake Bonneville); some lagoon basins include unexposed, thin, fine-grained deposits beneath the alluvial mud, laid down while the lagoon was active and the barriers were forming; thickness less than about 20 feet (6 m).

Qafy **Younger fan alluvium, post-Lake Bonneville** (Holocene to uppermost Pleistocene) – Poorly sorted gravel, sand, silt, and clay; deposited by streams, debris flows, and flash floods on alluvial fans and in mountain valleys; merges with unit Qal; includes alluvium and colluvium in canyon and mountain valleys; may include areas of eolian deposits and lacustrine fine-grained deposits below the Bonneville shoreline; includes active and inactive fans younger than Lake Bonneville, but may also include some older deposits above the Bonneville shoreline; in Puddle Valley and west of Cedar Mountains commonly includes eolian silt and sand cover typically less than 6 feet (2 m) thick; locally, unit Qafy spreads out on lake terraces and, due to limitations of map scale, is shown to abut Lake Bonneville shorelines even though it is not cut by these shorelines; Qafy also locally drapes over, but does not completely conceal shorelines; thickness variable, up to 50 feet (15 m) or more.

Qafo, Qafo?

Older fan alluvium, pre-Lake Bonneville (upper? to middle? Pleistocene) – Poorly sorted gravel, sand, silt, and clay; similar to unit Qafy, but forms higher level incised deposits that predate Lake Bonneville; includes fan surfaces of different levels; fans are incised by younger alluvial deposits and locally etched by Lake Bonneville; may locally include small areas of lacustrine or eolian deposits and younger alluvium; thickness variable, up to 100 feet (30 m) or more.

QTaf, QTaf?

Oldest fan alluvium (lower Pleistocene? to Pliocene?) – Poorly sorted gravel, sand, silt, and clay; unconsolidated to semi-consolidated with calcic soil development on upper surfaces; forms high-level deposits incised by younger alluvial deposits and locally etched by Lake Bonneville; may overlap in age with unit Tslc; may locally include small areas of lacustrine or younger alluvial deposits; only a few deposits mapped at northern Cedar and Stansbury Mountains; thickness variable, as much as 100 feet (30 m) or more.

Spring deposits

Qsm **Spring and marsh deposits** (Holocene) – Clay, silt, and sand that is variably organic-rich, calcareous, or saline; present in ephemerally or perennially saturated (marshy) areas near springs and seeps; form extensive areas mapped near Great Salt Lake and in Skull Valley; SWCA Environmental Consultants (2004) presented more detailed mapping of wetlands in Tooele Valley; thickness 0 to 30 feet (0–10 m).

Eolian deposits

Qes, Qes?

Eolian sand (Holocene) – Windblown sand and silt deposited as dunes and sheets; generally thin with no distinct bedding; mostly silty, well-sorted, fine-grained quartz sand; only thicker deposits mapped; also mapped in stacked units; less than 15 feet (5 m) thick.

Qeo **Eolian oolitic sand** (Holocene) – Windblown sand composed of oolites formed in Great Salt Lake; forms sparsely vegetated, active dunes on shores of Stansbury Island and northern Antelope Island; less than 10 feet (3 m) thick.

Qei **Eolian silt** (Holocene) – Windblown silt with minor clay and fine sand that is commonly oolitic; occurs as low-relief dunes that cap fine-grained lacustrine and alluvial deposits in lower Tooele Valley; thickness as much as 10 feet (3 m).

Lacustrine and deltaic deposits (Great Salt Lake)

Qly **Younger lacustrine deposits** (Holocene to upper Pleistocene?) – Silt, clay, and minor sand from higher levels of Great Salt Lake; form islands at paleo Jordan River delta and mudflats northeast of Magna; gradational upslope with fine-grained regressive Lake Bonneville deposits and downslope with units Qlmy and Qldy; near Magna unit Qly is incised by post-Lake Bonneville alluvium; locally covered with a loess veneer; thickness generally less than 15 feet (5 m).

Qdy **Younger deltaic deposits** (Holocene) – Silt, sand, and clay present in a lobate, paleo-Jordan River delta complex of the Baileys Lake and Browns Island area, lower Salt Lake Valley (McKean and Hylland, 2019); locally includes distributary channel fill and deltaic fan deposits and a loess veneer; deposits overlie units Qlmy and Qldy; exposed thickness less than 10 feet (3 m).

Qlk **Younger lacustrine carbonate-chip sand and gravel** (Holocene) – Lacustrine sand and gravel composed of calcium-carbonate clasts, including ooids, pellets, and rounded, irregularly shaped flakes and chips, with some pebbles of local rocks; formed on the floor of Great Salt Lake when adjacent mudflats (unit Qlpm) were submerged, or were precipitated from pore waters in mud and later reworked by waves; locally present in barrier bars and islands fringing Great Salt Lake and some beaches of Antelope Island; locally grades into units Qla and Qlpm; exposed thickness as much as 6 feet (2 m).

Qlmy **Younger lacustrine mud** (Holocene to upper Pleistocene?) – Mud composed of silt, clay, and minor sand; locally with thin salt deposits and some organic material; forms mudflats in lower Salt Lake Valley from the margin of Great Salt Lake extending upslope where it laterally interfingers with units Qly and Qldy; thickness probably less than 10 feet (3 m).

Qldy **Younger lacustrine and deltaic deposits** (Holocene to upper Pleistocene?) – Clay, silt, sand, and minor pebble gravel deposited by the ancestral Jordan River where it entered Great Salt Lake; locally includes a loess mantle; form a broad, gently sloping surface with some channel remnants; exposed thickness less than 10 feet (3 m).

Lacustrine deposits (Great Salt Lake and Lake Bonneville)

Qlb **Lacustrine boulders** (Holocene to upper Pleistocene) – Shorezone boulders of Lake Bonneville and locally of Great Salt Lake; boulders are in areas where finer-grained sediments were winnowed out by waves, leaving large boulders on bedrock knobs and headlands; form boulder fields and strandlines on hillsides of Antelope Island (after Doelling and others, 1990); not differentiated by age or elevation; thickness is probably as much as 10 feet (3 m).

Qlg, Qlg?

Lacustrine gravel (Holocene to upper Pleistocene) – Sandy gravel to boulders composed of locally derived rock fragments deposited in shore zones of Great Salt Lake and Lake Bonneville; clasts are typically well rounded and sorted; locally tufa-cemented (especially the Provo shoreline, figure 2) and draped on bedrock; not differentiated by lake or elevation; in Puddle Valley and west of Cedar Mountains commonly includes eolian silt and sand cover commonly less than 6 feet (2 m) thick; thickness variable, to 100 feet (30 m) or more.

Qlf, Qlf?

Lacustrine fine-grained deposits (Holocene to upper Pleistocene) – Sand, silt, marl, and calcareous clay of Great Salt Lake and Lake Bonneville; thin to very thick bedded; may include ostracode- and gastropod-rich layers; locally includes the white marl of Gilbert (1890); locally may include small areas of sand and gravel; can include thin eolian sand deposits at surface; in Puddle Valley and west of Cedar Mountains commonly includes eolian silt and sand cover commonly less than 6 feet (2 m) thick; near the margin of Great Salt Lake locally includes thin Qlk deposits at surface; thickness 10 to 100 feet (3–30 m) or more.

Lacustrine and deltaic deposits (Lake Bonneville)

Qls, Qls?

Lacustrine sand (upper Pleistocene) – Sand and silt deposited by transgressive and regressive phases of Lake Bonneville; generally thick bedded and well sorted; typically grades downslope to finer-grained lacustrine deposits; in Puddle Valley includes a barrier below the Stansbury level shoreline composed of sand and carbonate chips associated with the "Puddle Valley A shoreline" of Sack (1995); thickness up to 100 feet (30 m) or more.

Qlt **Lacustrine tufa** (upper Pleistocene) – Light-gray tufa (calcium carbonate precipitated at the shoreline of Lake Bonneville) with laminated and vuggy appearance; locally caps small hills in six small exposures located just below the Provo shoreline near Redlam Spring, east side of northern Cedar Mountains; other small unmapped deposits in northern Oquirrh Mountains; thickness as much as 10 feet (3 m).

Glacial deposits

Qgt **Glacial till** (upper to middle? Pleistocene) – Poorly sorted, angular, boulder to pebble gravel, sand, and mud in eroded moraines within and just below cirque basins in northern Stansbury and Oquirrh Mountains; locally includes glacial outwash and some small areas of younger alluvium and colluvium; deposits are undated, but till is likely associated with the younger Pinedale/Angel Lake glaciation, ~14 to 24 ka, and possibly the older Bull Lake/Lamoille glaciation (associated with Marine Oxygen Isotope Stage 6), ~ 130 to 190 ka (Lisiecki and Raymo, 2005; Laabs and Monroe, 2016; Pierce and others, 2018; Quirk and others, 2018, 2020); older till may be present downslope of the younger till, but more detailed mapping of the glacial deposits is needed; Osborn and Bevis (2001) reported on glacial deposits in the Stansbury and Oquirrh Mountains, and Valora (1968) reported on The Jumpoff (geographic feature of glacial origin) in the Oquirrh Mountains; probably as much as 50 feet (15 m) thick.

Mass-movement deposits

Qmct **Colluvium and talus** (Holocene to upper Pleistocene) – Local accumulations of mixed colluvium and talus throughout the map area; common near Lake Bonneville shorelines; thickness up to 15 feet (5 m).

Qms, Qms?

Landslide deposits (Holocene to middle? Pleistocene) – Poorly sorted, clay- to boulder-size debris, and large, displaced bedrock blocks; generally characterized by hummocky topography, main and internal scarps, and chaotic bedding in displaced bedrock; relatively few landslides in quadrangle; includes a few displaced bedrock blocks along the north end of the Oquirrh Mountains (Tooker and Roberts, 1971a; Solomon, 1993); we did not map the massive April 10, 2013, landslide at the Kennecott/Rio Tinto Bingham Canyon mine (see Pankow and others, 2014), which was subsequently altered to allow access to the mine operations; unit undivided as to inferred age because research shows that even landslides with subdued morphology (suggesting they are older and have not moved recently) may continue to creep or are capable of renewed movement (Ashland, 2003); age and stability determinations require detailed geotechnical investigations; thickness highly variable.

Mixed-environment deposits

Qlpm **Great Salt Lake and Playa mud** (Holocene) – Clay, silt, oolitic sand, and pelletal sand composing the bed of Great Salt Lake and some slightly higher adjacent areas, and much of the floor of northern Skull Valley; as mapped includes typical playa mud, which is subaerial in origin, and is washed in and/or derived from in-place weathering of the underlying deposits (probably less than 1 foot [0.3 m] in most places); also includes Great Salt Lake mud, which in many cases is difficult to distinguish from subaerial mud, and we did not attempt to separate them on the map; locally reworked by alluvial, eolian and lacustrine processes; locally mud is organic rich and contains carbonate chips; salts accumulate on playa surfaces as these deposits are locally and intermittently exposed depending on lake level; gradational with units Qal, Qlf, Qlk; the extent of Great Salt Lake is indicated on the map by the historical average elevation of 4200 feet (1280 m) (Baskin and Allen, 2005; U.S. Geological Survey, 2016); the historical highstand of Great Salt Lake (south arm) was 4212 feet (1284 m) in 1873, 1986, and 1987 (Mabey, 1986; U.S. Geological Survey, 2016); Atwood (2006) reported on shoreline superelevation in 1986–1987 that locally exceeded 4212 feet (1284 m) due to prevailing wind fetch; the historic lowstand (south arm) was 4191 feet (1278 m) in 1963 (U.S. Geological Survey, 2016); Great Salt Lake rose and fell frequently during post-Bonneville time (that is, during the past 13,000 years), but the precise ages and elevations of high stands and low stands has not been determined except for the high stand during the Gilbert episode at 11,600 yr B.P. (4250 feet or 1295 m) (Oviatt and others, in press); all highstands younger than the Gilbert episode have been lower than the Gilbert-episode lake; the sediments of Great Salt Lake are muddy, and the thickness is highly variable but generally less than 15 feet (5 m); unit Qlpm overlies Lake Bonneville deposits and pre-Bonneville deposits as recorded in several sediment cores within deeper parts of the Great Salt Lake basin (table A1); unit Qlpm ranges in thickness from about 1 inch (3 cm) to 50 feet (15 m) or more in fault zones on the floor of the lake (Spencer and others, 1984; Thompson and Oviatt, unpublished; Schnurrenberger and Haskell, 2001; Colman and others, 2002; McKean and others, 2019; Clark, unpublished data; Dinter, unpublished data).

Qla, Qla?

Lacustrine and alluvial deposits, undivided (Holocene to upper Pleistocene) – Sand, gravel, silt, and clay; consists of alluvial deposits reworked by lakes, lacustrine deposits reworked by streams and slopewash, and alluvial and lacustrine deposits that cannot be readily differentiated at map scale; grade into other lacustrine and alluvial deposits; west of Cedar Mountains includes more sand than typical gravelly exposures elsewhere, probably due to source material; in Puddle Valley and west of Cedar Mountains commonly includes eolian silt and sand cover commonly less than 6 feet (2 m) thick; thickness locally exceeds 30 feet (10 m).

Qac **Alluvial and colluvial deposits, undivided** (Holocene to upper Pleistocene) – Mixed alluvium and colluvium locally in upland valleys and along bases of slopes; clay- to boulder-size materials; locally grades into other deposits; thickness generally less than 20 feet (6 m).

QTlm **Lacustrine, mudflat and eolian deposits, undivided** (pre-Lake Bonneville) (Pleistocene to Pliocene) – Subsurface only. Basin-fill deposits consisting of light-gray to white marl with lacustrine ostracodes (lacustrine facies); mud, sandy mud, and fine sand; locally includes non-lacustrine ostracodes and gastropods, poorly sorted sandy mud, soil carbonate, and rootlet casts, and some massive sandy muds may be eolian ("marsh/mudflat facies" of Oviatt and others, 1999); relatively well-sorted beds of sand and/or gravel (fluvial or shorezone lacustrine facies) (Oviatt and others, 1999); deposits were encountered in several sediment cores (table A1) and drill holes (table A2); Williams (1994) reported ash beds in the Burmester core dated as about 0.11 to 3.29 Ma (table A4); unit QTlm underlies Lake Bonneville deposits and overlies the Salt Lake Formation; incomplete thickness is 1000 feet (300 m) in the Burmester and other "Eardley" cores (Saltair, S28 cores), and complete thickness roughly 4500 feet (1370 m) in the Amoco Antelope Island drill hole (Bortz and others, 1985; Bortz, 2002).

Human-derived deposits

Qh **Human disturbance** (historical) – Deposits and disturbed areas from human development; includes some Kennecott/Rio Tinto and other mining operations, gravel pits and quarries, waste management facilities, wastewater and storm water ponds, the Grantsville reservoir, motor sports area, and thicker fill for I-80 and its overpasses; also mapped in several stacked units; laterally extensive mine dumps, mine tailings, and evaporation ponds are mapped separately (see below); additional unmapped disturbed areas and smaller fill deposits are common throughout the map area; thickness generally less than about 20 feet (6 m).

Qhm **Mine dumps** (historical) – Unconsolidated mine waste rock at the Kennecott/Rio Tinto Bingham Canyon, Melco, and Barneys Canyon mines; dumps were mapped from 2011 orthophotos; nearly all of these mine dump areas are depicted on the map as patterned polygons (see geologic symbols) to show the underlying geology; mine dumps are principally coarse rock fragments with lesser sand- and silt-size particles; mine dump thickness is highly variable, but locally exceeds 200 feet (60 m).

Qht **Tailings impoundment** (historical) – Mine tailings disposal area of Kennecott/Rio Tinto located at the north end of the Oquirrh Mountains; above-ground diked area contains unconsolidated, fine-grained mine tailings that were slurried and pumped to this location; also includes some small areas of human disturbance; maximum thickness planned to be as much as 247 feet (75 m); maximum permitted elevation of the active north tailings pile is 4462 feet (1360 m), and the average elevation of the inactive south pile is 4430 feet (1350 m), with an original ground surface elevation in this area of ~4215 feet (~1285 m) (Leslie Heppler, Utah Division of Oil, Gas and Mining, verbal communication, June 21, 2016).

Qhe **Evaporation ponds** (historical) – Laterally extensive salt evaporation ponds (both active and inactive) operated by various companies near the southern margin of Great Salt Lake; lake water is pumped to a series of diked areas containing brine of varying concentrations that evaporates to form salt deposits; thickness is typically less than 6 feet (<2 m).

Stacked-unit deposits

Consist of thin surficial deposits covering underlying surficial deposit and bedrock geologic units. The stacked units are mapped judiciously here due to map-scale considerations, with a cover thickness typically exceeding 6 to 10 feet (2–3 m).

Qh/unit (Qh/Tsl, Qh/Tnf?, Qh/Tw?)

Human disturbance over unit (historical over Tertiary) – Disturbed areas and deposits from human development overlying various bedrock map units at the large gravel pit on the southeast side of Antelope Island; thickness of upper disturbed cover is highly variable.

Qei/Qlgf?

Eolian silt over lacustrine gravel to fine grained deposits? (Holocene over upper Pleistocene?) – Eolian silt forming a mantle on possible Lake Bonneville lacustrine gravel to fines; lacustrine feature may be related to Puddle Valley shoreline A of Sack (1995); cover unit thickness unknown, but possibly as much as 6 feet (2 m).

Qes/unit (Qes/Qafy, Qes/Qla, Qes/Qlg, Qes/Qls, Qes/Qlf, Qes/Qafo, Qes/Ks)

Eolian sand over unit (Holocene over Holocene, Pleistocene, Cretaceous) – Eolian sand forming a mantle on other surficial deposits and rock units, particularly along the flanks of the northern Cedar Mountains and southern Lakeside Mountains; cover unit thickness is highly variable, but possibly as much as 40 feet (12 m).

Qlf/Posc?

Lacustrine fine-grained deposits over Oquirrh Group, sandstone and limestone unit (Cedar thrust sheet?) (upper Pleistocene over Lower Permian) – Sand, silt, marl, and clay locally with tufa over bedrock unit in Puddle Valley; thickness of Qlf as much as 10 feet (3 m).

QTaf/Tslc

Oldest fan alluvium over Salt Lake Formation, conglomerate lithosome (lower Pleistocene? to Pliocene? over Pliocene? to Miocene) – Quartzite-clast gravel overlying conglomerate unit along east flank of northern Stansbury Mountains; difficult to differentiate units readily at this map scale; thickness of QTaf increases eastward and is from 0 to about 350 feet (105 m).

TERTIARY (NEOGENE-PALEOGENE) ROCK UNITS

T **Tertiary rocks, undivided** – Cross section only.

Tv **Tertiary volcanic rocks, undivided** – Cross section only.

Tsl, Tsl?

Salt Lake Formation, undivided (Pliocene? to Miocene) – Tuffaceous sandstone, conglomerate, volcanic ash, conglomeratic limestone, and possibly poorly consolidated sandstone that locally crops out on eastern Antelope Island in small exposures and as unit Qh/Tsl in a large sand and gravel pit (Doelling and others, 1990; Willis and Jensen, 2000), and in Hastings Canyon area, northern Cedar Mountains (Maurer, 1970, part of his "Tertiary unnamed unit"; this study); gray tuffaceous sandstone is very fine grained, moderately indurated, laminated to medium bedded, and locally cross-bedded; pale-gray conglomerate is crudely stratified, has clasts of quartzite and limestone cobbles that are subangular to subrounded, and a calcareous and sandy matrix; very light gray volcanic ash consisting of glass shards is present within poorly exposed fine-grained sediments; tephrochronology analyses from the east side of Antelope Island indicate ages from ~ 8 to 11 Ma (Willis and Jensen, 2000), and a fission-track age of 6.1 Ma (Bryant and others, 1989) appears too young (Willis and Jensen, 2000); no direct age dating from Hastings Canyon, but apparently interbedded with unit Tb; regionally Tsl age could extend into the Pliocene (Oaks and others, 1999); unit Tsl unconformably overlies older rock units; incomplete thickness is about 1800 feet (550 m) at Antelope Island (Doelling and others, 1990), and as much as 2200 feet (670 m) at Hastings Pass and Redlam Spring area in northern Cedar Mountains.

Salt Lake Formation, mapped as conglomerate lithosome in northern Stansbury Mountains.

Tslc **Salt Lake Formation, conglomerate lithosome** (Pliocene? to Miocene) – Conglomerate, tuffaceous sandstone and gritstone, minor limestone and volcanic ash; clast composition includes volcanic, quartzite, and carbonate rock types; mapped on east and west flanks of northern Stansbury Mountains; east flank exposures are mapped as unit QTaf/Tslc since overlying quartzite-clast fan gravels cannot be readily separated at map scale; tephrochronology age from South Willow Canyon is about 11 Ma (Cougar Point Tuff XIII) (Perkins and others, 1998; Clark and others, 2012, 2021); underlying basalt from Muskrat Canyon area is 12.1 Ma (K-Ar age) (Moore and McKee, 1983); may overlap in age with unit QTaf; regionally Tsl age could extend into the Pliocene (Oaks and others, 1999); Rigby (1958) reported on conglomerate composition in South Willow Canyon, but did not map the formation; Slentz (1955) measured sections in South Willow and Davenport Canyons; exposed (incomplete) thickness estimate as much as 3500 feet (1065 m).

Salt Lake Formation, divided into two lithosomes in western Salt Lake Valley.

Tslf **Salt Lake Formation, fine-grained lithosome** (Pliocene? to upper Miocene) – White to light-gray tuffaceous marlstone and micrite, lesser claystone, sandstone, unwelded rhyolitic tuff (volcanic ash), and minor limestone; appears to interfinger laterally with unit Tslg; typically poorly exposed with local exposures in cuts and pits near the Harkers Canyon-Clay Hollow area; previously called part of the Jordan Narrows unit (see Slentz, 1955; Biek and others, 2007; Solomon and others, 2007); new tephrochronology data indicate deposits contain Blacktail Creek ash (6.62 Ma), Walcott ash (6.4 Ma), and Wolverine Creek ash (5.6 Ma?) (UGS and others, 2015)(table A4), but there are no direct radiometric ages; yielded anomalously young fission-track age of 4.4 ± 1.0 Ma for a rhyolitic tuff from the reclaimed Pioneer pit (Bryant and others, 1989); regionally Tsl age could extend into the Pliocene (Oaks and others, 1999); exposed (incomplete) unit thickness is about 300 to 500 feet (90–150 m) (Biek and others, 2007; Solomon and others, 2007).

Tslg **Salt Lake Formation, gravel lithosome** (Pliocene? to upper Miocene) – Poorly sorted, unconsolidated gravel with sand, silt, and clay that locally contains unwelded rhyolitic tuff (volcanic ash); the unconsolidated gravel is not typical for the Salt Lake Formation; clasts are locally sourced from sedimentary and volcanic rocks; appears to interfinger laterally with unit Tslf; occurs as piedmont gravel that is deeply dissected and capped by an erosional surface along western Salt Lake Valley; upper part may be locally capped by thin Quaternary deposits based on tephrochronology data (M. Perkins, formerly Univ. of Utah, unpublished data, emails to Biek [2004] and Clark [2013]), and observations of Biek and others (2007) and Solomon and others (2007); previously called part of the Harkers fanglomerate (Slentz, 1955), and previously mapped as unit QTaf (oldest alluvial-fan deposits) (Biek and others, 2007; Solomon and others, 2007); two prior tephrochronology samples by Biek and others (2007) were reported to be the Walcott ash (6.4 Ma) (table A4); new tephrochronology data indicate the deposits contain Blacktail Creek ash (6.62 Ma) (UGS and others, 2015); (table A4); Bryant and others (1989) reported a fission-track age of 4.4 ± 1.0 Ma for a rhyolitic tuff from the reclaimed Pioneer pit in the Magna quadrangle (see Solomon and others, 2007); regionally Tsl age could extend into the Pliocene (Oaks and others, 1999); exposed (incomplete) thickness as much as 350 feet (100 m) (Biek and others, 2007; Solomon and others, 2007).

Tcu, Tcu?

Tertiary conglomerate, undivided (Oligocene? to Paleocene?) – Conglomeratic strata on eastern Antelope Island where relationship to units Tnf and

Tw? is unclear; pale-gray conglomerate with primarily carbonate and quartzite clasts that are very poorly sorted and range from pebble to boulder size (see unit 3, measured section S4, Willis and Jensen, 2000); exposed northwest of large gravel pit; Doelling and others (1990) previously mapped as part of lower member of unnamed conglomeratic unit; unconformably overlies the Farmington Canyon Complex and underlies the Salt Lake Formation; no age data; complete thickness about 190 feet (60 m) (Doelling and others, 1990).

Tnf? **Norwood Formation and Fowkes Formation, undivided?** (Oligocene? to Eocene) – Gray conglomerate with volcanic, metamorphic, carbonate, quartzite, and chert clasts (pebbles to boulders) with sandy, gritty matrix and calcite cement, and interbedded purple and gray bentonitic mudstone; mapped solely as stacked unit Qh/Tnf?, and overlies unit Qh/Tw? and Tw? and underlies Qh/Tsl at large gravel pit of eastern Antelope Island; yielded K-Ar ages of 42.9 Ma (claystone/bentonite), and 38.8 and 49.2 Ma on recycled volcanic clasts (Doelling and others, 1990), and regionally the unit could extend into the Oligocene (Coogan and King, 2016); uncertain correlation to Wasatch Range rocks; thickness is about 300 feet (90 m) (measured sections S1, S2, Willis and Jensen, 2000).

Tw? **Wasatch Formation?** (Eocene? to Paleocene?) – Grayish-red to dark-reddish-brown conglomerate and sedimentary breccia; contains angular clasts of local metamorphic rocks (pebbles to boulders) in a gritty, densely cemented matrix; present within (unit Qh/Tw?) and adjacent to large gravel pit at Antelope Island; unconformably overlies the Farmington Canyon Complex; queried since no direct age control, but lacks volcanic clasts; thickness is about 135 feet (40 m) (see lower parts of measured sections S1, S2, Willis and Jensen, 2000).

Tso, Tso?

Older Tertiary strata, undivided (Eocene to Paleocene?) – ***Northern Oquirrh Mountains*** have three exposures of silica-cemented conglomerate with subangular to subrounded pebbles to boulders of quartzite, sandstone, some black chert, and rare limestone; U-Pb detrital zircon maximum depositional age of 40 Ma from Harkers Canyon (Utah Geological Survey and O'Sullivan, 2017); unconformably overlies Permian and Pennsylvanian rock units; thickness about 30 to 500 feet (10–150 m) (Tooker and Roberts, 1971a; Biek and others, 2007; Solomon and others, 2007); ***northern Stansbury Mountains*** outcrops near Davenport Canyon consist of pale-reddish-orange conglomerate with primarily subrounded limestone and dolomite clasts and lesser sandstone and quartzite clasts; clasts typically less than 4 inches (10 cm) in a gritty, calcareous matrix; poorly bedded and exposed; previously called North Horn? Formation (Rigby, 1958); no direct age data, but underlies volcanic rocks (unit Tvs, 39–41 Ma); thickness as much as 400 feet (120 m) (Rigby, 1958); ***northern Cedar Mountains*** outcrops in easternmost Hastings Canyon consist of light-brown to light-gray sandstone and conglomerate, and one freshwater limestone bed; conglomerate clasts are sedimentary, likely from Permian and upper Oquirrh Group formations, and average 2 inches (5 cm) in diameter; bedding is poor, medium to thick, forming mostly slopes; previously called part of the "Tertiary unnamed unit" (Maurer, 1970); contains fossil gastropods *Physa* cf. *P. bridgerensis*, *Viviparus trochiformis*, and *Sphaerium* sp. of probable Eocene or late Paleocene age (LaRocque, in Maurer, 1970); unconformably overlies older rock units and overlain by unit Tb; incomplete thickness is 300 feet (90 m) (Maurer, 1970).

Volcanic Rocks of the Northern Cedar Mountains and Northern Stansbury Mountains

Tb **Trachybasalt and basalt** (Miocene?) – Dark-gray, locally vesicular, aphanitic, potassic trachybasaltic and basaltic lava flows; forms ledges and cliffs in northern Cedar Mountains (Hastings Canyon), northern Stansbury Mountains (Muskrat Canyon), and Salt Mountain area; geochemical data are available in Hogg (1972) and we obtained new data (Clark and Biek, 2017); prior K-Ar ages (whole rock) of 12.1 ± 0.3 Ma (northern Stansbury Mountains) and 13.8 ± 0.4 Ma (northern Cedar Mountains) (Moore and McKee, 1983), but Nevada Isotope Geochronology Laboratory (NIGL) reports that the groundmass on a sample from the northern Stansbury Mountains was too altered for a reliable $^{40}Ar/^{39}Ar$ age; thickness from 0 to 115 feet (0–35 m) (Davis, 1959; Maurer, 1970).

Tsh **Shoshonite** (Miocene?) – Moderate-gray, aphanitic, shoshonitic lava flows; forms cliffs, ledges, and slopes in Mack Canyon-Miners Canyon area of Stansbury Mountains; geochemical data are available in Hogg (1972) and we obtained new data (Clark and Biek, 2017); previously called basalt (Rigby, 1958; Davis, 1959); prior K-Ar age of 12.7 ± 0.2 Ma (Moore and McKee, 1983), but NIGL reports that the groundmass on a sample we submitted is too altered for a reliable $^{40}Ar/^{39}Ar$ age; thickness from 0 to about 125 feet (0–40 m) (Rigby, 1958).

Tm **Olivine melanephelinite** (Eocene?) – Dark-gray, porphyritic, melanephelinite lava flow(s); melanephelinite is a dark-colored rock with basaltic (low silica) character; contains olivine and lesser clinopyroxene and phlogopite phenocrysts in a fine-grained groundmass (clinopyroxene, olivine?, apatite, opaque oxides, nepheline or plagioclase) (Eric Christiansen, Brigham Young University, email to D.L. Clark, February 1, 2017); present in three small hills in northern Cedar Mountains near Interstate 80; geochemical data are similar to melanephelinite/minette at the Bingham district (Maughan and others, 2002; Eric Christiansen, BYU, email to D.L. Clark, December 6, 2016; Clark and Biek, 2017); no direct age data, but similar rocks at Bingham are about 38 Ma (Deino and Keith, 1997); exposed thickness less than about 30 feet (10 m).

Tvs, Tvsl

Rhyolitic to andesitic volcanic rocks of Stansbury Mountains (Eocene) – Interlayered volcanic and volcaniclastic rocks in eastern Stansbury Mountains and Salt Mountain area; includes gray to red to brown lava flows, ash-flow tuffs, lahars, debris avalanches, and tuffaceous sandstone; lahars and debris avalanches contain clasts of intermediate volcanic rocks; previously called latite volcanic series (Rigby, 1958) and andesites and associated rocks (Davis, 1959); in Davenport Canyon within unit Tvs is a pod of lacustrine limestone (unit Tvsl), up to about 200 feet (60 m) thick, that was previously mapped as Great Blue Limestone (Rigby, 1958); units Tvs and Tvsl form slopes, ledges, and cliffs; new geochemical data show compositional range from rhyolite to dacite, trachydacite, and andesite (Clark and Biek, 2017); prior K-Ar ages of 39.4 ± 0.5, 40.6 ± 1.7, and 41.8 ± 0.5 Ma (Moore and McKee, 1983), and new $^{40}Ar/^{39}Ar$ plateau ages on biotite of 39.68 ± 0.50 and 41.30 ± 0.60 Ma (Utah Geological Survey and Nevada Isotope Geochronology Laboratory, 2017); thickness of unit Tvs is 740 feet (225 m) (Salt Mountain) and 1630 feet (500 m) (eastern Stansbury Mountains) (Rigby, 1958; Davis, 1959).

Tirs **Rhyolite and trachydacite porphyry intrusions of Stansbury Mountains** (Eocene) – Light-gray to light-greenish-gray porphyritic rhyolite and trachydacite plugs, dikes, and sills; phenocrysts include plagioclase, hornblende, and biotite; present along axis of Deseret anticline and near North Willow and Mack Canyons; we obtained new geochemical data (Clark and Biek, 2017); mapped as monzonite porphyry (Rigby, 1958) and andesite and trachyandesite porphyry (Davis, 1959); Rigby's small monzonite? plug was not located; K-Ar ages of 39.0 ± 0.6 and 40.3 ± 0.5 Ma (Moore and McKee, 1983).

Volcanic Rocks of the Northern and Central Oquirrh Mountains

Tbx **Breccia pipes and bodies** (lower Oligocene? to upper Eocene?) – Unit includes the Kilkinny breccia, located on west side of the Bear Gulch porphyry, and Dalton breccia at Bingham Canyon mine (Smith, 1975; Swensen and others, 1991; KUCC, 2009); Kilkinny breccia is composed of intrusive and sedimentary fragments and is locally cut by latite porphyry dikes; Bear Gulch breccia has an intrusive matrix with small quartzite fragments; Dalton breccia appears as a hole filled with coarse crushed sedimentary fragments with no matrix (Smith, 1975); uncertain age of pipes and bodies, but likely post-mineralization (post ~37 Ma) (K.A. Krahulec, UGS, verbal communication to D.L. Clark, June 10, 2014); highly variable in diameter and depth.

Tvu **Volcanic rocks, undivided** (upper? to middle Eocene) – Combined unit of various volcanic rocks located under the mine dumps on east side of Bingham mine, where prior mapping does not match existing schemes of KUCC (2009) or Biek and others (2007); map unit also includes small intrusion northwest of Copperton (unit Tiu of Biek and others, 2007) and volcanic boulder lag (latite) overlying unit Tso near Harkers Canyon; geochemical data in Clark and Biek (2017); probably associated with older volcanic and intrusive suite rocks at Bingham (see below).

Younger Volcanic and Intrusive Suite (early Oligocene to late Eocene, ~30–37 Ma)

<u>Younger intrusive rocks</u>

Tir **Rhyolitic intrusion** (late Eocene) – Shaggy Peak plug or dome is light- to medium-gray porphyritic rhyolite that contains a border phase with abundant plagioclase, quartz, and biotite phenocrysts and generally near-vertical flow foliations, and an interior phase with slightly larger phenocrysts and little or no flow foliation (Biek, 2006a, 2006b); present at the southern map boundary in the Butterfield-Rose Canyon area; $^{40}Ar/^{39}Ar$ age of 35.49 ± 0.13 Ma (Biek and others, 2005); other rhyolitic intrusions are present south of the map area in Tickville Gulch, Dry Mountain-Ophir, and Eagle Hill-Mercur (Laes and others, 1997; Clark and others, 2012, 2021).

Older Volcanic and Intrusive Suite (upper to middle Eocene, ~37–41 Ma)

<u>Older extrusive and sedimentary rocks</u>

Tvfou **Older intermediate lava flows** (middle Eocene) – Dark-gray lava flows of intermediate composition derived from the Bingham intrusive complex; may locally include small areas of lahars and debris avalanches; interlayered with and difficult to differentiate from the older lahars and debris avalanches (unit Tvlo); present along the east flank of the Oquirrh Mountains; geochemical data in Clark and Biek (2017); $^{40}Ar/^{39}Ar$ age of 38.17 ± 0.09 Ma from recycled volcanic clast (Deino and Keith, 1997), and interlayered with Eocene lacustrine strata near Butterfield Canyon, south of map area (Biek and others, 2005); exposed thickness likely exceeds 1000 feet (300 m) (Biek and others, 2007).

Tvlo, Tvlo?

Older lahars and debris avalanches (middle Eocene) – Pebbles to boulders of intermediate-composition volcanic rocks in a matrix of lithic and crystal fragments; locally contain mostly mafic clasts and thin discontinuous lava flows of intermediate composition (Pulsifer, 2000; Maughan, 2001; Biek and others, 2005); generally form rubbly slopes along east flank of Oquirrh Mountains; Bingham area $^{40}Ar/^{39}Ar$ ages of 38.68 ± 0.13 Ma from waterlain tuff near top of unit (Maughan, 2001) and 39.18 ± 0.11 Ma from a volcanic clast near base of unit (Deino and Keith, 1997); also interlayered with Eocene lacustrine strata near Butterfield Canyon, south of map area (Biek and others, 2005); thickness may exceed 4000 feet (1200 m) (Biek and others, 2007).

Older intrusive rocks

Tipqm

Porphyritic quartz monzonite intrusions (late to middle Eocene) – Intrusions at the former Lark townsite and the Ohio Copper dike in Bingham mine; ***Lark intrusion*** (plug) is light- to medium-gray dacite porphyry with abundant phenocrysts of plagioclase and biotite and lesser hornblende in a fine-grained groundmass; typically weathers to grussy or clayey soils; present near mouth of Butterfield Canyon near former Lark townsite (Laes and others, 1997; Biek and others, 2005; Biek and others, 2007); geochemical data in Clark and Biek (2017); K-Ar ages from Bingham tunnel portal of 36.9 ± 0.9 Ma (hornblende) and 36.9 ± 1.0 Ma (biotite) (Moore and others, 1968); ***Ohio Copper dike*** (east of Bingham stock) is medium-gray to greenish-gray, porphyritic amphibole-biotite quartz monzonite with orthoclase and plagioclase phenocrysts in a phaneritic groundmass; a distinct late phase of Bingham and Last Chance (quartz) monzonite (KUCC, 2009); no direct age data, but probably between 37 and 38.5 Ma (K.A. Krahulec, UGS, verbal communication, July 2015); other similar intrusions are mapped in the Porphyry Hill/Knob area north of Mercur, Oquirrh Mountains (Laes and others, 1997).

Tiqmp **Quartz monzonite porphyry intrusion** (middle Eocene) – Forms west part of the Bingham stock at Bingham mine; light-gray, amphibole-biotite quartz monzonite porphyry; amphibole is altered to phlogopite and quartz, and plagioclase is altered to sericite and clay; there are no exposures of unaltered rock; inferred source of Bingham mineralizing fluids (KUCC, 2009); southwest part of unit Tiqmp is referred to as hybrid quartz monzonite porphyry by Kennecott (KUCC, 2009); U-Pb zircon age of 37.94 ± 0.08 Ma (von Quadt and others, 2011).

Tim **Monzonite intrusions** (middle Eocene) – Comprise Bingham and Last Chance stocks and associated intrusions at Bingham mine; medium- to dark-gray, augite-actinolite-phlogopite (quartz) monzonite; where altered, augite is replaced by actinolite, chlorite, phlogopite, and quartz, and some plagioclase is replaced by orthoclase; contains pyrite, chalcopyrite, bornite, and molybdenite mineralization; original magnetite is replaced by sulfide minerals; main Bingham ore host (KUCC, 2009); Last Chance stock has a U-Pb zircon age of 38.55 ± 0.19 Ma and $^{40}Ar/^{39}Ar$ age of 38.40 ± 0.16 Ma (Parry and others, 2001); similar monzonite intrusions occur south of the map area in the Spring Gulch and Calumet mine area (near Stockton), Soldier Canyon, and near axis of Long Ridge anticline (Lufkin, 1965; Laes and others, 1997; Krahulec, 2005).

Tilp **Latite to dacite porphyry sills and dikes** (middle Eocene) – Light- to dark-gray, latite to dacite porphyry (hornblende-augite-biotite quartz latite porphyry) with abundant phenocrysts of plagioclase and hornblende and lesser biotite; at Bingham mine includes the Fortuna sill, Main Hill, and Starless dikes, Bear Gulch porphyry, and apophyses (Laes and others, 1997; Biek and others, 2005; KUCC, 2009); geochemical data in Clark and Biek (2017); $^{40}Ar/^{39}Ar$ age of 38.84 ± 0.19 Ma (Deino and Keith, 1997), and U-Pb zircon age of 37.94 ± 0.13 Ma (von Quadt and others, 2011).

Tiqlp **Quartz latite porphyry dikes and sills** (late to middle Eocene) – Medium-brown and light-greenish-gray, hornblende-biotite quartz latite porphyry; hornblende is altered to phlogopite and/or chlorite within the Bingham pit area; distinguished from other latitic dikes and sills by the presence of relatively large quartz phenocrysts and higher percentage of aphanitic groundmass; groundmass usually contains considerable hornblende (KUCC, 2009); includes Raddatz porphyry dikes with large K-feldspar phenocrysts (Settlement Canyon area) (see Krahulec, 2005; new geochemical data in Clark and Biek, 2017), and the Andy Dike and apophyses at Bingham mine (KUCC, 2009); $^{40}Ar/^{39}Ar$ ages of 37.66 ± 0.08 and 37.72 ± 0.09 Ma (Deino and Keith, 1997), and U-Pb zircon age of 37.97 ± 0.11 Ma (von Quadt and others, 2011); also forms some small dikes (unmapped) east of Pass Canyon and near North Oquirrh thrust (Swensen and others, 1991) with K-Ar age of 36.5 ± 1.1 Ma (Moore, 1973); Raddatz dike has $^{40}Ar/^{39}Ar$ age of 39.4 ± 0.34 Ma (Kennecott in Krahulec, 2005).

CRETACEOUS TO NEOPROTEROZOIC ROCK UNITS

CRETACEOUS

Ks, Ks?

Cretaceous strata (Lower Cretaceous, Aptian) – Predominantly moderate-reddish-orange mudstone with lesser red and gray conglomerate, sandstone, and siltstone; becomes more coarse grained in northern outcrops; conglomerate clasts include sandstone, limestone, and chert (likely derived from Permian formations) as much as 18 inches (46 cm) in diameter; bedding is laminated to very thick; crops out as slopes and few ledges in western foothills between Hastings Canyon and Quincy Spring, northern Cedar Mountains; present in footwall of the Cedar thrust fault near Quincy Spring and unconformably overlies Triassic and Permian strata; gastropod fossils include *Gyraulus* sp. (LaRoque in Maurer, 1970); U-Pb detrital zircon maximum depositional age of 117 Ma (Utah Geological Survey and O'Sullivan, 2017); two palynology samples were barren; unit may be coeval with the Gannett Group in northern Utah; thickness from 0 to 1100+ feet (0–335+ m) (Maurer, 1970; this study).

TRIASSIC

Mz **Mesozoic rocks, undivided** – Cross section only. Could include Triassic rock units exposed in the Martin Fork syncline south of the map area (see Clark and others, 2012, 2021).

Ŧd? **Dinwoody Formation?** (Lower Triassic) – Moderate-brown limestone and lesser light-brown shale; laminated to thinly bedded forming slopes and ledges; mapped in two small outcrops located 2 miles (3 km) west-southwest of Hastings Pass, northern Cedar Mountains; no age data obtained to confirm assignment, regional age after Hintze and Kowallis (2009); Triassic exposures in the Grayback Hills area to the northwest are Thaynes Formation (Clark and others, 2020); disconformably overlies unit Pgp; incomplete thickness is about 100 feet (30 m) or less.

PALEOZOIC

Pz **Paleozoic rocks, undivided** – Cross sections only.

Pgp, Pgp?

Gerster Formation and Plympton Formation, undivided (middle to lower Permian, Guadalupian to Leonardian) – Light-brown and light-gray limestone, cherty limestone, and dolomite; locally common chert nodules (gray, tan, pink) (Maurer, 1970); Wardlaw and others (1979a, 1979b) reported dolomite, chert, mudstone and sparse limestone in the Cedar Mountains, but provided no details on measured section or fossil locations; unit is locally fossiliferous with macrofossils of brachiopods, pelecypods, and gastropods (Maurer, 1970; Wardlaw and others, 1979b); bedding is medium and thin, forming ledges and steep, rough slopes; crops out near the crest of the northern Cedar Mountains and south of Hastings Pass; Maurer (1970) considered the unit all Gerster Formation, whereas Wardlaw and others (1979a, 1979b) indicated the top part (~100 feet, 30 m) is Gerster Limestone and underlying part is the Plympton Formation; the Gerster contains *Kuvelousia* brachiopods there (Wardlaw and others, 1979b); Wardlaw and Collinson (1986) provided conodont fossil data from the Plympton in the Cedar Mountains that included *Hindeodus excavatus*, *Merrillina galeata*, *Neogondollella serrata*, *N. phosphoriensis*, and *N. bitteri*; Clark and others (2020) obtained *Neostreptognathodus sulcoplicatus* from the lower Plympton near Clive, Utah; the age of the Gerster and Plympton Formations is Guadalupian and Leonardian (Wordian, Roadian and Kungurian, global chronostratigraphy) (see Hintze and Kowallis, 2009; Wardlaw, 2015) [note that the Permian chronostratigraphic scale has changed over time]; the Gerster is considered correlative to the upper Rex Chert Member of the Phosphoria Formation (north) and the Franson Member of the Park City Formation (east), whereas the Plympton is considered correlative to the Murdock Mountain Formation (northwest), Rex Chert (north and east), and Meade Peak Member of the Phosphoria Formation (east) (Wardlaw and others, 1979b; Wardlaw, 2015; UGS unpublished data); the contact with underlying unit Ppm can be difficult to locate since the lower part of unit Pgp is cherty; complete thickness of unit Pgp is about 1000 feet (300 m) (this study), whereas Maurer (1970) and Wardlaw and others (1979a, 1979b) reported incomplete thicknesses of 511 to 840 feet (156–255 m), respectively.

Ppp, Ppp?

Park City Formation and Phosphoria Formation, undivided (middle to lower Permian, Guadalupian to

Leonardian) – Combined unit that contains the Franson and Grandeur Members of the Park City Formation separated by the Meade Peak Member of the Phosphoria Formation, following Solomon and others (2007), in the northeastern Oquirrh Mountains (Little Valley area southward to near Barneys Canyon); incomplete upper part (Franson) contains gray dolomite and tan quartzite (261+ feet [80+ m] thick); middle part (Meade Peak) includes platy, shaley dolomite, quartzite, sandstone, shale, chert, and phosphorite (284 feet [87 m] thick); lower part (Grandeur) consists of gray to light-brown limestone that is bioclastic, sandy, and cherty (215 feet [65 m] thick) (Tooker and Roberts, 1970; Solomon and others, 2007); overall, unit is thin to thick bedded and forms ledges and slopes; limestone from the Meade Peak yielded conodont fossil *Neostreptognathodus sulcoplicatus* of late Leonardian (Kungurian) age (table A8); several fossils from the lowermost limestone (Grandeur) indicate a Leonardian to possible Wordian? age (Gordan and Duncan in Tooker and Roberts, 1970), and this limestone also yielded conodont fossil *Neostreptognathodus* sp. of Leonardian age (table A8); the combined unit age is Guadalupian and Leonardian (Wordian, Roadian and Leonardian, global chronostratigraphy) (see Hintze and Kowallis, 2009; Wardlaw, 2015); may be conformable or disconformable with underlying unit Pu (see Tooker and Roberts, 1970); unit top eroded, but incomplete thickness of 760 feet (230 m) was measured by Tooker and Roberts (1970) at Coon Canyon, and Kennecott cross section at Barneys Canyon (Gunter, 1991, plate 4) indicates incomplete thickness of about 350 feet (110 m).

Ppm **Phosphoria Formation, Meade Peak Member** (middle to lower Permian, Leonardian) – Black and gray shaley phosphatic rock with interbedded chert and dolomite; contains oolitic phosphatic layers, and layers rich in brachiopods, vertebrate teeth, and skeletal fragments; bedding is laminated to medium, forms covered slopes at northern Cedar Mountains; contains fossil *Helicoprion* sp. (shark-like fish) and lingulid brachiopod molds (Maurer, 1970); Wardlaw and Collinson (1986) recovered conodont fossil *Neogondollella idahoensis* from the unit in the Cedar Mountains; regional age is Guadalupian and Leonardian (Roadian and Kungurian, global chronostratigraphy) (see Hintze and Kowallis, 2009; Wardlaw, 2015); the Meade Peak in part correlates to the Plympton to the west (Wardlaw, 2015); the unit is also known as the Meade Peak Phosphatic Shale Member and Meade Peak Tongue (U.S. Geological Survey geologic lexicon, 2020); measured thickness is 80 to 141 feet (25–43 m) (Maurer, 1970; Wardlaw and others, 1979a, 1979b), but Maurer's mapping suggests it may locally exceed those numbers.

Ppg **Park City Formation, Grandeur Member** (lower Permian, Leonardian) – Moderate-gray and light-brownish-gray limestone, dolomitic limestone, and dolomite that is finely crystalline and bioclastic; light-brown and gray chert is locally abundant and minor amounts occur throughout the member; can form two cliffs separated by a thin slope-forming unit of dolomite and chert (Maurer, 1970); Wardlaw and others (1979a, 1979b) report dolomite, cherty dolomite, siltstone and chert; bedding is typically medium to thick; crops out south of Hastings Pass, northern Cedar Mountains; Stokes (in Maurer, 1970) noted several brachiopod fossils had a faunal similarity to the Grandeur correlative Kaibab Limestone; Wardlaw and others (1979b) reported fossil brachiopods *Quadrochonetes*, *Echinauris*, and *Peniculauris* and Wardlaw and Collinson (1986) reported several conodont fossil types including *Hindeodus excavatus*, *Sweetina festiva*, *Neogondollella idahoensis*, *Neostreptognathodus pnevi*, *Ne. ruzhencevi*, *Ne. clinei*, *Ne. tschuvashovi*, *Ne. prayi*, *Ne.* sp. B, and *Ne. sulcoplicatus*; regional age is Leonardian (Kungurian, global chronostratigraphy) (see Hintze and Kowallis, 2009; Wardlaw, 2015); Clark uses terminology of Park City Formation rather than Group of some prior studies; UGS does not use Kaibab Limestone nomenclature in northwest Utah; measured thickness is 419 to 575 feet (128–175 m) (Maurer, 1970; Wardlaw and others, 1979a, 1979b).

Psl, Psl?

Permian sandstone, limestone and dolomite (lower Permian, Leonardian) – Gray to light-brown sandstone, limestone, and lesser dolomite; sandstone is fine to medium grained with calcareous cement and tabular cross-beds; carbonate rocks are finely crystalline, locally with chert and calcite nodules, and locally with brachiopods and gastropods; medium to thick bedded forming steep, ledgey slopes at northern Cedar Mountains; Leonardian age is from bracketing strata and fusulinids in the Cedar Mountains (sample D-77, Clark and others, 2016; Utah Geological Survey and Wells, 2017); may correlate with the Pequop Formation (west) and Diamond Creek Sandstone (east); forms few small outcrops along western map border (Grassy Mountains), and complete thickness at Cedar Mountains is 3953 feet (1205 m) (Maurer, 1970).

Pu **Permian strata, undivided** (lower Permian, Leonardian? to Wolfcampian?) – Combined unit at northern Oquirrh Mountains due to structural disturbance, limited age control, and poor exposure that includes units Pdk, Pofp, Pocp?; present below unit Ppp in a fault-bounded block containing a series of northeast-trending folds; unit contains interbedded light-brown to reddish-brown and light-gray quartzite, sandstone (calcareous, ferruginous, dolomitic), limestone, dolomite, dolomite breccia, and some thin chert beds; bedding is thin to medium; worm trails in ferruginous sandstone are common (Tooker and Roberts, 1970; Swensen, 1975); present east of the Garfield fault from near Harkers Canyon northward to the Arthur fault where it is poorly exposed and typically forms slopes and some ledges; fossil age data are very limited (see Tooker and Roberts, 1970); thickness is uncertain due to structural complications.

Pdk **Diamond Creek Sandstone and Kirkman Formation, undivided** (lower Permian, Leonardian? to Wolfcampian?) – Combined unit due to structural disturbance that extends across the northern Oquirrh Mountains from Flood and Pass Canyons (west) to near Barneys Canyon (east); stratigraphically higher beds in Flood and Pass Canyons consist of interbedded light-gray sandstone, quartzitic sandstone, and local beds of light-brownish-gray dolomite or dolomitic limestone that are typically contorted, lenticular, and discontinuous; there, lower part is light-gray to tan, calcareous sandstone breccia that includes lenses and slump blocks of limestone and dolomite; lower part of unit in upper Dry Fork consists of light-gray to tan calcareous sandstone that is locally brecciated, cross-bedded, and ripple-marked and is underlain by dark-gray, weathering to light- to medium-bluish-gray, limestone and arenaceous limestone that is thinly laminated and commonly contorted and brecciated (Welsh and James, 1961; Swensen, 1975); this combined unit typically forms slopes, and underwent both soft-sediment and tectonic deformation (Welsh and James, 1961; Schurer, 1979a, 1979b); Welsh (1998) reported the Diamond Creek Sandstone beds are in part brecciated because of collapse due to dissolution of anhydrite in the underlying Kirkman Formation in the Oquirrh Mountains and Wasatch Range; the unit has been structurally deformed between the North Oquirrh thrust fault (located near Nelson Peak) and Midas thrust (located in Bingham mine) and Bear fault (located west of Freeman Peak), and also south of the Arthur fault where included as unit Pu; contact with underlying Freeman Peak Formation is locally faulted, but is otherwise conformable (Schurer, 1979a; Gunter, 1991; Gunter and Austin, 1997); limited age control in Oquirrh Mountains (Swensen, 1975), regional age from Hintze and Kowallis (2009); thickness is uncertain due to structural complexity, but Swensen (1975) estimated about 2000 feet (600 m).

Oquirrh Group strata, subdivided into several formations, members, and units across the map area (see Notes on Stratigraphy section, figure 3, and tables A9 and A10).

Pℙo **Oquirrh Group, undivided** – Cross section only.

Oquirrh Group strata of the Grassy Mountains (Calcite and other thrust sheets), divided into three informal units (modified from Doelling, 1964; Jordan, 1979a, 1979b):

Pℙos **Oquirrh Group, sandstone and limestone unit** (lower Permian, Leonardian? to Wolfcampian to Upper Pennsylvanian, latest Virgilian) – Only three exposures in eastern Grassy Mountains of map area; platey dark-gray calcareous sandstone weathering to light and dark brown; bedding is thin and forms slopes and few ledges; in the Grassy Mountains and adjacent areas fossil fusulinids and conodonts were reported to indicate an early Leonardian through early Wolfcampian age (Doelling, 1964; Jordan, 1979a, 1979b; Clark and others, 2020); G.P. Wahlman (independent biostratigrapher) reevaluated the fusulinid data in Doelling (1964), results are provided in Clark and others (2020); Doelling (1964) reported other fossils in the Grassy Mountains including crinoids, brachiopods, pelecypods, sponges, trilobites, and bryozoans; unit Pℙos corresponds to Doelling's (1964) Oquirrh Formation units 6, 5, 4, 3 and upper part of unit 2; incomplete thickness in map area of about 1000 feet (300 m), Doelling (1964) reported a complete thickness of 7620 to 9004 feet (2323–2745 m) in the Grassy Mountains.

ℙosi, ℙosi?

Oquirrh Group, sandstone and siltstone unit (Upper Pennsylvanian, Virgilian) – Light-brown, light-gray, pale-red sandstone and calcareous sandstone and siltstone, lesser silty and sandy limestone; bedding is thin and forms slopes; fossil fusulinids from lower part were reported to be of Virgilian age (Doelling, 1964; Jordan, 1979a, 1979b); corresponds to Doelling's Oquirrh Formation unit 2, excluding the upper part (272 feet, 83 m) of limestone that is now placed in unit Pℙos; unconformably overlies unit ℙol (fossils indicate Missourian missing); locally queried near Puddle Valley where separation from unit Pℙos is difficult (see Doelling, 1964); incomplete thickness in map area of about 1600 feet (490 m), Doelling (1964) reported a complete thickness of 1934 feet (590 m) in the Grassy Mountains.

ℙol **Oquirrh Group, limestone unit** (Middle Pennsylvanian, Desmoinesian) – Medium-gray limestone and cherty limestone with minor interbedded light-brown sandstone; typically thick bedded, forming cliffs and ledges; fossil fusulinids and conodonts from adjacent areas indicated a Desmoinesian to late Atokan? age (Doelling, 1964; Jordan, 1979a, 1979b; Clark and others, 2020), and Doelling (1964) noted that it is uncertain if the lower part of the unit might contain Atokan- or Morrowan-age strata; other fossils include brachiopods, corals, trilobites, and bryozoans (Doelling, 1964); incomplete thickness of about 1000 feet (300 m) in map area, and Doelling (1964) reported an incomplete thickness of 1607 feet (490 m) in the Grassy Mountains.

Oquirrh Group strata of the western Cedar Mountains (Cedar thrust sheet), divided into three informal units:

Posc? **Oquirrh Group, sandstone and limestone unit, Cedar thrust sheet?** (Lower Permian, Leonardian? to Wolfcampian) – Dark-gray calcareous sandstone weathering to light and dark brown, and lesser moderate- to dark-gray fossiliferous limestone; bedding is thin to medium and forms slopes and ledges; Wolfcampian fusulinid *Schwagerina* obtained from Puddle Valley Knolls (table A8); unit queried in Puddle Valley as connection to Cedar thrust sheet is uncertain; Doelling (1964) included in Oquirrh Formation units 5 and 6; incomplete thickness is about 3300 feet (1000 m).

ℙosc **Oquirrh Group, sandstone and siltstone unit, Cedar thrust sheet** (Upper Pennsylvanian) – Dark-gray calcareous sandstone and siltstone weathering to light and dark brown, minor dark-gray and moderate-gray limestone, minor pale-red to moderate-gray shale; bedding is laminated to medium and forms slopes; conodonts from upper part in adjacent Bonneville Salt Flats quadrangle indicate a Virgilian age (Clark and Oviatt, 2020); Maurer mapped as Oquirrh Formation unit 4; incomplete thickness is roughly 1400 feet (425 m).

ℙolc, ℙolc?

Oquirrh Group, limestone unit, Cedar thrust sheet (Middle? Pennsylvanian) – Moderate-gray limestone and cherty limestone with minor interbedded light-brown calcareous sandstone; typically medium to thick bedded, forming cliffs and ledges; no fossils were found for biostratigraphic control; Maurer (1970) mapped as Oquirrh Formation unit 3; may include small outcrops of Manning Canyon Formation near base; incomplete thickness is roughly 1900 feet (580 m).

Oquirrh Group strata for the remainder of the quadrangle, divided into several units:

Pofc **Oquirrh Group, Freeman Peak Formation and Curry Peak Formation, undivided** (Lower Permian, Wolfcampian) – Combined unit in the northern Cedar Mountains and southern Lakeside Mountains, and on cross section C-C'; medium- to dark-gray, weathering to yellowish-gray, calcareous, fine-grained sandstone and siltstone with lesser interbedded very pale orange, medium-gray and pale-red quartz sandstone and orthoquartzite (particularly in upper part) and uncommon gray sandy limestone; laminated to thick-bedded unit typically breaks into chips and plates forming rounded hills and slopes with local ledges; worm trail markings common on bedding planes in lower part of unit; Wolfcampian fusulinids reported by Maurer (1970) and Clark and others (2016); appears to be conformable with underlying Bingham Mine Formation; Clark and others (2016) reported unit is 3500 feet (1065 m) in Cedar Mountains; incomplete thickness in southern Lakeside Mountains estimated at 2600 feet (790 m).

Pofp **Oquirrh Group, Freeman Peak Formation** (Lower Permian, Wolfcampian) – Light-gray to tan to brownish-tan, calcareous quartzite that is thick bedded and interbedded with some thin, calcareous sandstone and platy, argillaceous siltstone and shale (rarely exposed except in roadcuts or prospect tunnels); lacks worm tracks found in the Curry Peak Formation and fine banding of the Bingham Mine Formation; forms jointed blocks and distinctive talus-covered slopes; present along the nose of the Copperton anticline from Bingham Canyon north and west around to Freeman Peak and also to the west near Pass and Bates Canyons, northern Oquirrh Mountains (Welsh and James, 1961; Swensen, 1975); unconformable with underlying Curry Peak Formation; fusulinids *Schwagerina* and *Pseudoschwagerina* indicate a Wolfcampian age (Welsh and James, 1961); thickness is 2400 feet (730 m) at Freeman Peak, central Oquirrh Mountains (Swensen, 1975).

Pocp **Oquirrh Group, Curry Peak Formation** (Lower Permian, Wolfcampian) – Dark-gray, weathering to light-gray and tan, very fine grained, calcareous sandstone and siltstone that is thin bedded (poorly), and includes some minor quartzite and limestone; sandstone and siltstone locally weather with a darker brown, punky rind; sparsely fossiliferous, but worm tracks and trails are abundant on bedding planes; quartzite lacks fine color banding of Bingham Mine Formation (Welsh and James, 1961; Swensen, 1975); generally forms chippy slopes with few ledges; present on flanks of Copperton anticline north of the Midas thrust and west in the Markham Peak–Pole Canyon area, northern Oquirrh Mountains; unconformable on underlying Bingham Mine Formation (Welsh and James, 1961), but unconformity is not observed to the west (Clark and others, 2012, 2016, 2021); uppermost part of formation yielded fusulinids (*Triticites*, *Schwagerina*, *Pseudoschwagerina*) of Wolfcampian age (Welsh and James, 1961); thickness is 2450 feet (750 m) in section on south flank of Curry Peak, central Oquirrh Mountains (Swensen, 1975).

IPo, IPo?

Oquirrh Group, Pennsylvanian formations, undivided (Pennsylvanian) – Combined unit likely of Bingham Mine Formation?, Butterfield Peaks Formation, and West Canyon Limestone where backthrusted and structurally deformed along the east side of the northern Cedar Mountains; locally may include small outcrops of Manning Canyon Formation; also mapped in Skunk Ridge where there is no biostratigraphic control.

IPobm, IPobm?

Oquirrh Group, Bingham Mine Formation (Upper Pennsylvanian, Virgilian to Missourian) – Brown-weathering, fine-grained quartzitic sandstone, quartzite, and calcareous sandstone with lesser interbeds of medium- to dark-gray, fine-grained, sandy and cherty limestone; light-brown to pale-red sandstone is very fine grained, feldspathic, and cross-laminated; bedding is medium to thick, but can be poor; forms talus-covered slopes with some intervening ledges; Commercial and Jordan Limestone marker beds present at base of formation only in the central Oquirrh Mountains; in the northern Oquirrh Mountains, previously mapped as the Kessler Canyon Formation (Tooker and Roberts, 1970); fossil age data from the northern Oquirrh Mountains are limited (Tooker and Roberts, 1970; Welsh, 1998), but this area yielded conodont *Streptognathodus pawkuskaensis* of Virgilian (Gzhelian) age (table A8); fusulinids reported from Cedar Mountains by Maurer (1970) and Clark and others (2016), and northern Cedar Mountains and southern Lakeside Mountains yielded *Triticites* sp. (table A8); in northern Oquirrh Mountains, west of Garfield fault, incomplete lower part of formation is about 1000 to 2000 feet (300–600 m) thick (Tooker and Roberts, 1970, 1971a), and incomplete section between Garfield and Arthur faults is about 3400 feet (1040 m) thick (this study); complete thickness is 2700 feet (825 m) in Cedar Mountains (Clark and others, 2016), and possibly that thick in southern Lakeside Mountains where folded.

IPobmu, IPobmu?

Oquirrh Group, Bingham Mine Formation, upper member (Upper Pennsylvanian, Virgilian to Missourian) – Light-gray to tan, thinly color-banded and locally cross-bedded quartzite with interbedded thin, light- to medium-gray, calcareous, fine-grained sandstone, limestone, and siltstone; several of the thin calcareous units are locally important as marker beds; upper-lower member contact is placed at base of the Manefay limestone marker bed; unit is very similar to the lower member above the Commercial Limestone (Swensen, 1975); queried in three isolated outcrops at Tooele Army Depot that Tooker (1980) mapped as the Bingham Mine Formation, Markham Peak Member; Virgilian and Missourian fusulinids (*Triticites*) are reported from the Markham Peak section (R.C. Douglass, in Tooker and Roberts, 1970), and Welsh and James (1961) reported a Virgilian and Missourian age for the entire formation; 2200 feet (670 m) thick at the Bingham district (Swensen, 1975).

IPobml, IPobml?

Oquirrh Group, Bingham Mine Formation, lower member (Upper Pennsylvanian, Missourian) – Most of the unit consists of light-gray to tan, color-banded quartzite with thin, interbedded, light- to medium-gray, calcareous, fine-grained sandstone, limestone, siltstone, and minor shale; unit includes several limestone marker beds including the Commercial and basal Jordan Limestone beds (important Bingham ore hosts, but not mapped separately here due to scale limitations); the Commercial (100 feet [30 m] thick) consists of dark-gray to black, argillaceous, thin-bedded, silty and cherty limestone, whereas the Jordan (308 feet [94 m] thick) is thin-bedded, dark-gray, argillaceous and silty, cherty limestone and arenaceous limestone (Swensen, 1975); Missourian-age conodont fauna were recovered from the Jordan Limestone east of Tooele (S.M. Ritter, BYU, email to D.L. Clark, October 27, 2009) and Missourian fusulinids were also reported from this member (Welsh and James, 1961; R.C. Douglass, in Tooker and Roberts, 1970); thickness is about 3100 feet (945 m) near Middle Canyon, Bingham district (Swensen, 1975).

IPobw **Oquirrh Group, Butterfield Peaks Formation and West Canyon Limestone, undivided** (Middle to Lower Pennsylvanian) – Mapped as combined unit in eastern Stansbury Mountains and southern Lakeside Mountains, where contact is unclear due to sandy intervals in West Canyon Limestone; limited conodont data indicate Pennsylvanian age in southern Lakeside Mountains (S.M. Ritter, BYU, email to D.L. Clark, March 1, 2016); incomplete thickness about 550 feet (170 m) in northern Stansbury Mountains, and estimated at 4000 feet (1220 m) thick (where folded) in southern Lakeside Mountains.

IPobp, IPobp?

Oquirrh Group, Butterfield Peaks Formation (Middle to Lower Pennsylvanian, Desmoinesian to Morrowan) – Generally characterized by cyclically interbedded limestone and clastic intervals; limestone is medium gray and locally fossiliferous, arenaceous, cherty, and argillaceous in thin to thick beds and contains locally abundant brachiopod, bryozoan, coral, and fusulinid fauna; diagnostic black chert weathers brown and locally occurs as spherical nodules and laterally linked masses; light-brown quartzite and calcareous sandstone are thin to medium bedded and locally cross-bedded; includes some poorly exposed light-gray siltstone and mudstone interbeds; overall, limestone predominates over quartzite and sandstone, and clastic percentages increase upsection; unit forms ledges and cliffs with regularly intervening slopes; subdivided in the Bingham district into upper and lower members by Swensen (1975) and Laes and others (1997), but not differentiated in our map; fossil age data in Welsh and James (1961), Maurer (1970), Tooker and Roberts (1970), Douglass and others (1974), Swensen (1975), Davis and others (1989, 1994), Welsh (1998), Konopka (1999), Clark and others (2016), and Clark (this study) (see table A8); conodont data in the northern Oquirrh Mountains indicate the base of unit ℙobp is Atokan, but in the southern Oquirrh Mountains the base is Morrowan (Davis and others, 1994); complete thickness is 9072 feet (2766 m) at Butterfield Peaks, central Oquirrh Mountains (Tooker and Roberts, 1970), and 3606 feet (1099 m) measured by Tooker and Roberts (1970; their Erda Formation), and 3690 feet (1125 m) measured by Konopka (1999) near Rogers Canyon, northern Oquirrh Mountains; 4150 feet (1265 m) thick in Cedar Mountains (Clark and others, 2016).

ℙMwm **Oquirrh Group, West Canyon Limestone and Manning Canyon Formation, undivided** (Lower Pennsylvanian, Morrowan to Upper Mississippian, Chesterian) – Combined unit along the North Oquirrh thrust fault where separation of formations is difficult due to poor exposure and map scale.

ℙowc **Oquirrh Group, West Canyon Limestone** (Lower Pennsylvanian, Morrowan) – Light- to medium-gray limestone, fossiliferous limestone, and arenaceous limestone, with subordinate light-brown to light-gray calcareous sandstone and quartzite and minor dark-gray carbonaceous shale; limestone is medium to very thick bedded, and locally very fossiliferous, cherty, arenaceous, bioclastic, or bioturbated; fossils include crinoids, bryozoans, brachiopods, trilobites, foraminifera, corals, gastropods, sponges, calcareous algae, and pellets (Tooker and Roberts, 1970; Swensen, 1975; Davis and others, 1989); present in ledgy and cliffy exposures in the Kessler anticline, in the core of an unnamed anticline near Lake Point, along North Oquirrh thrust (Bates Canyon-Nelson Peak area), and in a few small exposures south of Henry Spring, northern Cedar Mountains; includes the upper two-thirds of the Lake Point Limestone of Tooker and Roberts (1970) in the northern Oquirrh Mountains based on lithofacies and age relations; there are uncertainties about picking consistent lithologic and fossil datum associated with the formation contacts (see Davis and others, 1989, 1994); microfossil and macrofossil data from northern and southern Oquirrh Mountains are available from Gordon and Duncan in Tooker and Roberts (1970), Welsh (1976), and Davis and others (1989, 1994); complete thickness of 1050 feet (320 m) (Green Ravine area, measured section units 109 to 10, northern Oquirrh Mountains, Davis and others, 1989, 1994); type and reference sections south of map area range from 1456 to 1007 feet (444–307 m) (Nygreen, 1958; Tooker and Roberts, 1970; Davis and others, 1994); 500 to 800 feet (150–245 m) in Cedar Mountains (Maurer, 1970).

Mmc, Mmc?

Manning Canyon Formation (Upper Mississippian, Chesterian) – The formation is an interval of regional décollement, commonly exhibiting substantial deformation, so regional thicknesses vary, but more reliable thicknesses of the formation are 1140 to 1559 feet (320–475 m) at Soldier Canyon, Oquirrh Mountains (Gilluly, 1932; Moyle, 1959) and 1176 feet (359 m) at the Lake Mountains (Biek and others, 2009). ***Northern Stansbury Mountains*** includes dark-gray to light-brown and pale-red shale and dark-gray carbonaceous limestone, and lesser sandstone and quartzite; bedding is very thinly laminated to medium; forms slopes and ledges on east flank from Broad to West Canyons; no fossil age data; thickness is about 1000 feet (300 m), greater than mapped by Rigby (1958). ***Northern Oquirrh Mountains*** includes light-gray to dark-gray limestone, sandy limestone, fossiliferous limestone and some thin shaley partings; limestone is thin to thick bedded with local black chert nodules, wispy sand layers, and intraformational conglomerate; macrofossils include brachiopods, crinoids, bryozoans, gastropods, corals, and trilobites (Tooker and Roberts, 1970; Davis and others, 1989); forms slopes and ledges on flanks of the Kessler anticline; includes the lower one-third of the Lakepoint Limestone of Tooker and Roberts (1970), which has similar age relations, but differing lithofacies (more limestone) compared to the typical Manning Canyon; upper contact placed at top of the prominent double-cliff limestone unit (units 9 and 8 of measured section by Davis and others, 1989, 1994; see also Tooker and Roberts, 1970, figure 8; Welsh, 1976); conodont and macrofossil data indicate a Chesterian age (Davis and others, 1989, 1994; Gordon and Duncan, in Tooker and Roberts, 1970); thickness in northern Oquirrh Mountains is 477 feet (145 m) (units 9 through 1 of measured section by Davis and others, 1989, 1994). ***Southern Lakeside Mountains and Northern Cedar Mountains*** include few exposures west of the Lakeside fault and associated with thrust faults in the Hastings Pass and Henry Spring areas; incomplete thickness as much as 500 feet (150 m) (Young, 1953; Doelling, 1964; Maurer, 1970); Maurer estimated a total thickness in the Cedar Mountains of 1500 to 2000 feet (460–610 m).

M **Mississippian rocks, undivided** – Cross section only.

Mgb, Mgb?

Great Blue Limestone (Upper Mississippian) – Primarily limestone with minor shale and sandstone; bluish-gray to medium- and dark-gray limestone is locally fossiliferous, cherty, and argillaceous; bedding is medium to very thick; locally black chert occurs as nodules, particularly near the top; macrofossils include brachiopods, corals, bryozoans, and crinoids (see Davis, 1956; M.K. Elias, in Arnold, 1956; Gordon and Douglas, in Tooker and Roberts, 1970); dark-gray to olive-gray shale occurs in middle part of section just south of the map area and in the lower part of the northern Oquirrh Mountains section; uncommon yellowish-brown sandstone beds locally occur; forms ledges and cliffs; complete thickness is from 650 to 1000 feet (200–300 m) at eastern Stansbury Mountains (Arnold, 1956; Rigby, 1958; this study), incomplete thickness at northern Oquirrh Mountains is about 1400 feet (430 m) (Tooker and Roberts, 1970), and incomplete thickness at southern Lakeside Mountains is 1537 feet (469 m) (Young, 1953).

Mh, Mh?

Humbug Formation (Upper Mississippian) – Light-brown and medium-blue-gray interbedded sandstone, quartzite, fossiliferous limestone, and sandy limestone; bedding is thin to thick; fossils include bryozoans, corals, brachiopods, and crinoid columnals (Davis, 1956; Rigby, 1958); forms slopes and ledges; queried in an isolated exposure near Skull Valley; thickness is 950 to 1300 feet (290–400 m) at northern Stansbury Mountains (Rigby, 1958; this study), 850 feet (260 m) in southern Lakeside Mountains (this study), and Palmer (1970) reported 350 feet (105 m) (where incomplete and structurally disturbed) at Stansbury Island, near Cedar Canyon.

MDdp **Deseret Limestone, Gardison Limestone, Fitchville Formation, Pinyon Peak Limestone, undivided** (Upper Mississippian to Upper Devonian, Famennian) – Combined unit in northern Stansbury Mountains, Salt Mountain, and west side of Stansbury Island where difficult to separate formations at map scale; primarily limestone and dolomite that is locally cherty and fossiliferous, see descriptions for units Md and MDgp; in Stansbury Mountains locally silicified near major Devonian unconformity, but elsewhere unit may conformably overlie Stansbury Formation; Clark excluded Pinyon Peak strata from the Stansbury Formation (following Rigby, 1958, Sandberg and Gutschick, 1979, Stock and Sandberg, 2019); Arnold (1956) and Rigby (1958) reported several fossils attributed to Meramecian, Osagean, and Kinderhookian ages; Sandberg and Gutschick (1979) reported on the Delle Phosphatic Member at Flux; Petersen (1969) reported ammonoids of early Meramecian age from the Delle Member in the northern Stansbury Mountains; fossils from the Fitchville and Pinyon Peak indicate Kinderhookian and Famennian ages (Sandberg and Gutschick, 1979; Nichols and others, 1992; Silberling in Trexler, 1992; Stock and Sandberg, 2019), and the fossil brachiopod *Paurorhyncha endlichi* reported by Rigby (1958) and Stokes and Arnold (1958) indicates Pinyon Peak strata (Stock and Sandberg, 2019); Sandberg and Gutschick (1979) used northern Utah stratigraphic nomenclature at Stansbury Island (table A9); thickness is from 800 to 2200 feet (245–670 m).

Md, Md?

Deseret Limestone (Upper to Lower Mississippian) – Locally mapped as separate unit at eastern Stansbury Island and an isolated exposure (queried) near Skull Valley; upper part is medium- to dark-gray cherty limestone, limestone, fossiliferous limestone, cherty dolomite, and medial part is light-olive-gray, weathering to light-brown, quartz sandstone; lower part (Delle Phosphatic Member, not mapped separately) includes poorly exposed phosphatic shale and medial cherty limestone (Palmer, 1970; Sandberg and Gutschick, 1984); bedding is thin to very thick; forms ledges and slopes; fossils locally include rugose corals, spiriferid brachiopods, bryozoans, and crinoids (Rigby, 1958; Palmer, 1970); thickness of 1150 feet (350 m), reported by Palmer (1970), may be excessive due to folding.

Mw **Woodman Formation** (Upper? to Lower Mississippian) – Upper part is pale-red, light-brown, moderate-gray, dolomitic, calcareous siltstone and fine-grained sandstone (called Needle Siltstone Member by Sandberg and Gutschick, 1984; Poole and Sandberg, 1991); lower part (Delle Phosphatic Member) is gray, black, and pale-red, phosphatic and cherty siltstone and mudstone with lesser nodular limestone and cherty limestone; formation is laminated to thinly bedded forming slopes with few ledges in southern Lakeside Mountains (Sandberg and Gutschick, 1984; Poole and Sandberg, 1991; Silberling and Nichols, 1992a, 1992b); yielded Osagean fossil data (Sandberg and Gutschick, 1984; Poole and

Sandberg, 1991; Silberling and Nichols, 1992b); correlates to the Deseret Limestone to the east (Poole and Sandberg, 1991); thickness is 445 feet (135 m) (Silberling and Nichols, 1992b).

MDgp, MDgp?

Gardison Limestone, Fitchville Formation, Pinyon Peak Limestone, undivided (Lower Mississippian, Osagean-Kinderhookian to Upper Devonian, Famennian) – Combined unit in the southern Lakeside Mountains (following Silberling and Nichols, 1992a), western Stansbury Mountains, and eastern Stansbury Island; upper part (Gardison) is moderate- to dark-gray silty limestone and limestone that is commonly cherty and fossiliferous; middle part (Fitchville) is moderate- to dark-gray limestone and silty limestone that is locally fossiliferous and cherty, locally with shale and sandstone near base; lower part (Pinyon Peak) is greenish-gray nodular silty limestone to light-gray to light-brown dolomite and sandstone and light-brown to pale-red shale that is typically poorly exposed; bedding is thin to very thick forming ledges, cliffs, and slopes; megafossils include corals, gastropods, brachiopods, bryozoa, and crinoid columnals, and conodonts range from Osagean to Kinderhookian to Fammenian (Rigby, 1958; Palmer, 1970; Howell, 1978; Sandberg and Gutschick, 1979, 1984; Silberling and Nichols, 1992a); unconformably overlies Devonian dolomite at southern Lakeside Mountains and conformably overlies the Stansbury Formation at eastern Stansbury Island; queried in isolated exposures; Sandberg and Gutschick (1979) and Poole and Sandberg (1991) used different stratigraphic nomenclature at Stansbury Island and the southern Lakeside Mountains (table A9); 640 to 1000 feet (195–300 m) thick in the southern Lakeside Mountains (Silberling and Nichols, 1992a; this study) and 1000 to 1200 feet (300–365 m) in western Stansbury Mountains and eastern Stansbury Island (Chapusa, 1969; Palmer, 1970; Howell, 1978; Sandberg and Gutschick, 1979; this study).

D **Devonian rocks, undivided** – Cross section only.

Dst, Dst(SOu)

Stansbury Formation (Upper Devonian, Famennian) – Enigmatic rock unit with complicated lithofacies relationships due to the Stansbury uplift (see Arnold, 1956; Stokes and Arnold, 1958; Rigby, 1958; Rigby, 1959; Nichols and others, 1992; Trexler, 1992). Clark's mapping (this study) follows Trexler (1992) except for reassigning the uppermost part (commonly covered) to the Pinyon Peak Limestone (see Rigby, 1958; Howell, 1978; Sandberg and Gutschick, 1979; Stock and Sandberg, 2019). In northern Stansbury Mountains (type section at Flux), the formation includes conglomerate with lesser quartz sandstone and quartzite, and some dolomite and limestone at the base; the distinctive conglomerate is gray dolomite-clast type in a dolomite matrix, and varies from matrix to clast supported; clasts are subrounded to subangular and up to 5 feet (2 m) in diameter; light-colored sandstone and quartzite has small-scale cross-lamination and can be laterally discontinuous; Stansbury Island section is different from the type section—it does not have conglomerate and it has roughly four times as much quartz sandstone compared to Flux (Trexler, 1992); bedding is thin to very thick, forming mostly ledges and slopes; unit Dst also includes three large slide blocks of Laketown-Ely Springs Dolomite, unit Dst(SOu), near Flux and Miners Canyon, Stansbury Mountains (Rigby, 1958; Stokes and Arnold, 1958; Trexler, 1992); major unconformity at base of formation (Rigby, 1958, 1959; Trexler, 1992); fossil data indicate the formation is Famennian in age (Sandberg and Gutschick, 1979; Mamet, in Trexler, 1992); Hollis (2015) reported U-Pb detrital zircon provenance data, but no maximum depositional age; the formation is limited in lateral extent (Rigby, 1958, 1959; Trexler, 1992), but appears to extend to the Wasatch Range near Salt Lake City (Bryant, 1990); thickness from 0 to about 1710 feet (0–520 m) at northern Stansbury Mountains and about 880 feet (270 m) at Stansbury Island (Trexler, 1992).

Dgs **Guilmette Formation and Simonson Dolomite, undivided** (Middle Devonian) – Combined unit in the southern Lakeside Mountains where not readily separable for mapping purposes; predominantly gray, color-banded dolomite and minor light-brown sandstone (Doelling, 1964); medium to thick bedded forming ledges; no biostratigraphic control, but regional ages on Devonian formations are in Hintze and Kowallis (2009); complete thickness is 1469 to 1850 feet (448–565 m) (Young, 1953; Doelling, 1964; this study).

Dss, Dss?

Simonson Dolomite and Sevy Dolomite, undivided (Middle to Lower Devonian) – Combined unit of dark- and light-gray dolomite that is medium to coarsely crystalline (Simonson) and light-gray dolomite that is finely crystalline with laminated surface appearance (Sevy); bedding is thin to very thick; occurs as ledges and slopes at Salt Mountain and Lone Rock (west of northern Stansbury Mountains); no fossils or other age data; unconformable on unit SOu; combined unit thickness is 375 feet (115 m) at Salt Mountain, but removed elsewhere by Devonian unconformity (Rigby, 1958, 1959).

Dsy **Sevy Dolomite** (Lower Devonian) – Light- to moderate-gray dolomite that is finely to coarsely crystalline with laminated surface appearance; bedding is medium to thick; lighter colored and less resistant than surrounding formations; contains fossil fish fragments (Young, 1953); mapped separately in the southern Lakeside Mountains; complete thickness is 220 to 242 feet (67–74 m) (Young, 1953; Petersen, 1956) and 341 feet (104 m) farther north (Doelling, 1964).

SOu **Laketown Dolomite, Ely Springs Dolomite, Eureka Quartzite, undivided** (Silurian to Upper Ordovician) – Combined unit of medium- to light-gray dolomite that is medium to coarsely crystalline (Laketown) and underlying, banded, dark- and medium-gray dolomite that is fine to medium crystalline (Ely Springs); in southern Lakeside Mountains also includes thin interval of Eureka Quartzite at base 15 to 35 feet (5–10 m) thick; bedding is medium to very thick; primarily forms ledges and cliffs; fossils include primarily brachiopods and corals (Young, 1953; Rigby, 1958; Doelling, 1964), regional age from Hintze and Kowallis (2009); stratigraphic study in Lakeside Mountains by Harris and Sheehan (1996); three slide blocks of SOu are included in unit Dst near Flux and Miners Canyon, Stansbury Mountains; complete thickness is 1075 feet (328 m) in southern Lakeside Mountains (Young, 1953), 925 feet (280 m) at Salt Mountain and northern Stansbury Mountains (Rigby, 1958), and 425 feet (130 m) at Stansbury Island where it is locally unconformable with overlying Stansbury Formation and younger rocks and with the underlying Pogonip Group (Chapusa, 1969; Palmer, 1970).

O **Ordovician rocks, undivided** – Cross section only.

Op, Op?

Pogonip Group (Middle to Lower Ordovician) – Medium-gray limestone and lesser dolomite (variably sandy and cherty) with yellowish-orange argillaceous partings and laminae interbedded with siltstone, shale, and intraformational pebble conglomerate; bedding is thin to medium, and soft-sediment deformation exists as wavy bedding, slump folds, and intraformational breccia; forms ledges and slopes; fossils include trilobites, brachiopods, cephalopods, graptolites, echinoderms, ostracodes, bryozoans, and algae (Young, 1953; Arnold, 1956; Rigby, 1958; Doelling, 1964); regional age from Hintze and Kowallis (2009); the thin upper formation (Kanosh Shale) is locally present only at Salt Mountain and southern Lakeside Mountains, but elsewhere the upper Pogonip Group (including the Kanosh) was eroded on the Ordovician unconformity (Tooele arch) (Rigby, 1958; Hintze, 1959); thickness as much as 1900 feet (580 m) at Stansbury Island (this study), 1200 feet (365 m) at northern Stansbury Mountains and Salt Mountain (Rigby, 1958), and 1137 to 1186 feet (345–360 m) at southern Lakeside Mountains (Young, 1953; Doelling, 1964).

Opk **Pogonip Group, Kanosh Shale** (Middle Ordovician) – Local marker unit that is an upper formation of the Pogonip Group; olive-green and black shale with minor argillaceous sandstone, limestone, and dolomite; forms slopes in Salt Mountain area; present but not mapped separately in southern Lakeside Mountains; fossils include graptolites and brachiopods (Rigby, 1958); thickness from 0 to about 100 feet (0–30 m) near Salt Mountain (Rigby, 1958; this study).

Ꞓ **Cambrian rocks, undivided** – Cross section only.

Ꞓum **Upper and Middle Cambrian strata, undivided** (lowermost Ordovician, upper to middle Cambrian) – Combined unit at Stansbury Island, where subdivision of several Cambrian formations could not be readily accomplished due to structural complications (also see Chapusa, 1969), as well as land access and time constraints; Clark considers western or northern Utah nomenclature more appropriate than the East Tintic area nomenclature applied by Palmer (1970).

Ꞓnp, Ꞓnp?

Notch Peak Formation (lowermost Ordovician? to upper Cambrian) – Dark-gray dolomite locally with very light gray intervals, bands and mottling; common chert nodules and stringers, *Girvanella* (microbial oncolites), pisolites, and calcite rods; medium to very thick bedded, forming ledges and cliffs; contains rare trilobite fossils (Arnold, 1956); Harlick (1989) and Garcia (2015) reported on the sedimentology, paleoecology and diagenesis of this unit in the southern Lakeside Mountains; no biostratigraphic control; for regional ages of the Notch Peak Formation and underlying Cambrian units refer to Hintze and Davis (2003); complete thickness is 750 to 900 feet (230–275 m) in northern Stansbury Mountains (Rigby, 1958; this study), and 1375 feet (420 m) at southern Lakeside Mountains, and incomplete in southernmost Stansbury Island.

Ꞓo, Ꞓo?

Orr Formation (upper Cambrian) – Upper part is light- to moderate-gray silty dolomitic limestone with rust-colored silty laminae and local rip-up clasts (possibly the Sneakover and Johns Wash Limestone Members), and intervening olive-green to pale-red shale (Corset Spring Shale Member) that includes trilobite *Housia varro* (Rigby, 1958); in southern Lakeside Mountains, upper part includes gray silty dolomite,

dolomite, limestone, moderate-brown sandstone, and light-brown weathering dolomite; lower part is light- and dark-gray dolomite (Big Horse Member) with calcite rods and blebs, pisolites, oolites, and *Girvanella*; bedding is typically medium to very thick bedded; formation forms ledges, slopes, and cliffs; thickness is 450 feet (135 m) at northern Stansbury Mountains, and 935 feet (285 m) at southern Lakeside Mountains.

Ꞓlt **Lamb Dolomite and Trippe Limestone, undivided** (upper to middle Cambrian) – Combined unit in northern Stansbury Mountains. ***Lamb*** includes thin upper part of moderate-gray silty limestone with rust-colored silty laminae and some oolites, and thicker lower part of light- and dark-gray dolomite; bedding is thin to thick; ***Trippe***, top part includes thin silty and shaley limestone and olive-green to pale-red shale (Fish Springs Member) that overlies moderate-gray limestone and lesser silty and shaley limestone; locally includes rip-up clasts/flat pebble conglomerate in limestone; fossils include inarticulate brachiopods and agnostid trilobite fragments (Rigby, 1958); bedding is thinly laminated to medium; combined map unit forms ledges, slopes, and cliffs; thickness is 1200 feet (365 m).

Ꞓl, Ꞓl? **Lamb Dolomite** (upper to middle Cambrian) – Mapped as separate formation in southern Lakeside Mountains; thin upper part of moderate-gray silty limestone with rust-colored silty laminae and some oolites, and thicker lower part of light- and dark-gray dolomite; bedding is thin to thick; complete thickness is 1075 feet (325 m).

Ꞓtp **Trippe Limestone and Pierson Cove Formation, undivided** (middle Cambrian) – Combined unit in southern Lakeside Mountains. ***Trippe***, upper part is olive-green shale and shaley nodular limestone (Fish Springs Member, the upper nodular limestone unit of Doelling, 1964) and lower part is moderate-dark-gray silty limestone, limestone, and dolomite that forms ledges; upper shale contains brachiopods (Doelling, 1964); ***Pierson Cove***, moderate-gray limestone (locally silty) and dolomite with calcite rods and local oolites; more resistant and poorly bedded (medium to thick), forming rounded ledges and cliffs; complete thickness is 975 feet (300 m) (Doelling, 1964).

Ꞓpc, Ꞓpc?

Pierson Cove Formation (middle Cambrian) – Mapped as separate formation in northern Stansbury Mountains; upper few beds of white and mottled dolomite (light and dark gray, called tiger-striped by Rigby [1958], and zebra-banding by Cohenour [1959]) underlain by light- and dark-gray silty limestone (silty laminae are tan, pale orange, and moderate to dark gray); locally dolomitized intervals are moderate-gray to mottled gray dolomite that is more resistant and with some calcite rods; bedding is thin to very thick; forms ledges, cliffs, and slopes; thickness is 575 feet (175 m).

Ꞓww **Wheeler Formation, Swasey Limestone, Whirlwind Formation, undivided** (middle Cambrian) – Combined unit in northern Stansbury Mountains. ***Wheeler***, upper part is olive-green shale and minor moderate-gray silty limestone interbeds with tan silty laminae, middle part is silty limestone, lower part is shale and some silty limestone and limey shale; bedding is thinly laminated to very thick; contains *Peronopsis* (agnostid trilobite) (Rigby, 1958); ***Swasey*** is moderate- to dark-gray limestone and silty limestone with some small oncolites; locally dolomitized; bedding is medium to thick; Rigby (1958) reported some fragments of *Elrathia* (trilobite); ***Whirlwind*** is pale-red and tan shale, and moderate-gray silty limestone; poorly exposed; fossils include *Ehmaniella* and *Ehmania* (trilobites) (Rigby, 1958); bedding is thinly laminated to medium; combined unit forms slopes, ledges, and few cliffs; thickness is 950 feet (290 m).

Ꞓwh **Wheeler Formation** (middle Cambrian) – Mapped as separate formation in southern Lakeside Mountains; gray silty limestone interbedded with lesser olive-green and grayish-green shale; bedding is laminated to thin and forms slopes; no fossil data; complete thickness is 441 feet (135 m) (Doelling, 1964).

Ꞓsw **Swasey Limestone** (middle Cambrian) – Mapped as separate formation in southern Lakeside Mountains; gray limestone and lesser silty limestone; bedding is thick to very thick; unit forms cliffs between less-resistant formations; sparse fossils include brachiopods and trilobites; complete thickness is 606 feet (185 m) (Doelling, 1964).

Ꞓwl **Whirlwind Formation** (middle Cambrian) – Mapped as separate formation in southern Lakeside Mountains; moderate-gray silty limestone with light-brown silty laminae interbedded with gray and green shale; bedding is laminated to medium; forms slopes with few ledges; fossils include trilobite debris; incomplete thickness is about 300 feet (90 m) (Doelling, 1964).

Ꞓdh, Ꞓdh?

Dome Limestone, Chisholm Formation, Howell Limestone, undivided (middle Cambrian) – ***Dome*** is moderate- to dark-gray silty limestone with tan and red silty laminae; bedding is thin to medium; in the southern Lakeside Mountains, it is orange-brown-weathering, medium-gray dolomite that is coarsely crystalline; ***Chisholm*** is olive-green shale (weathers brown), and lesser moderate-gray silty limestone and limestone with tan and orange silty laminae; bedding is thinly laminated to medium; contains uncommon *Glossopleura* (trilobite) (Rigby, 1958); ***Howell*** is moderate-gray silty limestone with orange silty laminae; bedding is thin to medium; combined unit forms ledges and slopes; complete thickness is 750 feet (230 m) at northern Stansbury Mountains, and an incomplete section in the southern Lakeside Mountains is 695 feet (210 m).

Ꞓp, Ꞓp?

Pioche Formation (middle to lower Cambrian) – Dark-greenish-gray and dark-reddish-gray (typically weathering to reddish brown or brown gray) graywacke sandstone, phyllitic shale and shale, quartzite, calcareous sandstone, and sandy and silty limestone; bedding is thin to medium; unit typically forms slopes and some ledges; on west flank of Stansbury Mountains south of Pass Canyon, formation contains more quartzite and sandstone and therefore is more difficult to separate from upper part of the Prospect Mountain Quartzite (see Rigby, 1958); complete thickness is 310 to 450 feet (95–135 m) at northern Stansbury Mountains (Rigby, 1958; this study), and about 500 feet (150 m) at Stansbury Island, north of Corral Canyon (Chapusa, 1969); about 545 feet (165 m) thick in the southern Lakeside Mountains where it is mostly quartzite.

Ꞓpm, Ꞓpm?

Prospect Mountain Quartzite (lower Cambrian to Neoproterozoic?) – Light-brown, light-gray, and white quartzite with scattered iron specks that is medium to coarse grained with cross-beds; bedding is medium to very thick; thin, uncommon conglomerate lenses occur with pebbles less than 1 inch (3 cm) diameter of quartzite and chert; in the Stansbury Mountains, uppermost part is reddish-brown colored and well bedded, forming ledges above the more easily eroded white-colored unit below (Rigby, 1958); forms ledges, slopes, and cliffs; detrital zircon data have not constrained the age for the formation (Yonkee and others, 2014); top of unit is conformable and base is not exposed; incomplete thickness is about 1150 to 2500 feet (350–760 m) at Stansbury Island (Chapusa, 1969; Palmer, 1970), and 4200 feet (1280 m) (nearly complete?) at the Stansbury Mountains (Rigby, 1958); incomplete thickness is 665 feet (200 m) at southern Lakeside Mountains.

NEOPROTEROZOIC

Z **Neoproterozoic rocks, undivided** – Cross section only.

Zm, Zm?

Mutual Formation (Neoproterozoic) – Light-brown to light-gray quartzite and quartzite conglomerate that weathers to moderate brown; conglomerate with rounded quartzite and chert pebbles in lenses and beds; common cross-bedding and some liesegang banding; thin to thick bedded; forms ledges and cliffs; detrital zircon analyses have not constrained the age of the formation (Yonkee and others, 2014); top part may not be exposed; incomplete thickness is about 1200 feet (365 m) at northern Stansbury Island.

Zi **Inkom Formation** (Neoproterozoic) – Grayish-green and maroon phyllitic shale and argillite, and minor quartzite and sandstone; thinly laminated to medium bedded; typically weathers to chips, and largely covered by surficial deposits forming a poorly exposed strike valley; detrital zircon maximum depositional age for the formation has not been constrained (Yonkee and others, 2014); complete thickness is about 200 to 300 feet (60–90 m) at northern Stansbury Island.

Zcc **Caddy Canyon Quartzite** (Neoproterozoic) – Very pale orange to white quartzite with orange and red liesegang banding; cross-bedding and local pebble conglomerate lenses; bedding is medium to very thick; forms ledges and cliffs; detrital zircon maximum depositional age for the formation has not been constrained (Yonkee and others, 2014); only top part of formation is exposed; incomplete thickness as much as 500 feet (150 m) at northern Stansbury Island.

Zp **Perry Canyon Formation** (Neoproterozoic) – Dark-brown and light-gray quartzite that is part of slate and quartzite member (see Balgord and others, 2013; Yonkee and others, 2014; Yonkee and others, in preparation); one small exposure in map area at the southernmost part of Carrington Island; detrital zircon data from Carrington Island are not yet available (Yonkee and others, in preparation), but data from Little Mountain (northeast of Fremont Island) indicate a maximum depositional age of 683 Ma (Balgord and others, 2013), and data from Fremont Island appear to reflect older sources (Yonkee and others, 2014); exposed (incomplete) thickness in map area is less than 100 feet (30 m).

CRETACEOUS TO PALEOPROTEROZOIC ROCK UNITS OF ANTELOPE ISLAND

CRETACEOUS

KXa Altered and deformed rocks (Cretaceous and Paleoproterozoic) – Older rocks (Farmington Canyon Complex) that were altered in the Cretaceous to dark-green to greenish-black chloritic, and dark-reddish-brown hematitic, gneiss, mylonite, and phyllonite (see Yonkee and Lowe, 2004; Willis and others, 2010); locally silicified and cut by quartz veins and pods (includes Kq unit of Doelling and others, 1990); found along shear zones, including a major shear zone in the central part of Antelope Island and near the contact with the overlying sedimentary cover; retrograde alteration and deformation of Farmington Canyon Complex protoliths is mostly Cretaceous in age (Yonkee and others, 1989; Willis and others, 2010), however, Bryant (1988) indicated some quartz veins and pods may be related to Precambrian alteration; in chloritic gneiss the original minerals are altered to sericite, fine-grained chlorite, biotite, stilpnomelane, epidote, and albite; phyllonite and mylonite contain sericite (6%–35%), chlorite (21%–31%), quartz (29%–51%), and feldspar (0%–30%) (Yonkee and others, 2000a); mapped as units XWfg and XWfs by Doelling and others (1990); unit KXa thickness is highly variable, and quartz veins and pods are <10 feet (3 m) to 400 feet (120 m) across (Doelling and others, 1990; Yonkee and others, 2000a).

CAMBRIAN

Ꞓt **Tintic Quartzite** (middle? to lower? Cambrian) – Tan to pale-gray to greenish-gray metaquartzite with interbeds of quartz pebble conglomerate; quartzite (60%) is dense, fine to medium grained; pebbly quartzite (20%) and conglomerate (20%) contain moderately well-sorted clasts of tan, white, and red polycrystalline quartz from 0.5 to 4 inches (1–10 cm) in diameter; bedding is medium to thick, and the unit commonly forms ledgey slopes and small blocky cliffs; quartzite is variably deformed with locally well-developed cleavage (stretched pebbles and micaceous partings), quartz-filled veins, and minor folds; unconformably overlies unit Zsd (Doelling and others, 1990; Yonkee and others, 2000b); detrital zircon data have not constrained the maximum depositional age (Yonkee and others, 2014); incomplete thickness is at least 800 feet (245 m), and top is not exposed (Doelling and others, 1990; Yonkee and others, 2000b).

NEOPROTEROZOIC

Zsm **Slate and dolomite unit and Mineral Fork Formation, undivided** (Neoproterozoic) – Combined unit in small exposures due to map scale.

Zsd **Slate and dolomite** (Neoproterozoic) – Consists of an upper slate member and thin lower dolomite member (Christie-Blick, 1983; Doelling and others, 1990; Yonkee and others, 2000b); the slate member consists of purple, greenish-gray, and reddish-brown slate, argillite, silty dolomite, and fine-grained metaquartzite that is thin bedded; the upper half consists mostly of purplish to reddish slate and fine-grained metaquartzite, and the lower half consists of multicolored slate with interbedded calcareous slate and silty dolomite; commonly forms smooth, covered slopes, but is locally well exposed; generally displays well-developed slaty cleavage, widespread minor folds, and locally complex quartz-filled veins developed during Mesozoic thrusting; slate grades downward to underlying light-gray to pink dolomite; the dolomite is finely crystalline to marbleized; bedding is finely laminated to thick bedded, partly reflecting recrystallization; the dolomite forms resistant cliffs; dolomite is generally weakly deformed and from 20 to 30 feet (6–10 m) thick; unit Zsd unconformably overlies the Mineral Fork Formation; previously called Kelley Canyon Formation (Doelling and others, 1990; Yonkee and others, 2000b; Willis and others, 2010), but the strata on Antelope Island may not be correlative with the Kelley Canyon Formation (W.A. Yonkee, Weber State University, email to D.L. Clark, February 24, 2014; Yonkee and others, 2014) and the nomenclature may not be appropriate for the eastern thrust system (cratonic) rock units; detrital zircon data were obtained from the unit on Antelope Island, but the maximum depositional age and correlation are unclear (Yonkee and others, 2014); unit thickness is variable from 70 to 280 feet (20–85 m) due to structural deformation (Doelling and others, 1990; Yonkee and others, 2000b).

Zmf **Mineral Fork Formation** (Neoproterozoic) – Dark-brownish-black, very poorly sorted, matrix-supported diamictite with minor interbedded argillite, metaquartzite, and conglomerate locally present near the top of the unit; clasts compose 20% to 60% of the diamictite and lie within a micaceous, gritty matrix; clast size is highly variable from pebbles to boulders 7 feet (2 m) across, but cobble-size clasts are abundant; clasts vary from angular to rounded, but many were altered and flattened during Mesozoic deformation; clast types include quartzo-feldspathic gneiss and granite, metaquartzite (including rare, but distinctive, chrome-green quartzite), schist, and amphibolite, with relative abundances varying between outcrops; diamictite has a well-developed cleavage formed during Mesozoic thrusting and is defined by subparallel partings in the matrix and flattened clasts; unit generally forms slopes, but cliffs are locally present; usually not bedded; locally chloritized and structurally deformed; unconformably overlies the Farmington Canyon Complex (Doelling and others, 1990; Yonkee and others, 2000b); a detrital zircon maximum depositional age of 700 Ma is given for the formation in the southern Wasatch Range (Yonkee and others, 2014) where it overlies the Big Cottonwood Formation (<766 Ma) (Dehler and others, 2010); unit Zmf (eastern thrust system/cratonic) is correlative to part of Perry Canyon Formation (western thrust system/passive margin) in the northern Wasatch Range (Yonkee and others, 2014); thickness is 0 to 200 feet (0–60 m) (Christie-Blick, 1983; Doelling and others, 1990; Yonkee and others, 2000b; Willis and others, 2010).

PALEOPROTEROZOIC

Farmington Canyon Complex, divided into eight informal units after Yonkee and others (2000a); also see Willis and others (2010). Considered Paleoproterozoic in age from about 1.6 to 1.7 Ga (Nelson and others, 2011, and references therein; also see Willis and others, 2010) (table A6), although debate remains whether it is older (W.A. Yonkee, Weber State University, verbal communication to D.L. Clark, October 22, 2015). Correlation with units of the Wasatch Range is presently unclear (Bryant, 1988; Yonkee and Lowe, 2004; Coogan and King, 2016). Map unit descriptions are modified from Yonkee and others (2000a) and Willis and others (2010).

Xfc **Farmington Canyon Complex, undivided** – Cross section only.

Xfcp **Granite and pegmatite** (Paleoproterozoic) – Mostly weakly to non-foliated, coarse-grained granite and pegmatite; only larger bodies mapped separately; unit includes pegmatitic granite that forms large bodies on the eastern part of the island, garnet-muscovite-bearing granite in small pods within and near layered gneiss, red granite that forms small plutons on the southern end of the island, and pegmatite in widespread dikes and pods within other units; larger outcrops of granite and pegmatite are generally white to gray to pink, variably fractured, and have a knobby appearance; contains quartz (25%–40%), plagioclase (20%–35%), K-feldspar (30%–50%) with minor muscovite, garnet, biotite, and accessory minerals, and is compositionally granite based on mineral modes; grain sizes variable from <1 to 10 mm in granite and locally >1 cm in pegmatite.

Xfcgr, Xfcg

Granitic gneiss (Paleoproterozoic) – Light- to pinkish-gray, weakly to strongly foliated, hornblende-bearing, quartz-feldspar gneiss with lenses of hornblende-plagioclase gneiss; intruded by widespread pegmatite dikes; unit includes a central body of weakly to moderately foliated, red granitic gneiss (unit Xfcgr) and a surrounding body of moderately to strongly foliated migmatitic granitic gneiss (Xfcg) that are mineralogically indistinguishable (Yonkee and others, 2000a); widely spaced, generally planar fractures produce a blocky appearance in most outcrops; exposed in a large elliptical area on the west-central part of the island and in a smaller area to the northeast; contains quartz (31%–36%), plagioclase (18%–32%), K-feldspar (27%–39%), hornblende and rare pyroxene (4%–8%), and accessory minerals, and has granitic compositions based on mineral modes; grain sizes from 0.1 to 10 mm.

Xfcb **Banded gneiss** (Paleoproterozoic) – Light- to pinkish-gray, strongly foliated and banded, locally migmatitic, hornblende-bearing, quartz-feldspar gneiss with lenses of hornblende-plagioclase gneiss; intruded by widespread pegmatite dikes; dominant rock type within the central and eastern parts of the island and surrounds the granitic gneiss unit; contains quartz (31%–34%), plagioclase (28%–38%), K-feldspar (16%–27%), hornblende (6%–12%), possible pyroxene and biotite, and accessory minerals, and is granitic to granodioritic in composition based on mineral modes; grain sizes from 0.1 to 3 mm.

Xfch **Hornblende-plagioclase gneiss** (Paleoproterozoic) – Dark-gray to black elongate pods of hornblende-plagioclase gneiss incorporated into granitic gneiss and banded gneiss, and light-gray to black plagioclase- to hornblende-rich gneiss that forms a large mafic body in the central part of the island; intruded by pegmatite dikes; contains hornblende (20%–60%), plagioclase (30%–60%), quartz (0%–15%), minor pyroxene, and accessory minerals, and varies compositionally from gabbro to diorite to tonalite based on mineral modes; grain sizes from 0.1 to 4 mm.

Xfcu **Metamorphosed ultramafic rock** (Paleoproterozoic) – Dark-green to black meta-ultramafic rock with amphibole, pyroxene, and rare olivine that are variably altered to chlorite, serpentine, and talc, and commonly with some surrounding hornblende-rich gneiss; forms small isolated pods within layered gneiss at the southern end of the island; contains anthophyllite and tremolite (~30%), orthopyroxene and clinopyroxene (15%), minor olivine, alteration minerals, and accessory minerals; grain size up to 3 mm.

Xfcq **Quartz-rich gneiss** (Paleoproterozoic) – White to pale-gray, quartz-plagioclase gneiss with minor layered gneiss and biotite schist; forms concordant lenses from 3 to 100 feet (1–30 m) wide within the layered gneiss; weathers to form vitreous, milky to greenish-gray, fractured and resistant outcrops; consists dominantly of quartz (79%–94%), with lesser amounts of plagioclase (5%–12%), biotite, muscovite, and accessory minerals; grain sizes from 0.2–5 mm.

Xfcl **Layered gneiss** (Paleoproterozoic) – Light- to dark-gray biotite- and garnet-bearing, migmatitic, quartz-feldspar gneiss with well-developed compositional layering (quartzo-feldspathic, biotite-rich, quartz-rich, amphibolite layers from 0.2 to 6 feet [0.05–2 m] thick); contains lenses of biotite schist and quartz-rich gneiss and rare pods of metamorphosed ultramafic and mafic rock; cut by widespread amphibolitic dikes; intruded by pegmatite dikes and granitic pods; forms heterogeneous, gray to brown to pink outcrops of variable erosional resistance in elongate regions within the southern and central parts of the island; layered gneiss mineral abundances are variable and contain quartz (18%–46%), plagioclase (27%–43%), K-feldspar (3%–16%), biotite (4%–32%), locally garnet, sillimanite, cordierite, and accessory minerals; grain sizes from 0.1–5 mm; U-Pb zircon age of 1691 ± 26 Ma from layered gneiss in southern Antelope Island (Nelson and others, 2011); biotite schist forms lenses up to 6 feet (2 m) wide; present locally with intercalated thin layers and pods of granitic material; relatively non-resistant, weathering to form brown slopes and subdued ledges; schist consists of biotite (38%–55%), quartz (1%–16%), coarser-grained muscovite (4%–7%), garnet (1%–4%), and lesser sillimanite and highly altered cordierite?, alteration to sericite (33%); grain sizes from 0.1–5 mm.

ACKNOWLEDGMENTS

We thank numerous individuals and entities for assistance in completion of this project. Kim Schroeder, Gerry Austin, and Brian Vinton (Kennecott Utah Copper/Rio Tinto) provided technical assistance, and Jeff Lachowski and Jeff Huber (Kennecott Utah Copper/Rio Tinto – Land, Water, and Energy) gave logistical assistance for work in the Oquirrh Mountains. ATK, U.S. Magnesium, Morton Salt, Broken Arrow Salt, Stansbury Park Wastewater, BLM, Tooele County, and Ensign Ranches helped provide access. Adolph Yonkee (Weber State University) reinterpreted the geology on Antelope Island and Carrington Island, and discussed the structural geology. Robert Baskin (USGS) provided Great Salt Lake bathymetry and shoreline data in digital form. The late John Welsh contributed to the understanding of Permian-Pennsylvanian strata of this region and shared much of his unpublished data. Barbara Nash (University of Utah) conducted tephrochronology analyses, and Michael Perkins (formerly University of Utah) also provided tephrochronology data. Geochemical and geochronologic laboratory work was by ALS Chemex, Nevada Isotope Geochronology Lab, and GeoSeparation Services. Scott Ritter (Brigham Young University [BYU]) identified microfossils for biostratigraphic control. Eric Christiansen (BYU) advised on volcanic rocks. Hellmut Doelling provided a colored version of his dissertation map and a digital text he revised (Doelling, 2003). Eric Christiansen, Ken Krahulec, and Jim Pechmann gave presentations during the field review. UGS staff conducted GPS profiles in Skull Valley (Adam McKean, Ben Erickson, Adam Hiscock, Emily Kleber), and Christian Hardwick provided updated gravity data in parts of the map area. Adolph Yonkee (Weber State University), David Miller (USGS), and Charles Sandberg (Emeritus USGS) provided brief geologic reviews. UGS staff, including Robert Biek, Grant Willis, Stefan Kirby, Stephanie Carney, Kimm Harty, and Michael Hylland, reviewed and improved this map; Ken Krahulec, Rich Giraud, Craig Morgan, Jon K. King, and Zach Anderson provided some technical assistance on geologic issues; Buck Ehler previously prepared the Tooele Valley Quaternary mapping data; Jay Hill, Lori Steadman, and Martha Jensen helped prepare the explanatory materials; Basia Matyjasik managed the GIS data and cartography.

REFERENCES

Adams, K.D, and Bills, B.G., 2016, Chapter 8, Isostatic rebound and palinspastic restoration of the Bonneville and Provo shorelines in the Bonneville basin, *in* Oviatt, C.G. and Shroder, J.F., editors, Lake Bonneville—A scientific update—Developments in Earth Surface Processes, Volume 20, Elsevier B.V., p. 145–164.

Arnold, D.E., 1956, Geology of the northern Stansbury Range, Tooele County, Utah: Salt Lake City, University of Utah, M.S. thesis, 57 p.

Arnow, T., and Mattick, R.E., 1968, Thickness of valley fill in the Jordan Valley east of the Great Salt Lake, Utah: U.S. Geological Survey Professional Paper 600-B, p. B79–B82.

Ashland, F.X., 2003, Characteristics, causes, and implications of the 1998 Wasatch Front landslides, Utah: Utah Geological Survey Special Study 105, 49 p., https://doi.org/10.34191/SS-105.

Atwood, G., 2006, Shoreline superelevation—evidence of coastal processes of Great Salt Lake, Utah: Utah Geological Survey Miscellaneous Publication 06-9, 231 p., https://doi.org/10.34191/MP-06-9.

Babcock, R.C., Jr., Ballantyne, G.H., and Phillips, C.H., 1995, Summary of the geology of the Bingham district, Utah, *in* Pierce, F.W., and Bolm, J.G., editors, Porphyry copper deposits of the American Cordillera: Arizona Geological Society Digest 20, p. 316–335.

Balgord, E.A., Yonkee, W.A., Link, P.K., and Fanning, C.M., 2013, Stratigraphic, geochronologic, and geochemical record of the Cryogenian Perry Canyon Formation, northern Utah—implications for Rodinia rifting and snowball Earth glaciation: Geological Society of America Bulletin, v. 125, no. 9–10, p. 1442–1467.

Barnhard, T.P., 1988, Fault-scarp studies in the Stansbury Mountains, Utah, *in* Machette, M.N., editor, In the footsteps of G.K. Gilbert—Lake Bonneville and neotectonics of the eastern Basin and Range Province, Guidebook for Field Trip 12, Geological Society of America Annual Meeting, Denver, Colorado: Utah Geological and Mineral Survey Miscellaneous Publication 88-1, p. 58–59, https://doi.org/10.34191/MP-88-1.

Barnhard, T.P., and Dodge, R.L., 1988, Map of fault scarps formed on unconsolidated sediments, Tooele 1° x 2° quadrangle, northwestern Utah: U.S. Geological Survey Miscellaneous Field Studies Map MF-1990, scale 1:250,000.

Best, M.G., and Christiansen, E.H., 1991, Limited extension during peak Tertiary volcanism, Great Basin of Nevada and Utah: Journal of Geophysical Research, v. 96, p. 13,509–13, 528.

Baskin, R.L., and Allen, D.V., 2005, Bathymetric map of the south part of Great Salt Lake, Utah: U.S. Geological Survey Scientific Investigations Map 2894.

Biek, R.F., 2006a, Geology of the Rose Canyon area, Salt Lake County, Utah—the exhumed flank of the Bingham volcanic center, *in* Harty, K.M., and Tabet, D.E., editors, Geology of northwest Utah: Utah Geological Association Publication 34, 21 p.

Biek, R.F., 2006b, Whole-rock geochemical and electron microprobe data for the Tickville Spring quadrangle, Utah: Utah Geological Survey Open-File Report 475, 7 p., https://doi.org/10.34191/OFR-475.

Biek, R.F., Clark, D.L., and Christiansen, E.H., 2009, Geologic map of the Soldiers Pass quadrangle, Utah County, Utah: Utah Geological Survey Map 235, 2 plates, scale 1:24,000, https://doi.org/10.34191/M-235.

Biek, R.F., Solomon, B.J., Keith, J.D., and Smith, T.W., 2005, Geologic map of the Tickville Spring quadrangle, Salt Lake and Utah Counties, Utah: Utah Geological Survey Map 214, 2 plates, scale 1:24,000, https://doi.org/10.34191/M-214.

Biek, R.F., Solomon, B.J., Smith, T.W., and Keith, J.D., 2007, Geologic map of the Copperton quadrangle, Salt Lake County, Utah: Utah Geological Survey Map 219, 2 plates, scale 1:24,000, https://doi.org/10.34191/M-219.

Black, J.E., and Babcock, R.C., editors, 1991, Guidebook to the geology and ore deposits of the Bingham mining district and northern Oquirrh Mountains, Utah: 1991 RTZ Group Mining and Exploration Conference, Salt Lake City, Utah, variously paginated, 6 plates.

Blackett, R.E., and Wakefield, S., compilers, 2004, Geothermal resources of Utah, 2004—a digital atlas of Utah's geothermal resources: Utah Geological Survey Open-File Report 431DM, scale 1:500,000, https://doi.org/10.34191/OFR-431DM.

Bortz, L.C., 2002, Heavy-oil deposit, Great Salt Lake, Utah, *in* Gwynn, J.W., editor, Great Salt Lake, an overview of change: Utah Geological Survey and Department of Natural Resources Special Publication, p. 243–250.

Bortz, L.C., Cook, S.A., and Morrison, O.J., 1985, Great Salt Lake area in Utah, *in* Gries, R.R., and Dyer, R.C., editors, Seismic Exploration of the Rocky Mountain Region: The Rocky Mountain Association of Geologists and the Denver Geophysical Society, Denver, CO, p. 275–281.

Bradley, M.D., and Bruhn, R.L., 1988, Structural interactions between the Uinta arch and the overthrust belt, north-central Utah—implications of strain trajectories and displacement modeling, *in* Schmidt, C.J. and Perry, W.J., editors, Interaction of the Rocky Mountain foreland and the Cordilleran thrust belt: Geological Society of America Memoir 171, p. 431–445.

Bray, R.E., and Wilson, J.C., editors, 1975, Guidebook to the Bingham mining district: Bingham Canyon, Utah: Society of Economic Geologists and Kennecott Copper Corporation, 156 p., 2 plates.

Brooks, L.E., 2006, Hydrology and simulation of ground-water flow, Lake Point, Tooele County, Utah: U.S. Geological Survey Scientific Investigations Report 2006-5310, 28 p.

Bryant, B., 1988, Geology of the Farmington Canyon Complex, Wasatch Mountains, Utah: U.S. Geological Survey Professional Paper 1476, 54 p., 1 plate, scale 1:50,000.

Bryant, B., 1990, Geologic map of the Salt Lake City 30' x 60' quadrangle, north-central Utah, and Uinta County, Wyoming: U.S. Geological Survey Miscellaneous Investigations Series Map I-1944, 3 plates, scale 1:100,000.

Bryant, B., Naeser, C.W., Marvin, R.F., and Mehnert, H.H., 1989, Ages of late Paleogene and Neogene tuffs and the beginning of rapid regional extension, eastern boundary of the Basin and Range Province near Salt Lake City, Utah: U.S. Geological Survey Bulletin 1787-K, 11 p.

Burr, T.N., and Currey, D.R., 1988, The Stockton Bar, *in* Machette, M.N., editor, In the footsteps of G.K. Gilbert—Lake Bonneville and neotectonics of the eastern Basin and Range Province, Guidebook for Field Trip 12, Geological Society of America Annual Meeting, Denver, Colorado: Utah Geological and Mineral Survey Miscellaneous Publication 88-1, p. 66–73, https://doi.org/10.34191/MP-88-1.

Cashman, P.H., 1992, Structural geology of the northeastern Stansbury Mountains, *in* Wilson, J.R., editor, Field guide to geologic excursions in Utah and adjacent areas of Nevada, Idaho, and Wyoming, for Geological Society of America, Rocky Mountain Section Meeting May 13–15, 1992: Utah Geological and Mineral Survey Miscellaneous Publication 92-3, p. 171–178, https://doi.org/10.34191/MP-92-3.

Chamberlin, C.K., and Clark, D.L., 1973, Trace fossils and conodonts as evidence for deep water deposits in the Oquirrh basin of central Utah: Journal of Paleontology, v. 47, p. 663–682.

Chapusa, F.W.P., 1969, Geology and structure of Stansbury Island, Tooele County, Utah: Salt Lake City, University of Utah, M.S. thesis, 83 p., 2 plates, map scale 1:24,000.

Chen, C.Y., and Maloof, A.C., 2017, Revisiting the deformed high shoreline of Lake Bonneville: Quaternary Science Reviews, v. 159, p. 169–189.

Chesley, J.T., and Ruiz, J., 1997, Preliminary Re-Os dating on molybdenite mineralization from the Bingham Canyon porphyry copper deposit, Utah, *in* John, D.A., and Ballantyne, G.H., editors, Geology and ore deposits of the Oquirrh and Wasatch Mountains, Utah: Society of Economic Geologists Guidebook Series 29, p. 165–169.

Christiansen, R.L., and Lipman, P.W., 1972, Cenozoic volcanism and plate tectonic evolution of the western United States—II, Late Cenozoic: Philosophical Transactions of the Royal Society of London, Series A, Mathematical and Physical Sciences, v. 271, no. 1213, p. 249-284.

Christiansen, R.L., and McKee, E.H., 1978, Late Cenozoic volcanic and tectonic evolution of the Great Basin and Columbia intermontane regions: Geological Society of America Memoir 152, p. 283–311.

Christie-Blick, N., 1983, Glacial-marine and subglacial sedimentation, Upper Proterozoic Mineral Fork Formation, Utah, *in* Molnia, B.F., editor, Glacial-marine Sedimentation: New York, Plenum Press, p. 703–775.

Clark, D.L., 2017, Tooele 30' x 60' quadrangle geologic map—faults, lakes, and resources: Utah Geological Survey Survey Notes, v. 49, no. 2, p. 1–3, https://doi.org/10.34191/SNT-49-2.

Clark, D.L., 2019, Northern Cedar Mountains Red Beds, Tooele County, *in* Milligan, M., Biek, R.F., Inkenbrandt, P., and Nielsen, P., editors, Utah Geosites: Utah Geological Association Publication 48, 5 p., https://doi.org/10.31711/geosites.v1i1.57.

Clark, D.L., 2020, The Uinta-Tooele structural zone—what's in a name?: Utah Geological Survey Survey Notes, v. 52, no. 2, p. 4–5.

Clark, D.L., and Biek, R.F., 2017, Whole-rock geochemical results for the Tooele 30' x 60' quadrangle and the Copperton 7.5' quadrangle, Utah: Utah Geological Survey Open-File Report 665, 1 p., https://doi.org/10.34191/OFR-665.

Clark, D.L., and Kirby, S.M., 2009, Reevaluating Cambrian stratigraphy in the Stansbury and northern Sheeprock Mountains, northwest Utah—a progress report, *in* Tripp, B.T., Krahulec, K., and Jordan, L., editors, Geology and geologic resources and issues of western Utah: Utah Geological Association Publication 38, p. 17–26.

Clark, D.L., Kirby, S.M., and Oviatt, C.G., 2012, Interim geologic map of the Rush Valley 30' x 60' quadrangle, Tooele, Utah and Salt Lake Counties, Utah: Utah Geological Survey Open-File Report 593, 65 p., 2 plates, scale 1:62,500, https://doi.org/10.34191/OFR-593.

Clark, D.L., Kirby, S.M., and Oviatt, C.G., 2021, Geologic map of the Rush Valley 30' x 60' quadrangle, Tooele, Utah and Salt Lake Counties, Utah: Utah Geological Survey Map, scale 1:62,500.

Clark, D.L., Oviatt, C.G., Hardwick, C.L., and Page, D., 2020, Interim geologic map of the Bonneville Salt Flats and east part of the Wendover 30' x 60' quadrangles, Tooele County, Utah—Year 3: Utah Geological Survey Open-File Report 731, 30 p., 2 plates, scale 1:62,500.

Clark, D.L., Oviatt, C.G., and Dinter, D.A., 2018a, Geologic map of the Tooele 30' x 60' quadrangle—an update to the geologic history of northwest Utah: Geological Society of America Abstracts with Programs, v. 50, no. 5, p. 27.

Clark, D.L., Oviatt, C.G., and Dinter, D.A., 2018b, Geologic map of the Tooele 30' x 60' quadrangle, Tooele, Salt Lake and Davis Counties, Utah: Lake Bonneville Geologic Conference and Short Course, Utah Department of Natural Resources, Salt Lake City, October 3–4, 2018 (poster).

Clark, D.L., Oviatt, C.G., and Page, D., 2016, Geologic map of Dugway Proving Ground and adjacent areas, Tooele County, Utah: Utah Geological Survey Map 274DM, 31 p., 2 plates, GIS data, scale 1:75,000, https://doi.org/10.34191/M-274DM.

Cohenour, R.E., 1959, Sheeprock Mountains, Precambrian and Paleozoic stratigraphy, igneous rocks, structure, geomorphology, and economic geology: Utah Geological and Mineral Survey Bulletin 63, 201 p., https://doi.org/10.34191/B-63.

Colman, S.M., Kelts, K.R., and Dinter, D.A., 2002, Depositional history and neotectonics in Great Salt Lake, Utah from high-resolution seismic stratigraphy: Sedimentary Geology, v. 148, p. 61–78.

Constenius, K.N., 1996, Late Paleogene extensional collapse of the Cordilleran foreland fold and thrust belt: Geological Society of America Bulletin, v. 108, p. 20–39.

Constenius, K.N., Esser, R.P., and Layer, P.W., 2003, Extensional collapse of the Charleston-Nebo salient and its relationship to space-time variations in Cordilleran orogenic belt tectonism and continental stratigraphy, *in* Raynolds, R.G., and Flores, R.M., editors, Cenozoic Systems of the Rocky Mountain Region, Rocky Mountain SEPM, Denver, CO, p. 303–343.

Constenius, K.N., Clark, D.L., King, J.K., and Ehler, J.B., 2011, Interim geologic map of the Provo 30' x 60' quadrangle, Utah, Wasatch, and Salt Lake Counties, Utah: Utah Geological Survey Open-File Report 586DM, 42 p., 2 plates, contains GIS data, scale 1:62,500, https://doi.org/10.34191/OFR-586DM.

Constenius, K.N, Coogan, J.C., and Clark, D.L., in preparation, Geologic map of the Provo 30' x 60' quadrangle, Utah, Wasatch, and Salt Lake Counties, Utah: Utah Geological Survey Map, scale 1:62,500.

Coogan, J.C., and Constenius, K.N., 2003, Structural continuity of the Sevier thrust belt across the Uinta arch: American Association of Petroleum Geologist Annual Meeting Field Trip 16, 25 p.

Coogan, J.C., and King, J.K., 2016, Interim geologic map of the Ogden 30' x 60' quadrangle, Box Elder, Cache, Morgan, Rich, Summit, Weber Counties, Utah, and Uinta County, Wyoming: Utah Geological Survey Open-File Report 653DM, 147 p., 3 plates, GIS data, scale 1:62,500, https://doi.org/10.34191/OFR-653DM.

Cook, K.L., Bankey, V., Mabey, D.R., and DePangher, M., 1989, Complete Bouguer gravity anomaly map of Utah: Utah Geological and Mineral Survey Map 122, 1 plate, scale 1:500,000, https://doi.org/10.34191/M-122.

Crittenden, M.D., Jr., 1963, New data on the isostatic deformation of Lake Bonneville: U.S. Geological Survey Professional Paper 454-E, 31 p.

Crittenden, M.D., Jr., 1976, Stratigraphic and structural setting of the Cottonwood area, Utah, *in* Hill, J.G., editor, Geology of the Cordilleran hingeline: Denver, Rocky Mountain Association of Geologists, p. 363–379.

Currey, D.R., 1980, Coastal geomorphology of Great Salt Lake and vicinity, *in* Gwynn, J.W., editor, Great Salt Lake—a scientific, historical, and economic overview: Utah Geological and Mineral Survey Bulletin 116, p. 69–82, https://doi.org/10.34191/B-116.

Currey, D.R., 1982, Lake Bonneville—selected features of relevance to neotectonic analysis: U.S. Geological Survey Open-File Report 82-1070, 30 p., 1 plate, scale 1:500,000.

Currey, D.R., and Oviatt, C.G., 1985, Durations, average rates, and probable causes of Lake Bonneville expansions, stillstands, and contractions during the last deep lake cycle, 32,000 to 10,000 years ago, *in* Kay, P.A., and Diaz, H.F., editors, Problems of and prospects for predicting Great Salt Lake levels: University of Utah Center for Public Affairs and Administration, p. 9–24.

Currey, D.R., Oviatt, C.G., and Plyler, G.B., 1983, Lake Bonneville stratigraphy, geomorphology, and isostatic deformation in west-central Utah, *in* Gurgel, K.D., editor, Geologic excursions in neotectonics and engineering geology in Utah, Guidebook—Part IV: Utah Geological and Mineral Survey Special Studies 62, p. 63–82, https://doi.org/10.34191/SS-62.

Dames & Moore, The Ralph M. Parsons Company, and Roger Foott Associates, Inc., 1987, Site proposal for the Superconducting Super Collider, Cedar Mountains site—Appendix A, Geotechnical Report, Site Geologic Map 1:50,000 scale: Utah Department of Business and Economic Development, 2 volumes, variously paginated.

Davis, D.E., 1956, A taxonomic study of Mississippian corals of central Utah: Brigham Young University Research Studies, Geology Series, v. 3, no. 5, 50 p.

Davis, B.L., 1959, Petrology and petrography of the igneous rocks of the Stansbury Mountains, Tooele County, Utah: Brigham Young University Geology Studies, v. 6, no. 2, 56 p.

Davis, O.K., 1998, Palynological evidence for vegetation cycles in a 1.5 million year pollen record from the Great Salt Lake, Utah, USA: Palaeogeography, Palaeoclimatology, Palaeoecology, v. 138, p. 175–185.

Davis, L.E., Dyman, T.S., Webster, G.D., and Schwarz, D., 1989, Measured stratigraphic sections of West Canyon Limestone and equivalent strata (upper Mississippian-middle Pennsylvanian), lower Oquirrh Group, northern Utah and southeastern Idaho: U.S. Geological Survey Open-File Report 89-292, 47 p.

Davis, L.E., Webster, G.D., and Dyman, T.S., 1994, Correlation of the West Canyon, Lake Point, and Bannock Peak Limestones (Upper Mississippian to Middle Pennsylvanian), basal formations of the Oquirrh Group, northern Utah and southeastern Idaho: U.S. Geological Survey Bulletin 2088, 30 p., 1 plate.

DeCelles, P.G., 2004, Late Jurassic to Eocene evolution of the Cordilleran thrust belt and foreland basin system, western U.S.A.: American Journal of Science, v. 304, p. 105–168.

DeCelles, P.G., and Coogan, J.C., 2006, Regional structure and kinematic history of the Sevier fold-and-thrust belt, central Utah: Geological Society of America Bulletin, v. 118, p. 841–864.

Dehler, C.M., Fanning, C.M., Link, P.K., Kingsbury, E.M., and Rybczynski, D., 2010, Maximum depositional age and provenance of the Uinta Mountain Group and Big Cottonwood Formation, northern Utah—paleogeography of rifting western Laurentia: Geological Society of America Bulletin, v. 122, no. 9/10, p. 1686–1699.

Deino, A., and Keith, J.D., 1997, Ages of volcanic and intrusive rocks in the Bingham mining district, Utah, *in* John, D.A., and Ballantyne, G.H., editors, Geology and ore deposits of the Oquirrh and Wasatch Mountains, Utah: Society of Economic Geologists Guidebook Series, v. 29, p. 91–100.

Dinter, D., Haskell, B., Valero-Garcés, B., Schnurrenberger, D., Heil, C., Dean, W., and Kruger, N., 2001, GLAD1, Great Salt Lake Site 3, *in* Schnurrenberger, D., and Haskell, B., editors, Initial reports of the global lakes drilling program, volume 1, Glad1, Great Salt Lake, Utah and Bear Lake, Utah/Idaho: Limnological Research Center, Minneapolis, University of Minnesota, p. 30–36.

Dinter, D.A., and Pechmann, J.C., 2001?, Paleoseismology of the East Great Salt Lake fault (Phase 3): Final Technical Report for U.S. Geological Survey, award number 00HQGR0099, 7 p.

Dinter, D.A., and Pechmann, J.C., 2014, Paleoseismology of the Promontory segment, East Great Salt Lake fault: Final Technical Report for U.S. Geological Survey, award number 02HQGR0105, 23 p.

Dinter, D.A., and Pechmann, J.C., 2015, Paleoseismology of the northern segments of the Great Salt Lake fault: Utah Quaternary Fault Parameters Working Group Meeting February 10, 2015, https://geology.utah.gov/docs/pdf/UQFPWG-2015_Presentations.pdf.

Doelling, H.H., 1964, Geology of the northern Lakeside Mountains and the Grassy Mountains and vicinity, Tooele and Box Elder Counties, Utah: Salt Lake City, University of Utah, Ph.D. dissertation, 354 p., 5 plates, scale 1:31,680.

Doelling, H.H., 2003, Unpublished digital update to 1964 Ph.D. dissertation: UGS files, text variously paginated, 6 colored maps, 10 colored cross sections.

Doelling, H.H., Solomon, B.J., and Davies, S.F., 1994, Geologic map of the Grayback Hills quadrangle, Tooele County, Utah: Utah Geological Survey Map 166, 22 p., 2 plates, scale 1:24,000, https://doi.org/10.34191/M-166.

Doelling, H.H., Willis, G.C., Jensen, M.E., Hecker, S., Case, W.F., and Hand, J.S. (with contributions by Davis, F.D., Klauk, R.H., Gwynn, J.W., Bishop, C.E., and Atwood, G.), 1990, Geologic map of Antelope Island, Davis County, Utah: Utah Geological Survey Map 127, 2 plates, 27 p., scale 1:24,000, https://doi.org/10.34191/M-127.

Douglass, R.C., Moore, W.J., and Huddle, J.W., 1974, Stratigraphy and microfauna of the Oquirrh Group in the western Traverse Mountains and northern Lake Mountains, Utah: U.S. Geological Survey Journal of Research, v. 2, no. 1, p. 97–104.

Eardley, A.J., 1939, Structure of the Wasatch-Great Basin region: Geological Society of America Bulletin, v. 50, p. 1277–1310.

Eardley, A.J., and Gvosdetsky, V., 1960, Analysis of Pleistocene core from Great Salt Lake, Utah: Geological Society of America Bulletin, v. 71, p. 1323–1344.

Eardley, A.J., Shuey, R.T., Gvosdetsky, V., Nash, W.P., Picard, M.D., Grey, D.C., and Kukla, G.J., 1973, Lake cycles in the Bonneville basin, Utah: Geological Society of America Bulletin, v. 84, p. 211–216.

Economic Geology (11 papers), 1978, v. 73, no. 7, p. 1215–1365.

Eleogram, B., 2014, The application of zircon (U-Th)/He thermochronology to determine the timing and slip rate of the Willard thrust, Sevier fold and thrust belt, northern Utah: Las Vegas, University of Nevada, M.S. thesis, 131 p.

Erickson, A.J., Jr., 1974, The Uinta-Gold Hill trend—an economically important lineament, *in* Hodgson, R.A., Gay, S.P., Jr., Benjamins, J.Y., editors, Proceedings from the first international conference on the new basement tectonics: Utah Geological Association Publication 5, p. 126–138.

Erskine, M.C., 1997, The Oquirrh basin revisited: American Association of Petroleum Geologists Bulletin, v. 81 no. 4, p. 624–636.

Foose, M.P., 1989, Geologic map of the northern Stansbury Mountains Wilderness Study Area, Tooele County, Utah: U.S. Geological Survey Miscellaneous Field Studies Map MF-2061, scale 1:24,000.

Garcia, P.E., 2015, Paleoecology of the Upper Cambrian carbonate units, House Range and South Lakeside Mountains, Utah: Salt Lake City, University of Utah, M.S thesis, 122 p.

Geunthner, W.R., Reiners, P.W., DeCelles, P.G., and Kendall, J., 2015, Sevier belt exhumation in central Utah constrained from complex zircon (U-Th)/He data sets—radiation damage and He inheritance effects on partially reset detrital zircons: Geological Society of America Bulletin, v. 127, no. 3/4, p. 323–328.

Gilbert, G.K., 1890, Lake Bonneville: U.S. Geological Survey Monograph 1, 438 p.

Gilluly, J., 1932, Geology and ore deposits of the Stockton and Fairfield quadrangles, Utah: U.S. Geological Survey Professional Paper 173, 171 p., 12 plates, scale 1:62,500.

Godsey, H.S., Currey, D.R., and Chan, M.A., 2005, New evidence for an extended occupation of the Provo shoreline and implications for regional climate change, Pleistocene Lake Bonneville, Utah, USA: Quaternary Research, v. 63, p. 212–223.

Godsey, H.S., Oviatt, C.G., Miller, D.M., and Chan, M.A., 2011, Stratigraphy and chronology of offshore to nearshore deposits associated with the Provo shoreline, Pleistocene Lake Bonneville, Utah: Palaeogeography, Palaeoclimatology, Palaeoecology, v. 310, Issues 3/4, p. 442–450.

Green, S.A., and Currey, D.R., 1988, The Stansbury shoreline and other transgressive deposits of the Bonneville lake cycle: Utah Geological and Mineral Survey Miscellaneous Publication 88-1, p. 55–57, https://doi.org/10.34191/MP-88-1.

Gruen, G., Heinrich, C.A., and Schroeder, K., 2010, The Bingham Canyon porphyry Cu-Mo-Au Deposit, II—vein geometry and ore shell formation by pressure-driven rock extension: Economic Geology, v. 105, no. 1, p. 69–90.

Gunter, W.L., 1991, The geology of the Barneys Canyon and Melco gold deposits, Salt Lake County, Utah, *in* Black, J.E., and Babcock, R.C., editors, Guidebook to the geology and ore deposits of the Bingham mining district and northern Oquirrh Mountains, Utah: 1991 RTZ Group Mining and Exploration Conference, Salt Lake City, Utah, 21 p.

Gunter, W.L., and Austin, G.W., 1997, Geology of the Melco gold deposit, Oquirrh Mountains, Utah, *in* John, D.A., and Ballantyne, G.H., editors, Geology and ore deposits of the Oquirrh and Wasatch Mountains, Utah: Society of Economic Geologists Guidebook Series, v. 29, p. 227–240.

Gwynn, J.W., editor, 1980, Great Salt Lake—a scientific, historical, and economic overview: Utah Geological and Mineral Survey Bulletin 116, 400 p., 2 plates, https://doi.org/10.34191/B-116.

Gwynn, J.W., editor, 2002, Great Salt Lake—an overview of change: Utah Geological Survey Special Publication, 584 p.

Harlick, A.J., 1989, Sedimentology, paleoecology and diagenesis of the Upper Cambrian St. Charles Formation, southern Lakeside Mountains, Utah: Salt Lake City, University of Utah, M.S. thesis, 277 p.

Harris, M.T., and Sheehan, P.M., 1996, Upper Ordovician-Lower Silurian depositional sequences determined from middle shelf sections, Barn Hills and Lakeside Mountains, eastern Great Basin, *in* Witzke, B.J., Ludvigson, G.A., and Day, J., editors, Paleozoic sequence stratigraphy—views from the North American Craton: Geological Society of America Special Paper 306, p. 161–176.

Helm, J.M., 1994, Structure and tectonic geomorphology of the Stansbury fault zone, Tooele County, Utah, and the effect of crustal structure on Cenozoic faulting patterns: Salt Lake City, University of Utah, M.S. thesis, 128 p., 2 plates.

Helm, J.M., 1995, Quaternary faulting in the Stansbury fault zone, Tooele County, Utah, *in* Lund, W.L., editor, Environmental & engineering geology of the Wasatch front region: Utah Geological Association Publication 24, p. 31–44.

Hintze, L.F., 1959, Ordovician regional relationships in north-central Utah and adjacent areas, *in* Williams, N.C., editor, Guidebook to the geology of the Wasatch and Uinta Mountains transition area: Intermountain Association of Petroleum Geologists Tenth Annual Field Conference Guidebook, p. 46–53.

Hintze, L.F., 1988, Geologic history of Utah: Brigham Young University Geology Studies, Special Publication 7, 202 p.

Hintze, L.F., and Davis, F.D., 2003, Geology of Millard County, Utah: Utah Geological Survey Bulletin 133, 305 p., https://doi.org/10.34191/B-133.

Hintze, L.F., and Kowallis, B.J., 2009, Geologic history of Utah: Brigham Young University Geology Studies, Special Publication 9, 225 p.

Hintze, L.F., Willis, G.C., Laes, D.Y.M., Sprinkel, D.A., and Brown, K.D., 2000, Digital geologic map of Utah: Utah Geological Survey Map 179DM, https://doi.org/10.34191/M-179DM.

Hogg, N.C., 1972, Shoshonitic lavas in west-central Utah: Brigham Young University Geology Studies, v. 19, part 2, p. 133–184.

Hollis, N., 2015, Tracking Late Devonian reactivation of the Tooele Arch with detrital zircon provenance, Great Basin: Pocatello, Idaho State University, M.S. thesis, 74 p.

Hood, J.W., and Waddell, K.M., 1968, Hydrologic reconnaissance of Skull Valley, Tooele County, Utah: Utah Department of Natural Resources Technical Publication no. 18, 57 p., 2 plates.

Houston, R.S., editor, 1993, The Wyoming Province (Chapter 3), *in* Reed, J.C., Jr. and others, editors, Precambrian—Conterminous U.S.: Geological Society of America, The Geology of North America, v. C-2, p. 121–170.

Howell, J.R., 1978, Stratigraphy and paleontology of the Fitchville Formation (Lower Mississippian) on Stansbury Island, Great Salt Lake, Utah: Salt Lake City, University of Utah, M.S. thesis, 134 p.

Hylland, M.D., DuRoss, C.B., McDonald, G.N., Olig, S.S., Oviatt, C.G., Mahan, S.A., Crone, A.J., and Personius, S.F., 2012, Basin-floor Lake Bonneville stratigraphic section as revealed in paleoseismic trenches at the Baileys Lake site, West Valley fault zone, Utah, *in* Hylland, M.D., and Harty, K.M., editors, Selected topics in engineering and environmental geology in Utah: Utah Geological Association Publication 41, p. 175–193.

Hylland, M.D., DuRoss, C.B., McDonald, G.N., Olig, S.S., Oviatt, C.G., Mahan, S.A., Crone, A.J., and Personius, S.F., 2014, Late Quaternary paleoseismology of the West Valley fault zone—insights from the Baileys Lake trench site, *in* DuRoss, C.B., and Hylland, M.D., Evaluating surface faulting chronologies of graben-bounding faults in Salt Lake Valley, Utah—new paleoseismic data from the Salt Lake City segment of the Wasatch fault zone and the West Valley fault zone: Utah Geological Survey Special Study 149, Paleoseismology of Utah Volume 24, 76 p., 12 appendices, 2 plates, https://doi.org/10.34191/SS-149.

International Commission on Stratigraphy, International Chronostratigraphic Chart v 2020/01: Online, http://www.stratigraphy.org/index.php/ics-chart-timescale, accessed May 1, 2020.

Janecke, S.U., and Evans, J.P., 2017, Revised structure and correlations of the Great Salt Lake, North Promontory, Rozel and Hansel Valley fault zones revealed by the 2015–2016 low stand of Great Salt Lake: Utah Geological Association Publication 46, variously paginated, electronic appendices [omitted].

John, D.A., and Ballantyne, G.H., editors, 1997, Geology and ore deposits of the Oquirrh and Wasatch Mountains, Utah: Society of Economic Geologists Guidebook Series, v. 29, 256 p., 2 plates.

Jordan, T.E., 1979a, Evolution of the Late Pennsylvanian-Early Permian western Oquirrh basin, Utah: Palo Alto, California, Stanford University, Ph.D. thesis, 253 p.

Jordan, T.E., 1979b, Lithofacies of the Upper Pennsylvanian and Lower Permian western Oquirrh Group, northwest Utah: Utah Geology v. 6, no. 2, p. 41 to 56.

Jordan, T.E., and Douglass, R.C., 1980, Paleogeography and structural development of the late Pennsylvanian to early Permian Oquirrh Basin, northwestern Utah, *in* Paleozoic paleogeography of the west-central United States, Rocky Mountain Section, Society of Economic Paleontologists and Mineralogists, Denver, p. 217–238.

Keaton, J.R., and Currey, D.R., 1989, Earthquake hazard evaluation of the West Valley fault zone in the Salt Lake City urban area, Utah: Technical report to U.S. Geological Survey, Salt Lake City, under Contract 14-08-001-G1397, 69 p.

Keaton, J.R., Currey, D.R., and Olig, S.J., 1987, Paleoseismicity and earthquake hazards evaluation of the West Valley fault zone, Salt Lake urban area: Technical report to U.S. Geological Survey, under Contract 14-08-0001-22048, April 1986 (Draft), 18 p.

Kenney, T.A., Wright, S.J., and Stolp, B.J., 2006, Ground-water movement and water quality in Lake Point, Tooele County, Utah, 1999–2003: U.S. Geological Survey Scientific Investigations Report 2006-5124, 13 p.

Kennecott Utah Copper Corporation (KUCC), 2009, Geologic map of the Bingham Canyon mine (using detailed mapping 1982–2009): unpublished map by Rio Tinto Corporation, prepared by Bingham mine geology staff, scale 1:4800.

Kleber, E.J., McKean, A.P., Hiscock, A.I., Hylland, M.D., Hardwick, C.L., McDonald, G.N., Anderson, Z.W., Bowman, S.D., Willis, G.C., and Erickson, B.A., 2020, Geologic Setting, Ground Effects, and Proposed Structural Model for the 18 March 2020 M_w 5.7 Magna, Utah, Earthquake: Seismological Research Letters, 15 p., https://doi.org/10.1785/0220200331.

Kloppenburg, A., Grocott, J., and Hutchinson, D., 2010, Structural setting and synplutonic fault kinematics of a Cordilleran Cu-Au-Mo porphyry mineralization system, Bingham mining district, Utah: Economic Geology, v. 105, no. 1, p. 743–761.

Konopka, E.H., 1999, Stratigraphy and sedimentology of the Butterfield Peaks Formation (Middle Pennsylvanian), Oquirrh Group, in central Utah: Madison, University of Wisconsin, Ph.D. dissertation, 259 p.

Kowalewska, A., and Cohen, A.S., 1998, Reconstruction of paleoenvironments of the Great Salt Lake basin during the late Cenozoic: Journal of Paleolimnology, v. 20, p. 381–407.

Krahulec, K.A., 2005, Rush Valley mining district, Tooele County, Utah, *in* Rasmussen, H., Crafford, E.J., O'Malley, P., and Callicrate, T., editors, Porphyry deposits of the Great Basin, Field Trip Guidebook 9: Geological Society of Nevada Symposium 2005 Window to the World, p. 75–80.

Kwon, S., and Mitra, G., 2004, Strain distribution, strain history, and kinematic evolution associated with the formation of arcuate salient in fold-thrust belts—the example of the Provo salient, Sevier orogeny, Utah: Geological Society of America Special Paper 383, p. 205–223.

Laabs, B.J.C., and Carson, E.C., 2005, Glacial geology of the southern Uinta Mountains, *in* Dehler, C.M., Pederson, J.L., Sprinkel, D.A., and Kowallis, B.J., editors, Uinta Mountain geology: Utah Geological Association Publication 33, p. 235–253.

Laabs, B.J.C., and Monroe, J.S., 2016, Chapter 17, Late Pleistocene mountain glaciation in the Lake Bonneville basin, *in* Oviatt, C.G. and Shroder, J.F., editors, Lake Bonneville—a scientific update—developments in earth surface processes, volume 20: Elsevier B.V., p. 462–503.

Laes, D.Y.M., Krahulec, K.A., and Ballantyne, G.H., compilers, 1997, Geologic map of the Oquirrh Mountains, Utah, *in* John, D.A., and Ballantyne, G.H., editors, Geology and ore deposits of the Oquirrh and Wasatch Mountains, Utah: Society of Economic Geologists Guidebook Series, v. 29, plate 1, scale 1:62,500.

Lambert, P.M., 1995, Numerical simulation of ground-water flow in basin-fill material in Salt Lake Valley, Utah: Utah Department of Natural Resources Technical Publication 110-B, 58 p.

Lambert, P.M., and West, J.C., 1988, Continuous seismic-reflection survey of the Great Salt Lake, Utah—east of Antelope and Fremont Islands: U.S. Geological Survey Water-Resources Investigations Report 88-4157, 17 p., 1 plate.

Landtwing, M.R., Furrer, C., Redmond, P.B, Pettke, T., Guillong, M., and Heinrich, C.A., 2010, The Bingham Canyon porphyry Cu-Mo-Au deposit, III—zoned copper-gold ore deposition by magmatic vapor expansion: Economic Geology, v. 105, no. 1, p. 91–118.

Langenheim, V.E., 2016, Aeromagnetic map of northwest Utah and adjacent parts of Nevada and Idaho: Utah Geological Survey Miscellaneous Publication 16-4, 8 p., 1 plate, scale 1:200,000, https://doi.org/10.34191/MP-16-4.

Lanier, G., John, E.C., Swensen, A.J., Reid, J., Bard, C.E., Caddey, S.W., and Wilson, J.C., 1978, General geology of the Bingham mine, Bingham Canyon, Utah: Economic Geology, v. 73, no. 7, p. 1228–1241.

Lawton, T.F., Boyer, S.E., Schmitt, J.G., 1994, Influence of inherited taper on structural variability and conglomerate distribution, Cordilleran fold and thrust belt, western United States: Geology, v. 22, p. 339–342.

LeBas, M.J., Le Maitre, R.W., Streckheisen, A., and Zanettin, B., 1986, A chemical classification of volcanic rocks based on the total alkali-silica diagram: Journal of Petrology, v. 27, p. 745–750.

Lipman, P.W., Prostka, H.J., and Christiansen, R.L., 1972, Cenozoic volcanism and plate tectonic evolution of western United States—Part 1, Early and Middle Cenozoic, in A discussion on volcanism and structure of the Earth: Philosophical Transactions of the Royal Society of London, Series A, v. 271, no. 1213, p. 217–248.

Lisiecki, L.E., and Raymo, M.E., 2005, A Pliocene-Pleistocene stack of 57 globally distributed benthic $\delta^{18}O$ records: Paleoceanography, v. 20, PA1003, https://doi.org/10.1029/2004PA001071.

Lowe, M., and Wallace, J., 1999, Protecting groundwater quality through aquifer classification—examples from Cache, Ogden, and Tooele Valley, Utah, *in* Spangler, L.E., and Allen, C.J., editors, Geology of Northern Utah and vicinity: Utah Geological Association Publication 27, p. 275–312.

Lowe, M., Wallace, J., Butler, M., Riding, R., and Johnson, A., 2004, Ground-water sensitivity and vulnerability to pesticides, Tooele Valley, Tooele County, Utah: Utah Geological Survey Miscellaneous Publication 04-3, 23 p., https://doi.org/10.34191/MP-04-3.

Lufkin, J.L., 1965, Geology of the Stockton stock and related intrusives, Tooele County, Utah: Brigham Young University Geology Studies, v. 12, p. 149–164.

Mabey, D.R., 1986, Notes on the historic high level of Great Salt Lake: Utah Geological and Mineral Survey Survey Notes, v. 20, no. 2, p. 13-15.

Mabey, D.R., Tooker, E.W., and Roberts, R.J., 1963, Gravity and magnetic anomalies in the northern Oquirrh Mountains, Utah, *in* Geological Survey Research 1962: U.S. Geological Survey Professional Paper 450-E, p. E28–31.

Maughan, D.T., 2001, Mafic to intermediate alkaline rocks of the the Bingham district, Utah: Provo, Utah, Brigham Young University, M.S. thesis, 238 p.

Maughan, D.T., Keith, J.D., Christiansen, E.H., Pulsipher, T., Hattori, K., and Evans, N.J., 2002, Contributions from mafic alkaline magmas to the Bingham porphyry Cu-Au-Mo deposit, Utah, U.S.A.: Mineralium Deposita, v. 37, p. 14–37.

Maurer, R.E., 1970, Geology of the Cedar Mountains, Tooele County, Utah: Salt Lake City, University of Utah, Ph.D. dissertation, 184 p., 10 plates, scale 1:43,700.

McKean, A.P., 2019, Geologic map of the Saltair NE quadrangle, Salt Lake and Davis Counties, Utah: Utah Geological Survey Map 282DM, 28 p., 2 plates, scale 1:24,000, https://doi.org/10.34191/M-282DM.

McKean, A.P., Doelling, H.H., Willis, G.C., and Yonkee, W.A., 2019, Geologic map of the Antelope Island South quadrangle, Salt Lake, Davis, and Tooele Counties, Utah: Utah Geological Survey Map 280DM, 28 p., 2 plates, scale 1:24,000, https://doi.org/10.34191/M-280DM.

McKean, A.P., and Hylland, M.D., 2019, Geologic map of the Baileys Lake quadrangle, Salt Lake and Davis Counties, Utah: Utah Geological Survey Map 281DM, 28 p., 2 plates, scale 1:24,000, https://doi.org/10.34191/M-281DM.

McNeil, B.R., and Smith, R.B., 1992, Upper crustal structure of the northern Wasatch Front, Utah, from seismic reflection and gravity data: Utah Geological Survey Contract Report 92-7, 62 p., 2 plates, https://doi.org/10.34191/CR-92-7.

Middlemost, E.A.K., 1994, Naming materials in the magma/igneous rock system: Earth-Science Reviews, v. 37, p. 215–224.

Miller, D.M., 2016, Chapter 7, The Provo Shoreline of Lake Bonneville, *in* Oviatt, C.G. and Shroder, J.F., editors, Lake Bonneville—a scientific update—developments in earth surface processes, volume 20: Elsevier B.V., p. 127–144.

Miller, D.M. and Phelps, G.A., 2016, Chapter 3, The Pilot Valley Shoreline—an early record of Lake Bonneville dynamics, *in* Oviatt, C.G. and Shroder, J.F., editors, Lake Bonneville—a scientific update—developments in earth surface processes, volume 20: Elsevier B.V., p. 60–74.

Miller, D.M., Clark, D.L., Wells, M.L., Oviatt, C.G., Felger, T.J., and Todd, V.R., 2020, Interim geologic map of the Grouse Creek and Utah part of the Jackpot 30' x 60' quadrangles, Box Elder County, Utah and Cassia County, Idaho: Utah Geological Survey Open-File Report 716DM, 31 p., 1 plate, scale 1:62,500, https://doi.org/10.34191/OFR-716DM.

Miller, D.M., Clark, D.L., Wells, M.L., Oviatt, C.G., Felger, T.J., and Todd, V.R., in preparation, Geologic map of the Grouse Creek and east part of the Jackpot 30' x 60' quadrangles, Box Elder County, Utah and Cassia County, Idaho: Utah Geological Survey Miscellaneous Publication, scale 1:62,500.

Miller, D.M., Felger, T.J., and Langenheim, V.E., 2020, Geologic and geophysical maps of the Newfoundland Mountains and part of the adjacent Wells 30' x 60' quadrangles, Box Elder County, Utah: Utah Geological Survey Miscellaneous Publication 173DM, 26 p., 2 plates, scale 1:62,500, https://doi.org/10.34191/MP-173DM.

Miller, D.M., Felger, T.J., and Langenheim, V.E., in preparation, Geologic map of the Tremonton 30' x 60' quadrangle, Box Elder County, Utah: Utah Geological Survey Miscellaneous Publication, scale 1:62,500.

Miller, D.M., Nilsen, T.H., and Bilodeau, W.L., 1992, Late Cretaceous to early Eocene geologic evolution of the U.S. Cordillera (Chapter 6), *in* Burchfiel, B.C., Lipman, P.W., and Zoback, M.L., editors, The Cordilleran Orogen—conterminous U.S.: Geological Society of America, The Geology of North America, v. G-3, p. 205–260.

Moore, W.J., 1973, A summary of radiometric ages of igneous rocks in the Oquirrh Mountains, north-central Utah: Economic Geology, v. 68, no. 1, p. 97–101.

Moore, W.J., and Lanphere, M.A., 1971, The age of porphyry-type copper mineralization in the Bingham mining district, Utah—a refined estimate: Economic Geology, v. 66, p. 331–334.

Moore, W.J., Lanphere, M.A., and Obradovich, J.D., 1968, Chronology of intrusion, volcanism, and ore deposition at Bingham, Utah: Economic Geology, v. 63, no. 6, p. 612–621.

Moore, W.J., and McKee, E.H., 1983, Phanerozoic magmatism and mineralization in the Tooele 1° x 2° quadrangle, Utah, *in* Miller, D.M., Todd, V.R., and Howard, K.A., editors, Tectonic and stratigraphic studies in the eastern Great Basin: Geological Society of America Memoir 157, p. 183–190.

Moore, W.J., and Sorensen, M.L., 1979, Geologic map of the Tooele 1° x 2° quadrangle, Utah: U.S. Geological Survey Miscellaneous Investigation Series Map I-1132, scale 1:250,000.

Moutoux, T.E., 1995, Palynological and tephra correlations among deep wells in the modern Great Salt Lake, Utah, USA—implications for a Neogene through Pleistocene climatic reconstruction: Tucson, University of Arizona, M.S. thesis, 30 p.

Moyle, R.W., 1959, Stratigraphy of the southern Oquirrh Mountains, Manning Canyon Shale: Utah Geological Society Guidebook 14, p. 59–92.

Murchison, S.B., 1989, Fluctuation history of Great Salt Lake, Utah, during the last 13,000 years: Salt Lake City, University of Utah Limnotectonics Laboratory Technical Report 89-2, 137 p.

Murchison, S.B., and Mulvey, W.E., 2000, Late Pleistocene and Holocene shoreline stratigraphy on Antelope Island, *in* King, J.K., and Willis, G.C., editors, The geology of Antelope Island, Davis County, Utah: Utah Geological Survey Miscellaneous Publication 00-1, p. 77–83, https://doi.org/10.34191/MP-00-1.

Nelson, S.T., Hart, G.L., and Frost, C.D., 2011, A reassessment of Mojavia and a new Cheyenne Belt alignment in the eastern Great Basin: Geosphere, v. 7, no. 2, p. 513–527.

New Mexico Geochronology Research Laboratory and Utah Geological Survey, 2006, $^{40}Ar/^{39}Ar$ geochronology results for the Cave Canyon, Fountain Green North, Hilgard Mountain, Pine Park, Skinner Peaks, Tickville Spring, and Veyo quadrangles, Utah: Utah Geological Survey Open-File Report 473, variously paginated, https://doi.org/10.34191/OFR-473.

Nichols, K.M., Silberling, N.J., Cashman, P.H., and Trexler, J.H., Jr., 1992, Extraordinary syorogenic and anoxic deposits amidst sequence cycles of the Late Devonian-Early Mississippian carbonate shelf, Lakeside and Stansbury Mountains, Utah, *in* Wilson, J.R., editor, Field guide to geologic excursions in Utah and adjacent areas of Nevada, Idaho, and Wyoming, prepared for the Geological Society of America Rocky Mountain Section meeting in Ogden, Utah, May 13–15, 1992: Utah Geological Survey Miscellaneous Publication 92-3, p. 123–130, https://doi.org/10.34191/MP-92-3.

Nishizawa, S., Currey, D.R., Brunelle, A., and Sack, D., 2013, Bonneville basin shoreline records of large lake intervals during Marine Isotope Stage 3 and the Last Glacial Maximum: Palaeogeography, Palaeoclimatology, Palaeoecology, v. 386, p. 374–391.

Nygreen, P.W., 1958, The Oquirrh formation—stratigraphy of the lower portion in the type area and near Logan, Utah: Utah Geological and Mineral Survey Bulletin, no. 61, 67 p., https://doi.org/10.34191/B-61.

Oaks, R.Q., Jr., Smith, K.A., Janecke, S.U., Perkins, M.E., and Nash, W.P., 1999, Stratigraphy and tectonics of Tertiary strata of southern Cache Valley, north-central Utah, *in* Spangler, L.E., and Allen, C.J., editors, Geology of northern Utah and vicinity: Utah Geological Association Publication 27, p. 71–110.

Olig, S.S., Lund, W.R., Black, B.D., and Mayes, B.H., 1996, Paleoseismic investigation of the Oquirrh fault zone, Tooele County, Utah, *in* Lund, W.R., editor, The Oquirrh fault zone, Tooele County, Utah—surficial geology and paleoseismology (Paleoseismology of Utah, v. 6): Utah Geological Survey Special Study 88, p. 18–64, 1 plate, https://doi.org/10.34191/SS-88.

Osborn, G., and Bevis, K., 2001, Glaciation in the Great Basin of the western United States: Quaternary Science Reviews, v. 20, p. 1377–1410.

Oviatt, C.G., 2014, The Gilbert episode in the Great Salt Lake basin, Utah: Utah Geological Survey Miscellaneous Publication 14-3, 20 p., https://doi.org/10.34191/MP-14-3.

Oviatt, C.G., 2015, Chronology of Lake Bonneville, 30,000 to 10,000 yr B.P.: Quaternary Science Reviews, v. 110, p. 166–171.

Oviatt, C.G., Atwood, G., and Thompson, R.S., in press, History of Great Salt Lake, Utah, USA, since the termination of Lake Bonneville, *in* Rosen, M.R., Park-Bousch, L., and Finkelstein, D.B., editors, Limnogeology—Progress, challenges and opportunities—A tribute to Beth Gierlowski-Kordesch: Springer.

Oviatt, C.G., Currey, D.R., and Miller, D.M., 1990, Age and paleoclimatic significance of the Stansbury shoreline of Lake Bonneville, northeastern Great Basin: Quaternary Research, v. 33, p. 291–305.

Oviatt, C.G, Currey, D.R., and Sack, D., 1992, Radiocarbon chronology of Lake Bonneville, eastern Great Basin, USA: Palaeogeography, Palaeoclimateology, Palaeoecology, v. 99, p. 225–241.

Oviatt, C.G., Madsen, D.B., and Schmitt, D.N., 2003, Late Pleistocene and early Holocene rivers and wetlands in the Bonneville basin of western North American: Quaternary Research, v. 60 p. 200–210.

Oviatt, C.G. and Miller, D.M., 1997, New explorations along the northern shores of Lake Bonneville, field trip guidebook: Brigham Young University Geology Studies, v. 42, part II, p. 345–371.

Oviatt, C.G., and Shroder, J., editors, 2016, Lake Bonneville—a scientific update—developments in earth surface processes, volume 20: Elsevier B.V., 659 p.

Oviatt, C.G., Thompson, R.S., Kaufman, D.S., Bright, J., and Forester, R.M., 1999, Reinterpretation of the Burmester core, Bonneville basin, Utah: Quaternary Research v. 52, p. 180–184.

Palmer, D.E., 1970, Geology of Stansbury Island, Tooele County, Utah: Brigham Young University Geology Studies, v. 17, pt. 2, p. 3–30, 1 plate, map scale 1:24,000.

Pan-American Center for Earth and Environmental Studies, 2012, North American gravity and magnetic database, University of Texas, El Paso: Online, http://irpsrvgis08.utep.edu/viewers/FlexGravityMagnetic GravityMagnetic_CyberShare, accessed September 17, 2012; site is inactive.

Pang, G., Koper, K.D., Mesimeri, M., Pankow, K.L., Baker, B., Farrell, J., Holt, J., Hale, J.M, Roberson, P., Burlacu, R., Pechmann, J.C., Whidden, K., Holt, M.M, Allam, A., and DuRoss, C., 2020, Seismic analysis of the 2020

Magna, Utah, earthquake sequence—Evidence for a listric Wasatch fault: Geophysical Research Letters, v. 47, 10 p., e2020GL089798, https://doi.org/10.1029/2020GL089798.

Pankow, K.L., Moore, J.R., Hale, J.M., Koper, K.D., Kubacki, T., Whidden, K.M., and McCarter, M.K., 2014, Massive landslide at Utah copper mine generates wealth of geophysical data: GSA Today, v. 24, no. 1, p. 4–9.

Parry, W.T., Wilson, P.N., Moser, D., and Heizler, M.T., 2001, U-Pb dating of zircon and $^{40}Ar/^{39}Ar$ dating of biotite at Bingham, Utah: Economic Geology, v. 96, p. 1671–1683.

Patrickson, S., Sack, D., Brunelle, A.R., and Moser, K.A., 2010, Late Pleistocene to early Holocene paleoclimate insights from Bonneville paleolake dynamics, Stansbury Island, Utah: Quaternary Research, v. 73, p. 237–246.

Paulsen, T., and Marshak, S., 1999, Origin of the Uinta recess, Sevier fold-thrust belt, Utah—influence of basin architecture on fold-thrust geometry: Tectonophysics, v. 312, p. 203–216.

Perkins, M.E., Brown, F.H., Nash, W.P., McIntosh, W., and Williams, S.K., 1998, Sequence, age, and source of silicic fallout tuffs in middle to late Miocene basins of the northern Basin and Range Province: Geological Society of America Bulletin, v. 110, no. 3, p. 344–360.

Personius, S.F., and Scott, W.E., 1992, Surficial geology of the Salt Lake City segment and parts of adjacent segments of the Wasatch fault zone, Davis, Salt Lake, and Utah Counties, Utah: U.S. Geological Survey Miscellaneous Investigations Series Map I-2106, scale 1:50,000.

Petersen, M.S., 1956, Devonian strata of central Utah: Brigham Young University Research Studies, Geology Series, v. 3, no. 3, 36 p., 4 plates.

Petersen, M.S., 1969, The occurrence of ammonoids from the lower Deseret Limestone, northern Stansbury Mountains, Tooele County, Utah: Proceedings Geological Society of America, Rocky Mountain Section, p. 63.

Pierce, K.L., 2004, Pleistocene glaciations of the Rocky Mountains, *in* Gillespie, A.R., Porter, S.C., and Atwater, B.F., editors, The Quaternary period in the United States: Developments in Quaternary Science, v. 1, Amsterdam, Elsevier, p. 63–76.

Pierce, K.L., Licciardi, J.M., Good, J.M., and Jaworowski, C., 2018, Plieistocene Glaciation of the Jackson Hole area, Wyoming: U.S. Geological Survey Professional Paper 1835, 68 p.

Poole, F.G., and Sandberg, C.A., 1991, Mississippian paleogeography and conodont biostratigraphy of the western United States, *in* Cooper, J.D., and Stevens, C.H., editors, Paleozoic Paleogeography of the western United States-II: Pacific Section Society of Economic Paleontologists and Mineralogists, v. 67, p. 107–136.

Porter, J.P., Schroeder, K., and Austin, G., 2012, Geology of the Bingham Canyon porphyry Cu-Mo-Au Deposit, Utah, *in* Hedenquist, J.W., Harris, M., and Camus, F., editors, Geology and genesis of major copper deposit and districts of the world—a tribute to Richard H. Sillitoe: Society of Economic Geologists Special Publication 16, p. 127–146.

Presnell, R.D., 1997, Structural controls on the plutonism and metallogeny in the Wasatch and Oquirrh Mountains, Utah, *in* John, D.A., and Ballantyne, G.H., editors, Geology and ore deposits of the Oquirrh and Wasatch Mountains, Utah: Society of Economic Geologists Guidebook Series, v. 29, p. 1–9.

Pulsifer, T., 2000, The correlation of Eocene extrusive block and ash flows to intrusions at the Bingham copper porphyry system, Utah: Provo, Utah, Brigham Young University, M.S. thesis, 104 p.

Quirk, B.J., Moore, J.R., Laabs, B.J.C., Caffee, M.W., and Plummer, M.A., 2018, Termination II, last glacial maximum, and lateglacial chronologies and paleoclimate from Big Cottonwood Canyon, Wasatch Mountains, Utah: Geological Society of America Bulletin, v. 130, no. 11/12, p. 1889-1902.

Quirk, B.J., Moore, J.R., Laabs, B.J.C., Plummer, M.A., and Caffee, M.W., 2020, Latest Pleistocene glacial and climate history of the Wasatch Range, Utah: Quaternary Science Reviews, v. 238, 17 p.

Radkin, H., Murphy, M., and Schuster, G.T., 1989, Subsurface map and seismic risk analysis of the Salt Lake Valley: Utah Geological and Mineral Survey Open-File Report 152, 82 p., 4 plates, https://doi.org/10.34191/OFR-152.

Raines, G.L., Sawatzky, D.L., and Connors, K.A., 1996, Great Basin geoscience data base: U.S. Geological Survey Data Series 41, CD.

Redmond, P.B., and Einaudi, M.T., 2010, The Bingham Canyon porphyry Cu-Mo-Au deposit, I—sequence of intrusions, vein formation, and sulfide deposition: Economic Geology, v. 105, no. 1, p. 43–68.

Rigby, J.K., 1958, Geology of the Stansbury Mountains, eastern Tooele County, Utah, *in* Rigby, J.K., editor, Geology of the Stansbury Mountains, Tooele County, Utah: Utah Geological Society, Guidebook to the Geology of Utah, no. 13, p. 1–134. Includes geologic map of the Timpie [15'] quadrangle, northern Stansbury Mountains, Tooele County, Utah (plate 1) and geologic cross sections (plate 3), scale 1:63,360.

Rigby, J.K., 1959, Upper Devonian unconformity in central Utah: Geological Society of America Bulletin, v. 70, p. 207–218.

Roberts, R.J., Crittenden, M.D., Tooker, E.W., Morris, H.T., Hose, R.K., and Cheney, T.M., 1965, Pennsylvanian and Permian basins in northwestern Utah and northeastern Nevada and south-central Idaho: American Associaton of Petroleum Geologists Bulletin, v. 40, no. 11, p. 1926–1956.

Rowley, P.D., 1998, Cenozoic transverse zones and igneous belts in the Great Basin, western United States—their tectonic and economic implications, *in* Faulds, J.E., and Stewart, J.H., editors, Accomodation zones and transfer zones—the regional segmentation of the Basin and Range Province: Geological Society of America Special Paper 323, p. 195–228.

Sack, D., 1993, Quaternary geologic map of Skull Valley, Tooele County, Utah: Utah Geological Survey Map 150, 16 p., 1 plate, scale 1:100,000, https://doi.org/10.34191/M-150.

Sack, D., 1995, The shoreline preservation index as a relative-age dating tool for late Pleistocene shorelines—an example from the Bonneville Basin, U.S.A.: Earth Surface Processes and Landforms, v. 20, p. 363–377.

Saltus, R.W., and Blakely, R.J., 2011, Unique geologic insights from "non-unique" gravity and magnetic interpretation: GSA Today, v. 21, no. 12, p. 4–11.

Sandberg, C.A., and Gutschick, R.C., 1979, Guide to conodont biostratigraphy of Upper Devonian and Mississippian rocks along the Wasatch Front and Cordilleran Hingeline, *in* Sandberg, C.A., and Clark, D.L., editors, Conodont biostratigraphy of the Great Basin and Rocky Mountains: Brigham Young University Geology Studies, v. 26, pt. 3, p. 107–134.

Sandberg, C.A., and Gutschick, R.C., 1984, Distribution, microfauna, and source-rock potential of Mississippian Delle Phosphatic Member of Woodman Formation and equivalents, Utah and adjacent states, *in* Woodward, J., Meissner, F.F., and Clayton, J.L., editors, Hydrocarbon source rocks of the Greater Rocky Mountain region: Denver, Colorado, Rocky Mountain Association of Geologists, p. 137–178.

Schnurrenberger, D., and Haskell, B., editors, 2001, Initial reports of the global lakes drilling program. Volume 1. GLAD 1—Great Salt Lake, Utah, and Bear Lake, Utah/Idaho. Covering Expedition GLAD1 of the Drilling Barge Kerry Kelts and the GLAD800 Drilling System, 10 August, 2000 to 4 September, 2000: Limnological Research Center, Minneapolis, University of Minnesota, 315 p.

Schurer, V.C., 1979a, Structural geology of the Kirkman-Diamond Creek Formation, west-central Oquirrh Mountains, Utah: Salt Lake City, University of Utah, M.S. thesis, 46 p., 3 plates, scale 1:12,000.

Schurer, V.C., 1979b, A basin and range chaos in the Oquirrh Mountains, sedimentary or tectonic?, *in* Newman, G.W., and Goode, H.D., editors, Basin and Range symposium and Great Basin field conference: Rocky Mountain Association of Geologists (Denver, CO) and Utah Geological Association (Salt Lake City, UT), p. 267–271.

Silberling, N.J., and Nichols, K.M., 1992a, Depositional cycles of the Upper Devonian-Lower Mississippian Limestone succession in the southern Lakeside Mountains, Utah, with an appendix on the identification and age interpretations of conodont faunas by R.G. Stamm, *in* Wilson, J.R., editor, Field guide to geologic excursions in Utah and adjacent areas of Nevada, Idaho, and Wyoming, prepared for the Geological Society of America Rocky Mountain Section meeting in Ogden, Utah, May 13–15, 1992: Utah Geological Survey Miscellaneous Publication 92-3, p. 131–145, https://doi.org/10.34191/MP-92-3.

Silberling, N.J., and Nichols, K.M., 1992b, Petrology and regional significance of the Mississippian Delle Phosphatic Member, Lakeside Mountains, northwestern Utah, *in* Wilson, J.R., editor, Field guide to geologic excursions in Utah and adjacent areas of Nevada, Idaho, and Wyoming, prepared for the Geological Society of America Rocky Mountain Section meeting in Ogden, Utah, May 13–15, 1992: Utah Geological Survey Miscellaneous Publication 92-3, p. 147–159, https://doi.org/10.34191/MP-92-3.

Slentz, L.W., 1955, Tertiary Salt Lake Group in the Great Salt Lake Basin: Salt Lake City, University of Utah, Ph.D. dissertation, 62 p., 3 plates, scales 1:24,000 and 1:8000.

Smith, W.H., 1975, General structural geology of the Bingham mining district, *in* Bray, R.E., and Wilson, J.C., editors, Guidebook to the Bingham mining district: Bingham Canyon, Utah, Society of Economic Geologists and Kennecott Copper Corporation, p. 41–48.

Smith, R.P., Breckenridge, R.P., and Wood, T.R., 2011, Preliminary assessment of geothermal resource potential at the UTTR: Idaho National Laboratory, prepared for the U.S. Department of Energy, Assistant Secretary for Energy Efficiency and Renewable Energy, Under DOE Idaho Operations Office, Contract DE-AC07-05ID14517, 30 p.

Solomon, B.J., 1993, Quaternary geologic maps of Tooele Valley and the west desert hazardous industry area, Tooele County, Utah: Utah Geological Survey Open-File Report 296, 20 plates, 48 p., scale 1:24,000, https://doi.org/10.34191/OFR-296.

Solomon, B.J., 1996, Surficial geology of the Oquirrh fault zone, Tooele County, Utah, *in* Lund, W.L., editor, Paleoseismology of Utah, Volume 6: Utah Geological Survey Special Study 88, 17 p., 1 plate, scale 1:24,000, https://doi.org/10.34191/SS-88.

Solomon, B.J., Biek, R.F., and Smith, T.W., 2007, Geologic map of the Magna quadrangle, Salt Lake County, Utah: Utah Geological Survey Map 216, 2 plates, scale 1:24,000, https://doi.org/10.34191/M-216.

Spencer, RJ., Baedecker, M.J., Eugster, H.P., Forester, R.M., Goldhaber, M.B., Jones, B.F., Kelts, K., McKenzie, J., Madsen, D.B., Retting, S.L., Rubin, M., and Bowser, C.J., 1984, Great Salt Lake, and precursors, Utah—the last 30,000 years: Contributions to Mineralogy and Petrology, v. 86, p. 321–334.

Stein, H.J., Bankey, V, Cunningham, C.G, Zimbelman, D.R., Brickey, D.W., Shubat, M., Campbell, D.L., and Podwysocki, M.H., 1989, Tooele 1x2 degree quadrangle, northwest Utah—a CUSMAP preassessment study: U.S. Geological Survey Open-File Report 89-0467, 134 p., 22 plates.

Stock, C.W., and Sandberg, C.A., 2019, Latest Devonian (Famennian, *expansa* Zone) conodonts and sponge-microbe symbionts in Pinyon Peak Limestone, Star Range, southwestern Utah, lead to reevaluation of global Dasberg Event: Palaeogeography, Palaeoclimatology, Palaeoecology, v. 534, 14 p., https://doi.org/10.1016/j.palaeo.2019.109271.

Stokes, W.L., 1963, Geologic map of the northwest quarter of Utah: Utah State Land Board, 1 plate, scale 1:250,000.

Stokes, W.L., 1986, Geology of Utah: Utah Museum of Natural History and Utah Geological and Mineral Survey, 280 p.

Stokes, W.L., and Arnold, D.E., 1958, Northern Stansbury Range and the Stansbury Formation, *in* Rigby, J.K., editor, Geology of the Stansbury Mountains, Tooele County, Utah: Utah Geological Society, Guidebook to the Geology of Utah, no. 13, p. 135–149.

Stolp, B.J., and Brooks, L.E., 2009, Hydrology and simulation of ground-water flow in the Tooele Valley ground-water basin, Tooele County, Utah: U.S. Geological Survey Scientific Investigations Report 2009-5154, 85 p., 1 plate.

SWCA Environmental Consultants, 2004, Tooele Valley wetland classification map (plate 1), *in* Burk, N., Bishop, C., and Lowe, M., 2005, Wetlands in Tooele Valley, Utah—an evaluation of threats posed by groundwater development and drought: Utah Geological Survey Special Study 117, 37 p., 1 plate, scale 1:40,000, https://doi.org/10.34191/SS-117.

Swan, F.H., Hanson, K.L., Youngs, R.R., and Angell, M.M., 2005, Paleoseismic investigations of the Stansbury and mid-valley faults, Skull Valley, Utah, *in* Lund, W.L., editor, Proceedings, Basin and Range Province seismic hazard summit II: Utah Geological Survey Miscellaneous Publication MP-05-2, 21 p., https://doi.org/10.34191/MP-05-2.

Swensen, A.J., 1975, Sedimentary and igneous rocks of the Bingham mining district, *in* Bray, R.E., and Wilson, J.C., editors, Guidebook to the Bingham mining district: Bingham Canyon, Utah, Society of Economic Geologists and Kennecott Copper Corporation, p. 21–39.

Swensen, A.J., and Kennecott staff, compilers, 1991, Geologic map of the Bingham district, *in* Black, J.E., and Babcock, R.C., editors, Guidebook to the geology and ore deposits of the Bingham mining district and northern Oquirrh Mountains, Utah: RTZ Group Mining and Exploration Conference, Salt Lake City, Utah, map (plate 1), scale 1:24,000.

Teichert, J.A., 1959, Geology of the southern Stansbury Range, Tooele County, Utah: Utah Geological and Mineralogical Survey Bulletin 65, 75 p., https://doi.org/10.34191/B-65.

Thiros, S.A., 1995, Chemical composition of groundwater, hydrologic properties of basin-fill materials, and groundwater movement in Salt Lake Valley, Utah: Utah Department of Natural Resources Technical Publication 110-A, 60 p., 2 plates.

Thomas, G., 1957, Oquirrh Range, Garfield quadrangle: Bear Creek Mining Company unpublished geologic map, scale 1:24,000.

Thompson, R.S., Toolin, L.J., Forester, R.M., and Spencer, R.J., 1990, Accelerator-mass spectrometer (AMS) radiocarbon dating of Pleistocene lake sediments in the Great Basin: Palaeogeography, Palaeoclimatology, Palaeoecology, v. 78, p. 301–313.

Tooker, E.W., 1980, Preliminary geologic map of the Tooele quadrangle, Utah: U.S. Geological Survey Open-File Report 80-623, 1 plate, scale 1:24,000.

Tooker, E.W., 1983, Variations in structural style and correlation of thrust plates in the Sevier foreland thrust belt, Great Salt Lake area, Utah, *in* Miller, D.M., editor, Tectonic and stratigraphic studies in the eastern Great Basin: Geological Society of America Memoir 157, p. 61–73.

Tooker, E.W., 1999, Geology of the Oquirrh Mountains, Utah: U.S. Geological Survey Open-File Report 99-571, map scale 1:50,000.

Tooker, E.W., and Roberts, R.J., 1970, Upper Paleozoic rocks in the Oquirrh Mountains and Bingham mining district, Utah, with a section on biostratigraphy and correlation by Gordon, M., Jr., and Duncan, H.M.: U.S. Geological Survey Professional Paper 629-A, 76 p.

Tooker, E.W., and Roberts, R.J., 1971a, Geologic map of the Garfield quadrangle, Salt Lake and Tooele Counties, Utah: U.S. Geological Survey Geologic Quadrangle Map GQ-992, 1 plate, scale 1:24,000.

Tooker, E.W., and Roberts, R.J., 1971b, Geologic map of the Mills Junction quadrangle, Tooele County, Utah: U.S. Geological Survey Geologic Quadrangle Map GQ-924, 1 plate, scale 1:24,000.

Tooker, E.W., and Roberts, R.J., 1998, Geologic map of the Oquirrh Mountains and adjoining south and western Traverse Mountains, Tooele, Salt Lake, and Utah Counties, Utah: U.S. Geological Survey Open-File Report 98-581, 2 plates, scale 1:50,000.

Trexler, J.H., Jr., 1992, The Devonian-Mississippian Stansbury Formation at Stansbury Island and in the northeastern Stansbury Mountains, Utah, *in* Wilson, J.R., editor, Field guide to geologic excursions in Utah and adjacent areas of Nevada, Idaho, and Wyoming, prepared for the Geological Society of America Rocky Mountain Section meeting in Ogden, Utah, May 13–15, 1992: Utah Geological Survey Miscellaneous Publication 92-3, p. 161–169, https://doi.org/10.34191/MP-92-3.

Tripp, B.T., Shubat, M.A., Bishop, C.E., Blackett, R.E., and Gloyn, R.W., 1989, Mineral occurrences of the Tooele 1° x 2° quadrangle and part of the Elko 1° x 2° quadrangle, west-central Utah: Utah Geological and Mineral Survey Open-File Report 153, 85 p., 3 plates, scale 1:48,000, https://doi.org/10.34191/OFR-153.

U.S. Geological Survey, 2016, Utah Water Science Center, Great Salt Lake—lake elevations and elevation changes: Online, https://ut.water.usgs.gov/greatsaltlake/elevations/, accessed June 14, 2016.

U.S. Geological Survey geologic lexicon: Online, https://ngmdb.usgs.gov/Geolex/search, accessed July 2, 2020.

Utah Division of Oil, Gas and Mining (UDOGM), Oil and gas information database: Online, https://oilgas.ogm.utah.gov/oilgasweb/live-data-search/lds-main.xhtml, accessed January 2017.

Utah Division of Oil, Gas and Mining (UDOGM), Mineral mines in Utah database: Online, https://utahdnr.maps.arcgis.com/apps/webappviewer/index.html?id=fc09fb46b4934a19a60714c37154667c, accessed March 23, 2018.

Utah Division of Water Rights (UDWR), Well database: Online, http://maps.waterrights.utah.gov/EsriMap/map.asp?layersToAdd=wellsearch, accessed March 1, 2017.

Utah Geological Survey, Quaternary fault & fold map: Online, https://geology.utah.gov/apps/qfaults/index.html, accessed March 23, 2018

Utah Geological Survey, Nash, B.P., and Perkins, M.E., 2015, Tephrochronology results for the Copperton, Lofgreen, and Magna quadrangles, Utah: Utah Geological Survey Open-File Report 649, 3 p., https://doi.org/10.34191/OFR-649.

Utah Geological Survey and Nevada Isotope Geochronology Laboratory, 2017, $^{40}Ar/^{39}Ar$ geochronology results for the North Willow Canyon quadrangle, Utah: Utah Geological Survey Open-File Report 666, variously paginated, https://doi.org/10.34191/OFR-666.

Utah Geological Survey and O'Sullivan, P.B., 2017, U-Pb zircon geochronology results for the Angle, Donkey Flat, Farnsworth Peak, Fort Douglas, and Quincy Spring quadrangles, Utah: Utah Geological Survey Open-File Report 660, variously paginated, https://doi.org/10.34191/OFR-660.

Utah Geological Survey and Wells, A.J., 2017, Fossil fusulinid evaluation results for the Rush Valley, Wildcat Mountain, Grouse Creek, and Tremonton 30' x 60' quadrangles, Utah: Utah Geological Survey Open-File Report 664, 64 p., https://doi.org/10.34191/OFR-664.

Valora, P.J., 1968, Glaciation of The Jumpoff, Oquirrh Mountains, Utah: Provo, Utah, Brigham Young University, M.S. thesis, 132 p.

Vogel, T.A., Cambray, F.W., and Constenius, K.N., 2001, Origin and emplacement of igneous rocks in the central Wasatch Mountains, Utah: Rocky Mountain Geology, v. 36, p. 119–162, https://doi.org/10.2113/gsrocky.36.2.119.

von Quadt, A., Erni, M., Martinek, K., Moll, M., Peytcheva, I., and Heinrich, C.A., 2011, Zircon crystallization and the lifetimes of ore-forming magmatic-hydrothermal systems: Geology, v. 39, p. 731–734.

Wahlman, G.P., 2013, Pennsylvanian to Lower Permian (Desmoinesian-Wolfcampian) fusulinid biostratigraphy of Midcontinent North America: Stratigraphy, v. 10, nos. 1-2, p. 73-104.

Waite, K.A., 1996, Petrogenesis of the volcanic and intrusive rocks associated with the Bingham porphyry Cu-Mo deposit, Utah: Provo, Utah, Brigham Young, University, M.S. thesis, 143 p.

Waite, K.A., Keith, J.D., Christiansen, E.H., Whitney, J.A., Hattori, K., Tingey, D.G., and Hook, C.J., 1997, Petrogenesis of the volcanic and intrusive rocks associated with the Bingham Canyon porphyry Cu-Au-Mo deposit, Utah, *in* John, D.A., and Ballantyne, G.H., editors, Geology and ore deposits of the Oquirrh and Wasatch Mountains, Utah: Society of Economic Geologists Guidebook Series, v. 29, p. 69–90.

Wardlaw, B.R., 2015, Gondolellid condonts and depositional setting of the Phosphoria Formation: Micropaleontology, v. 61, nos. 4-5, p. 335–368.

Wardlaw, B.R., and Collinson, J.W., 1986, Paleontology and deposition of the Phosphoria Formation: Contributions to Geology, University of Wyoming, v. 24, no. 2, p. 107–142.

Wardlaw, B.R., Collinson, J.W., and Ketner, K.B., 1979a, Regional relations of Middle Permian rocks in Idaho, Nevada, and Utah, in Newman, G.W., and Goode, H.D., editors, 1979 Basin and Range Symposium: Rocky Mountain Association of Geologists and Utah Geological Association Symposium Guidebook, p. 277–283.

Wardlaw, B.R., Collinson, J.W., and Maughan, E.K., 1979b, Stratigraphy of Park City Group equivalents (Permian) in southern Idaho, northeastern Nevada, and northwestern Utah, *in* Wardlaw, B.R., editor, Studies of Permian Phosphoria Formation and related rocks, Great Basin-Rocky Mountain region: U.S. Geological Survey Professional Paper 1163-C, p. 9–16.

Warnaars, F.W., Smith, W.H., Bray, R.E., Lanier, G., and Shafiquallah, M., 1978, Geochronology of igneous intrusion and porphyry copper mineralization at Bingham, Utah: Economic Geology, v. 73, p. 1242–1249.

Webb, G.W., 1958, Middle Ordovician stratigraphy in eastern Nevada and western Utah: American Association of Petroleum Geologists, v. 42, no. 10, p. 2335–2377.

Welsh, J.E., 1976, Relationships of Pennsylvanian-Permian stratigraphy to the late Mesozoic thrust belt in the eastern Great Basin, Utah and Nevada, *in* Hill, J.G., editor, Symposium on geology of the Cordilleran hingeline: Rocky Mountain Association of Geologists, Denver, Colorado, p. 153–160.

Welsh, J.E., 1983, Differences in the Oquirrh Group and the Granger Mountain Group between the Oquirrh Mountains and Wallsburg Ridge, Wasatch Mountains, Utah: Geological Society of America Abstracts with Programs, v. 15, p. 290.

Welsh, J.E., 1998, unpublished maps, stratigraphic sections, well logs, and reports provided to the Utah Geological Survey.

Welsh, J.E., and Bissell, H.J., 1979, The Mississippian and Pennsylvanian (Carboniferous) Systems in the United States: U.S. Geological Survey Professional Paper 1110-Y, 35 p.

Welsh, J.E., and James, A.H., 1961, Pennsylvanian and Permian stratigraphy of the central Oquirrh Mountains, Utah, *in* Cook, D.R., editor, Geology of the Bingham mining district and northern Oquirrh Mountains: Utah Geological Society Guidebook to the Geology of Utah, no. 16, p. 1–16.

Welsh, J.E., and James, A.H., 1998 (revised), Reconnaissance traverse and measured section of part of the South Mountain quadrangle, Tooele County, Utah: unpublished data submitted to the Utah Geological Survey.

Williams, S.K., 1994, Late Cenozoic tephrochronology of deep sediment cores from the Bonneville basin, northwest Utah: Geological Society of America Bulletin, v. 105, p. 1517–1530.

Willis, G.C., 2017, History and evolution of geologic mapping in Utah with emphasis on the Wasatch area, *in* Lund, W.R., Emerman, S.H., Wang, W., and Zanazzi, A., editors, Geology and resources of the Wasatch—back to front: Utah Geological Association Publication 46, p. 375–398.

Willis, G.C., 1999, The Utah thrust system—an overview, *in* Spangler, L.E., and Allen, C.J., editors, Geology of northern Utah and vicinity: Utah Geological Association Publication 27, p. 1–9.

Willis, G.C., and Jensen, M.E., 2000, Tertiary rocks of Antelope Island, Davis County, Utah, *in* King, J.K., and Willis, G.C., editors, Geology of Antelope Island, Davis County, Utah: Utah Geological Survey Miscellaneous Publication 00-1, p. 49–70, https://doi.org/10.34191/MP-00-1.

Willis, G.C., Yonkee, W.A., Doelling, H.H., and Jensen, M.E., 2010, Geology of Antelope Island State Park, *in* Sprinkel, D.A., Chidsey, T.C., Jr., and Anderson, P.B., editors, Geology of Utah's parks and monuments: Utah Geological Association Publication 28 (third edition), p. 349–377.

Wong, I., Olig, S., Green, R., Moriwaki, Y., Abrahamson, N., Baures, D.,Silva, W., Somerville, P., Davidson, D., Pilz, J., and Dunne, B., 1995, Seismic hazard evaluation of the Magna tailings impoundment, *in* Lund, W.R., editor, Environmental and Engineering Geology of the Wasatch Front Region: Utah Geological Association Publication 24, p. 95-110.

Working Group on Utah Earthquake Probabilities (WGUEP), Wong, I., Lund, W., DuRoss, C., Thomas, T., Arabasz, W., Crone, A., Hylland, M., Luco, N., Olig, S., Pechmann, J., Personius, S., Petersen, M., Schwartz, D., Smith, R., and Bowman, S., 2016, Earthquake probabilities for the Wasatch Front region in Utah, Idaho, and Wyoming: Utah Geological Survey Miscellaneous Publication 16-3, variously paginated, https://doi.org/10.34191/MP-16-3.

Yonkee, W.A., Dehler, C.D., Link, P.K., Balgord, E.A., Keeley, J.A., Hayes, D.S., Wells, M.L., Fanning, C.M., and Johnston, S.M., 2014, Tectono-stratigraphic framework of Neoproterozoic to Cambrian strata, west-central U.S.—protracted rifting, glaciation, and evolution of the North American Cordilleran margin: Earth-Science Reviews, v. 136, p. 59–95.

Yonkee, W.A., and Lowe, M., 2004, Geologic map of the Ogden 7.5-minute quadrangle, Weber and Davis Counties, Utah: Utah Geological Survey Map 200, 2 plates, 42 p., scale 1:24,000, https://doi.org/10.34191/M-200.

Yonkee, W.A., Parry, W.T., Bruhn, R.L., and Cashman, P.C., 1989, Thermal models of thrust faulting—Constraints from fluid inclusion observations, Willard thrust sheet, Idaho-Utah-Wyoming thrust belt: Geological Society of America Bulletin, v. 101, p. 304–313.

Yonkee, W.A., and Weil, A.B., 2011, Evolution of the Wyoming salient of the Sevier fold-thrust belt, northern Utah to western Wyoming, *in* Sprinkel, D.A., Yonkee, W.A., and Chidsey, T.C., Jr., editors, Sevier thrust belt—northern and central Utah and adjacent areas: Utah Geological Association Publication 40, 56 p.

Yonkee, W.A., Willis, G.C., and Doelling, H.H., 2000a, Petrology and geologic history of the Precambrian Farmington Canyon Complex, Antelope Island, Utah, *in* King, J.K., and Willis, G.C., editors, Geology of Antelope Island, Davis County, Utah: Utah Geological Survey Miscellaneous Publication 00-1, p. 5–36, https://doi.org/10.34191/MP-00-1.

Yonkee, W.A., Willis, G.C., and Doelling, H.H., 2000b, Proterozoic and Cambrian sedimentary rocks and low-grade metasedimentary rocks of Antelope Island, *in* King, J.K., and Willis, G.C., editors, Geology of Antelope Island, Davis County, Utah: Utah Geological Survey Miscellaneous Publication 00-1, p. 38–47, https://doi.org/10.34191/MP-00-1.

Yonkee, W.A., and several others, in preparation, Geologic maps of Little Mountain, Fremont Island, Carrington Island, Hat Island and the Perry Canyon Formation, Utah: Utah Geological Survey Miscellaneous Publication.

Young, J.C., 1953, Geology of the southern Lakeside Mountains, Utah: Salt Lake City, University of Utah, M.S. thesis, 90 p., 3 plates, scale 1:31,680.

Young, J.C., 1955, Geology of the southern Lakeside Mountains, Utah: Utah Geological and Mineral Survey Bulletin 56, 110 p., 1 plate, scale 1:73,000, https://doi.org/10.34191/B-56.

Zoback, M.L., 1983, Structure and Cenozoic tectonism along the Wasatch fault zone, Utah: Geological Society of America Memoir 157, p. 3–27.

APPENDIX A:

TABLES

Table A1. Summary of sediment cores for the Tooele 30' x 60' quadrangle.

Map Number	Core Name	Date Cored	7.5' Quadrangle	Latitude (°N) NAD83	Longitude (°W) NAD83	Total Depth (ft)	Total Depth (m)	Basin	Reference
SC1	Saltair	prior to 1960	Baileys Lake	40.7879	112.1247	649	198	SE Antelope Island	Eardley and Gvosdetsky, 1960
SC2	S28	1960s	Baileys Lake	40.7869	112.0687	764	233	Salt Lake?	Williams, 1994
SC3	Burmester	1970	Burmester	40.6549	112.4526	1007	307	N Tooele Valley	Eardley and others, 1973; Oviatt and others, 1999
SC4	Spencer core A	late 1970s	Plug Peak NW	40.9501	112.4778	12.5	3.8	S Arm Great Salt Lake	Spencer and others, 1984
SC5	Spencer core C	late 1970s	Plug Peak NW	40.9880	112.4491	19.0	5.8	S Arm Great Salt Lake	Spencer and others, 1984
SC6	Spencer core G	late 1970s	Plug Peak SE	40.8224	112.2608	16.4	5.0	S Arm Great Salt Lake	Spencer and others, 1984
SC7	Spencer core H	late 1970s	Plug Peak NE	40.9930	112.3330	11.2	3.4	S Arm Great Salt Lake	Spencer and others, 1984
SC8	USGS core 95-2	1995	Plug Peak NE	40.9963	112.3012	34.60	10.55	S Arm Great Salt Lake	USGS, unpublished
SC9	GLAD core 3A	2000	Antelope Island	40.8968	112.2461	187.9	57.3	S Arm Great Salt Lake	Dinter and others, 2001; Schnurrenberger and Haskell, 2001
SC10	GLAD core 3B	2000	Antelope Island	40.8969	112.2433	74.98	22.86	–	Dinter and others, 2001; Schnurrenberger and Haskell, 2001

Notes:

Map number corresponds to plate 1.
The Saltair, S28, and Burmester cores were taken by A. Eardley (Univ. of Utah).
Core locations are approximate except for GLAD cores 3A, 3B.
Basin indicates major Neogene-Recent basins within quadrangle.
See table A3 (radiocarbon age data) and table A4 (tephrochrology data) for selected sediment cores.

Table A2. *Summary of oil and gas exploration drill hole and selected water well data for the Tooele 30' x 60' quadrangle.*

Exploration Drill Holes (UDOGM)

Map Number	API Number	Well Name	Company	Year Completed	7.5' Quadrangle	Latitude (°N) NAD83	Longitude (°W) NAD83	Total Depth (ft)	Total Depth (m)	Basin	Lithology Notes/Unit Tops
DH1	4301130002	ST OF UT E 1 (Antelope Island)	AMOCO PRODUCTION COMPANY	1979	Plug Peak NE	40.97917	112.34907	10,419	3177	S Arm Great Salt Lake	Pleistocene 0 ft, Pliocene ~3000 ft, Miocene ~4500 ft, Precambrian ? ft–TD (Bortz and others, 1985; Bortz, 2002)
DH2	4301130003	ANTELOPE ISLAND 9-17	ANSCHUTZ CORPORATION, THE	2007	Antelope Island	40.99440	112.20243	100	30	-	-
DH3	4303511442	WHITLOCK-MORTON SALT CO 1	WHITLOCK, L E	1956	Antelope Island South	40.80631	112.13131	4231	1290	SE Antelope Island	Quaternary 0 ft, Tertiary 1432 ft, Oligocene-Eocene volcanics 2330–2807 ft, Tertiary clastics? 2807–3654 ft, Precambrian metamorphics 3654 ft –TD (Ritzma, UGS files, 1975; Willis and Jensen, 2000)
DH4	4303516540	JONNIE FEE 1	GEOTRONIC DEVELOPMENT CO	1959	Baileys Lake	40.79658	112.00159	565	172	Salt Lake?	Quaternary to TD (McKean and Hylland, 2019)
DH5	4303516542	FROST 1	BYRD-FROST INC	1951	Baileys Lake	40.85080	112.05632	1916	584	Salt Lake?	Quaternary?
DH6	4303530002	SALTAIR 1	MOUNTAIN FUEL SUPPLY CO	1975	Baileys Lake	40.78945	112.09911	3265	995	Salt Lake?	Quaternary 0 ft, Tertiary 1328 ft, Precambrian 3070 ft (Willis and Jensen, 2000)
DH7	4303530003	SALTAIR 2	MOUNTAIN FUEL SUPPLY CO	1975	Baileys Lake	40.81804	112.07980	3207	978	SE Antelope Island	unreliable data (Willis and Jensen, 2000)
DH8	4303530005	GILLMOR 3	PEASE OIL & GAS COMPANY	1976	Baileys Lake	40.79176	112.05118	2119	646	Salt Lake?	Quaternary 0 ft, Tertiary? 1048 ft (McKean and Hylland, 2019)
DH9	4304510468	CASSITY 2	HICKEY OIL CORP	1955	Mills Junction	40.64683	112.36731	3540	1079	N Tooele Valley	Tertiary at TD
DH10	4304511428	WOODLAY-GARSON-CASSITY 1	WHITLOCK, L E	1956	Burmester	40.64285	112.38391	7993	2437	N Tooele Valley	Quaternary 0 ft, Tertiary? 920? ft, Tertiary at TD
DH11	4304520100	NATIONAL OIL & GAS CO 1	NATIONAL OIL & GAS CO	1917	Burmester	40.69093	112.46330	1127	344	N Tooele Valley	-
DH12	4304520102	CASSITY 1	HICKEY OIL CORP	1955	Mills Junction	40.64620	112.36881	5540	1689	N Tooele Valley	Quaternary 0 ft, Tertiary? 892 ft, Oquirrh? 4880 ft-TD (Slentz, 1955)
DH13	4304520104	C WORTHINGTON 1	BONNEVILLE OIL & GAS EXPLO	1948	Burmester	40.64530	112.48848	3115	950	N Tooele Valley	-
DH14	4304530010	ST OF UT N 1 (Sandbar)	AMOCO PRODUCTION COMPANY	1980	Plug Peak SE	40.75522	112.30556	7864	2398	N Tooele Valley	Paleozoics at TD (Bortz and others, 1985)
DH15	4304530018	SIX MILE RANCH 1	TRINITY EXPLOR & PROD INC	1984	Mills Junction	40.63555	112.34703	5150	1570	N Tooele Valley?	Valley fill to 4365 ft, Paleozoics below
DH16	4304530024	STRATIGRAPHIC TEST 1	ROSSBERG, KENNETH	1988	Mills Junction	40.64302	112.26422	700	213	N Tooele Valley	Valley fill to TD
DH17	4304530025	SKULL VALLEY FED 26-3	PIERCE, ANDY	1989	Hastings Pass SE	40.53327	112.83311	2108	643	-	Tertiary 50 ft, Oquirrh 211 ft, Manning Canyon 1250 ft
DH18	4304530029	FEDERAL 26 1-2	SAXON OIL COMPANY	1994	Hastings Pass SE	40.53336	112.83280	6392	1979	-	Manning Canyon and Mississippian 1300 ft, palynology samples
DH19	4304530031	SKULL VLY FED 21-1	VA RESOURCES, LLC	2011	Hastings Pass SE	40.53768	112.86424	8051	2455	-	-
DH20	4304530032	TEST WELL 2	STODDARD DRILLING COMPANY	1978	Grantsville	40.54273	112.39792	1483	452	N Tooele Valley?	Valley fill to TD
DH21	4304530033	TEST WELL 7	STODDARD DRILLING COMPANY	1978	Grantsville	40.57068	112.45638	1522	464	N Tooele Valley	Valley fill to TD
DH22	4304530034	TOOELE VALLEY TEST 8	STODDARD DRILLING COMPANY	1978	Tooele	40.56765	112.27222	1511	461	-	Valley fill to TD
DH23	4304530035	TOOELE VALLEY 6	STODDARD DRILLING COMPANY	1978	Grantsville	40.59996	112.45659	1516	462	N Tooele Valley	Valley fill to TD
DH24	4304530036	TOOELE VALLEY 1	STODDARD DRILLING COMPANY	1977	Grantsville	40.60091	112.38033	1513	461	N Tooele Valley	Valley fill to TD
DH25	4304530037	TOOELE VALLEY 4	STODDARD DRILLING COMPANY	1978	Tooele	40.60200	112.28484	1500	457	-	Valley fill to TD
DH26	4304530038	TEST WELL 5	STODDARD DRILLING COMPANY	1978	Mills Junction	40.67451	112.26698	1176	359	-	Valley fill to TD
DH27	4304530039	TOOELE VALLEY 10	STODDARD DRILLING COMPANY	1978	Mills Junction	40.64575	112.26658	992	302	-	Valley fill? to TD

Notes:
Data from Utah Division of Oil, Gas and Mining (UDOGM) database.
Lithology notes compiled from UDOGM files and other sources.
Basin indicates major Neogene-Recent basins within quadrangle.

Selected Water Wells/Groundwater Monitoring Wells (UDWR and Kennecott)

Map No.	Well ID No.	Well Type	Owner	Year Completed	7.5' Quadrangle	UTM27-12E	UTM27-12N	Total Depth (ft)	Total Depth (m)	Basin	Lithology Notes
W1	427887	water well	SITLA (GSL Marina)	1966	Farnsworth Peak	397718	4509900	485	148	-	Valley fill to 475 ft, limestone and quartzite to TD
W2	12621	water well	Kennecott Utah Copper	1964	Farnsworth Peak	401044	4509870	886	270	-	Valley fill to 882 ft, limestone to TD, well abandoned
W3	ECG1114	monitoring well	Kennecott		Copperton	407510	4488550	3000	915	Salt Lake?	QT to 235', Tv 235' to 2900', Paleozoics to TD
W4	ECG1113	monitoring well	Kennecott		Copperton	408375	4488103	980	299	Salt Lake?	QT to 775', Tv 775' to TD
W5	ECG1143	monitoring well	Kennecott		Copperton	409085	4488366	1150	351	Salt Lake?	QT to 1036', Tv to TD
W6	ECG1131	monitoring well	Kennecott		Copperton	409701	4488758	1090	332	Salt Lake?	QT to 710', Tsl 710' to TD
W7	P273	monitoring well	Kennecott		Copperton	409695	4488389	340	104	Salt Lake?	QT gravel to TD
W8	P241	monitoring well	Kennecott		Copperton	411654	4488554	1007	307	Salt Lake?	QT gravel to TD

Notes:
Map number corresponds to plate 1.
UDWR is Utah Division of Water Rights.
Water well locations are approximate.
Kennecott groundwater monitoring wells on the Copperton quadrangle geologic map are related to the 1998 Remedial Investigation/Feasibility Study.
Basin indicates major Neogene-Recent basins within quadrangle.

Table A3. *Summary of radiocarbon age analyses for the Tooele 30' x 60' quadrangle.*

Map Number	Core/Location	Collection Date	Latitude (°N) NAD83	Longitude (°W) NAD83	Depth (cm)	Radiocarbon Age (yr B.P.)	Lab Number	Reference
SC9	GLAD core 3A	2000	40.8968	112.2461	1137-1147	8704±50	AA54639	Dinter and others, 2001; Dinter and Pechmann, 2001?; Schnurrenberger and Haskell, 2001
SC9	GLAD core 3A	2000	40.8968	112.2461	1141-1142	9068±66	AA55094	Dinter and others, 2001; Dinter and Pechmann, 2001?; Schnurrenberger and Haskell, 2001
SC10	GLAD core 3B	2000	40.8969	112.2433	37-41	804±38	AA43718	Dinter and others, 2001; Dinter and Pechmann, 2001?; Schnurrenberger and Haskell, 2001
SC10	GLAD core 3B	2000	40.8969	112.2433	50-54	1027±44	AA44469	Dinter and others, 2001; Dinter and Pechmann, 2001?; Schnurrenberger and Haskell, 2001
SC10	GLAD core 3B	2000	40.8969	112.2433	633-644	5711±50	AA53426	Dinter and others, 2001; Dinter and Pechmann, 2001?; Schnurrenberger and Haskell, 2001
SC10	GLAD core 3B	2000	40.8969	112.2433	842-846	7186±66	AA44475	Dinter and others, 2001; Dinter and Pechmann, 2001?; Schnurrenberger and Haskell, 2001
SC5	Spencer core C	late 1970s	40.9880	112.4491	334	9680±130	AA-663	Thompson and others, 1990
SC5	Spencer core C	late 1970s	40.9880	112.4491	337	11,970±180	AA-667	Thompson and others, 1990
SC5	Spencer core C	late 1970s	40.9880	112.4491	350	12,100±130	AA-666	Thompson and others, 1990
SC5	Spencer core C	late 1970s	40.9880	112.4491	360	12,400±300	AA-662	Thompson and others, 1990
SC5	Spencer core C	late 1970s	40.9880	112.4491	380	13,300±140	AA-661	Thompson and others, 1990
SC5	Spencer core C	late 1970s	40.9880	112.4491	414	15,860±180	AA-660	Thompson and others, 1990
SC5	Spencer core C	late 1970s	40.9880	112.4491	425	17,760±150	AA-3948	Thompson and others, 1990
SC5	Spencer core C	late 1970s	40.9880	112.4491	430	18,110±120	AA-3949	Thompson and others, 1990
SC5	Spencer core C	late 1970s	40.9880	112.4491	458	19,540±140	AA-3950	Thompson and others, 1990
SC5	Spencer core C	late 1970s	40.9880	112.4491	461	22,500±190	AA-3951	Thompson and others, 1990
SC5	Spencer core C	late 1970s	40.9880	112.4491	489	21,050±320	AA-664	Thompson and others, 1990
SC5	Spencer core C	late 1970s	40.9880	112.4491	496	26,460±320	AA-657	Thompson and others, 1990
SC5	Spencer core C	late 1970s	40.9880	112.4491	560	31,000±650	W-4809	Spencer and others, 1984
SC5	Spencer core C	late 1970s	40.9880	112.4491	560	>41,000	W-4669	Spencer and others, 1984
-	USGS core 95-1	1995	41.0000	112.4522	123	11,850±60	WW-786	Thompson and Oviatt, unpublished data
-	USGS core 95-1	1995	41.0000	112.4522	246	12,420±70	WW-787	Thompson and Oviatt, unpublished data
SC8	USGS core 95-2	1995	40.9963	112.3012	50	2660±60	WW-788	Thompson and Oviatt, unpublished data
SC8	USGS core 95-2	1995	40.9963	112.3012	420	6000±60	WW-835	Thompson and Oviatt, unpublished data
SC8	USGS core 95-2	1995	40.9963	112.3012	260	6580±60	WW-834	Thompson and Oviatt, unpublished data
SC8	USGS core 95-2	1995	40.9963	112.3012	585	7260±60	WW-792	Thompson and Oviatt, unpublished data
SC8	USGS core 95-2	1995	40.9963	112.3012	100	8410±70	WW-833	Thompson and Oviatt, unpublished data
SC8	USGS core 95-2	1995	40.9963	112.3012	745	8900±60	WW-793	Thompson and Oviatt, unpublished data
SC8	USGS core 95-2	1995	40.9963	112.3012	905	9550±60	WW-794	Thompson and Oviatt, unpublished data
SC8	USGS core 95-2	1995	40.9963	112.3012	1055	10,330±60	WW-795	Thompson and Oviatt, unpublished data
-	Magna spit	1980s; 1990s	40.709	112.044	-	10,285±265	GX-6614	Currey and others, 1983; Oviatt, 2014
-	Magna spit	1980s; 1990s	40.709	112.044	-	10,300±310	GX-6949	Currey and others, 1983; Oviatt, 2014
-	Magna spit	1980s; 1990s	40.709	112.044	-	10,570±60	Beta-159195	Currey and others, 1983; Oviatt, 2014
-	Tooele Valley	2000s	40.708	112.215	-	14,370±240	Beta-5697	Godsey and others, 2005
-	Tooele Valley	2000s	40.512	112.215	-	15,080±90	Beta-151451	Godsey and others, 2005
-	Tooele Valley	2000s	40.510	112.215	-	15,060±50	Beta-169099	Godsey and others, 2005
-	Tooele Valley	2000s	40.512	112.215	-	13,580±40	Beta-159810	Godsey and others, 2005
-	Tooele Valley	2000s	40.465	112.215	-	14,730±140	Beta-146004	Godsey and others, 2005
-	Tooele Valley	2000s	40.512	112.215	-	11,940±130	Beta-156660	Godsey and others, 2005
-	Stansbury Island	2000s	40.791	112.517	-	7510±40	Beta-208972	Patrickson and others, 2010
-	Stansbury Island	2000s	40.791	112.517	-	19,370±80	Beta-195845	Patrickson and others, 2010
-	Stansbury Island	1980s	40.791	112.517	-	20,710±310	Beta-5566	Currey and others, 1983
-	Stansbury Island	2000s	40.791	112.517	-	20,990±150	Beta-209904	Nishizawa and others, 2013
-	Stansbury Island	2000s	40.791	112.517	-	23,630±240	Beta-151447	Nishizawa and others, 2013
-	Stansbury Island	2000	40.791	112.517	-	23,270±160	Beta-119851	Oviatt, 2015
-	Stansbury Island	1980s	40.791	112.517	-	24,870±410	Beta-8343	Currey and Oviatt, 1985
-	Antelope Island	1990s	40.96	112.17	-	3450±250	Beta-25289	Murchison and Mulvey, 2000
-	Antelope Island	1990s	40.96	112.17	-	5890±120	Beta-26629	Murchison and Mulvey, 2000
-	Antelope Island	1990s	40.96	112.17	-	7650±90	Beta-25290	Murchison and Mulvey, 2000
-	Baileys Lake fault trench	2010	40.795	112.012	~80	675±30	OS-86491	Hylland and others, 2012, 2014
-	Baileys Lake fault trench	2010	40.795	112.012	~80	1800±25	OS-86573	Hylland and others, 2012, 2014
-	Baileys Lake fault trench	2010	40.795	112.012	~20	3890±30	OS-86492	Hylland and others, 2012, 2014
-	Baileys Lake fault trench	2010	40.795	112.012	~20	4280±30	OS-86494	Hylland and others, 2012, 2014
-	Baileys Lake fault trench	2010	40.795	112.012	~35	5400±30	OS-86493	Hylland and others, 2012, 2014
-	Baileys Lake fault trench	2010	40.795	112.012	~440	31,400±350	OS-86572	Hylland and others, 2012, 2014

Notes:
Map number corresponds to plate 1.
Core/sample locations are approximate except for GLAD cores 3A and 3B, Tooele Valley, and Baileys Lake fault trench.
nd is no data.
B.P. is before present (present = A.D. 1950).

Table A4. *Summary of tephrochronology data for the Tooele 30' x 60' quadrangle.*

Map Number	Sample Number/Core	7.5' Quadrangle	Latitude (°N) NAD27	Longitude (°W) NAD27	Tephra Name	Depth (ft.in)	Depth (m)	Correlation Age (Ma)	Error (Ma)	Laboratory	Reference
Antelope Island											
AT1	AITT-0840	Antelope Island	40°56'36"	112°10'52"	Rush Valley? or unamed?	–	–	7.9 or 9.2	0.5	Univ of Utah, Perkins and Nash	Willis and Jensen, 2000
AT2	AITT-1200	Antelope Island	40°54'32"	112°10'20"	Rush Valley? or unamed?	–	–	7.9 or 9.2	0.5	Univ of Utah, Perkins and Nash	Willis and Jensen, 2000
AT3	AITT-1030	Antelope Island	40°55'59"	112°11'02"	unamed (SW MT?)	–	–	~9.8		Univ of Utah, Perkins and Nash	Willis and Jensen, 2000
AT4	AITT-1090	Antelope Island	40°54'08"	112°10'16"	unamed (SW MT?)	–	–	~9.8		Univ of Utah, Perkins and Nash	Willis and Jensen, 2000
AT5	AITT-1220	Antelope Island	40°54'38"	112°10'18"	unamed (Mink Creek SE ID?)	–	–	9.5 to 10.5		Univ of Utah, Perkins and Nash	Willis and Jensen, 2000
AT6	AITT-0700	Antelope Island	40°55'36"	112°10'35"	Cougar Point Tuff XIII	–	–	10.94	0.03	Univ of Utah, Perkins and Nash	Willis and Jensen, 2000
AT7	AITT-1020	Antelope Island	40°56'00"	112°11'05"	unknown (Group A, Trapper Ck, ID?)	–	–	8.0? to 10.5?		Univ of Utah, Perkins and Nash	Willis and Jensen, 2000
Western Salt Lake Valley											
			Latitude (°N) NAD83	**Longitude (°W) NAD83**							
CT1	C51104-1	Copperton	40°36'30.0"	112°06'45.0"	Walcott	–	–	6.4	0.1	University of Utah, Perkins	Biek and others, 2007
CT2	C51804-2	Copperton	40°32'09.3"	112°05'40.7"	Walcott	–	–	6.4	0.1	University of Utah, Perkins	Biek and others, 2007
			Latitude (°N) WGS84	**Longitude (°W) WGS84**							
T8	T8	Copperton	40.60838	112.11254	Blacktail Creek	–	–	6.62	0.03	University of Utah, Nash	UGS and others, 2015
T9	T9	Copperton	40.60836	112.11912	Blacktail Creek	–	–	6.62	0.03	University of Utah, Nash	UGS and others, 2015
T10	T10	Copperton	40.61457	112.08536	Blacktail Creek	–	–	6.62	0.03	University of Utah, Nash	UGS and others, 2015
T11	T11	Copperton	40.61081	112.07180	Wolverine Creek	–	–	5.6?		University of Utah, Nash	UGS and others, 2015
T12	T12	Copperton	40.56779	112.10096	Blacktail Creek	–	–	6.62	0.03	University of Utah, Nash	UGS and others, 2015
T14	T14	Copperton	40.62013	112.07592	Walcott	–	–	6.27	0.04	University of Utah, Nash	UGS and others, 2015
T15	T15	Magna	40.67666	112.08463	unknown	–	–	–		University of Utah, Nash	UGS and others, 2015
T16	T16	Magna	40.67688	112.08638	unknown	–	–	–		University of Utah, Nash	UGS and others, 2015
			Latitude (°N) NAD83	**Longitude (°W) NAD83**							
SC2	**S28 Core**	Baileys Lake	40.7869	112.0687							
					Natural Trap?	112.9	–	0.11*		University of Utah	Williams, 1994
					Lava Creek B	467.9	142.6	0.62		University of Utah	Williams, 1994
					Ranch Canyon	505.4	–			University of Utah	Williams, 1994
					Rye Patch Dam	505.8	154.1			University of Utah	Williams, 1994
					Bishop	–	–	0.759		University of Utah	Williams, 1994
SC1	**Saltair Core**	Baileys Lake	40.7879	112.1247							
					Natural Trap?	–	–	0.11*		University of Utah	Williams, 1994
					Lava Creek B	547.6	–	0.62		University of Utah	Williams, 1994
					Bishop	–	–	0.759		University of Utah	Williams, 1994
SC3	**Burmester Core**	Burmester	40.6549	112.4526							
					Hansel Valley	–	2	0.03		–	Oviatt and others, 1999
					Natural Trap?	50.6	15.4	0.11*		University of Utah	Williams, 1994
					Paoha Island	–	23.4	0.16*		University of Utah	Williams, 1994
					Lava Creek B	281.9, 283.1, 285.2	86.9	0.62		University of Utah	Williams, 1994
					Bishop	–	96.6	0.759		University of Utah	Williams, 1994
					Bailey	–	148.8	1.15*		University of Utah	Williams, 1994
					BUR-498.11	498.11	152.1	1.17*		University of Utah	Williams, 1994
					BUR-523.3	523.3	159.5	1.22*		University of Utah	Williams, 1994
					Mesa Falls	547.8	166.9	1.27		University of Utah	Williams, 1994
					Rio Dell	605	184.4	1.44*		University of Utah	Williams, 1994
					BUR-621.3	621.3	189.4	1.49*		University of Utah	Williams, 1994
					Last Chance Bench	744.4	226.9	1.91*		University of Utah	Williams, 1994
					Huckleberry Ridge	756.1, 760.8	231.9	2.06		University of Utah	Williams, 1994
					Hogsback?	812.6	247.7	2.65*		University of Utah	Williams, 1994
					BUR-841.2	840.4, 841.2	256.4	2.77*		University of Utah	Williams, 1994
					BUR-871.11	871.11	265.8	2.90*		University of Utah	Williams, 1994
					Upper Horse Hill	914.2, 915.0	278.9	3.04*		University of Utah	Williams, 1994
					BUR-962.8	960.2, 962.8	293.5	3.15*		University of Utah	Williams, 1994
					Nomlaki	989.4, 993.0, 996.0	303.6	3.29*		University of Utah	Williams, 1994

Table A4. *Continued.*

Map Number	Sample Number/Core	7.5' Quadrangle	Latitude (°N) NAD27	Longitude (°W) NAD27	Tephra Name	Depth (ft.in)	Depth (m)	Correlation Age (Ma)	Error (Ma)	Laboratory	Reference
SC4	**Spencer core A**	Plug Peak NW	40.9501	112.4778							
					Mazama	–	1.4	0.0763		–	Spencer and others, 1984
					Hansel Valley?	–	?			–	Oviatt, unpublished data
SC5	**Spencer core C**	Plug Peak NW	40.9880	112.4491							
					Mazama	–	1.4	0.0763		–	Spencer and others, 1984
					Hansel Valley	–	5	0.03		–	Spencer and others, 1984; Thompson and others, 1990
SC6	**Spencer core G**	Plug Peak SE	40.8224	112.2608							
					Mazama	–	3.8	0.00763		–	Spencer and others, 1984
					Hansel Valley?	–	?			–	Oviatt, unpublished data
SC7	**Spencer core H**	Plug Peak NE	40.9930	112.3330							
					Mazama	–	3.1	0.00763		–	Spencer and others, 1984
					Hansel Valley?	–	?			–	Oviatt, unpublished data
SC9	**GLAD core 3A**	Antelope Island	40.8968	112.2461							
					Mazama	–	8.555	0.00763		–	Dinter and others, 2001; Schnurrenberger and Haskell, 2001
					Hansel Valley	–	17.08	0.03		–	Dinter and others, 2001; Schnurrenberger and Haskell, 2001
SC10	**GLAD core 3B**	Antelope Island	40.8969	112.2433							
					Mazama	–	8.45	0.00763		–	Dinter and others, 2001; Schnurrenberger and Haskell, 2001
					Hansel Valley	–	17.14	0.03		–	Dinter and others, 2001; Schnurrenberger and Haskell, 2001
SC8	**USGS core 95-2**	Plug Peak NE	40.9963	112.3012							
					Mazama	–	6.86, 7.89	0.00763		–	Thompson and Oviatt, unpublished data
DH14	**Amoco Sandbar well**	Plug Peak SE	40.75522	112.30556							
					Lava Creek	–	250	0.62		not analyzed	Kowalewska and Cohen, 1998
					Bishop	–	277	0.759		not analyzed	Kowalewska and Cohen, 1998

Notes:

Map number corresponds to plate 1.
Correlation ages are based on geochemical correlation of glass composition to the database of analyses/stratigraphic data/age dates for late Cenozoic vitric tephra layers in the Western U.S. assembled at the University of Utah, Dept. of Geology and Geophysics. Refer to Williams (1994) for methods and sources of actual radiometric ages on various ash beds. Lanphere and others (2002) have updated the radiometric age on the Lava Creek ash to 0.64 Ma.
S28, Saltair, Burmester, Spencer A, C, G, H, and USGS 95-2 core locations are approximate.
* Estimated age in Burmester core (Williams, 1994)
Corrected coordinates provided for C51804-2 of Biek and others (2007).

Table A5. *Summary of radiometric age analyses of Tertiary rocks for the Tooele 30' x 60' quadrangle and adjacent areas.*

Map Number	Sample Number	Map Unit	Rock Name	7.5' Quadrangle	Location	Latitude (N)	Longitude (W)	Location Coordinate System	Age (Ma)	Material Dated	Laboratory	Analysis Type	Comments	Reference
-	TS33104-4	Tir	rhyolite	Tickville Spring	W Traverse Mtns	40°29'44.1"	112°05'05.7"	NAD83	35.49 ± 0.13	sanidine	NMGRL	$^{40}Ar/^{39}Ar$	single-crystal laser fusion	Biek and others, 2005; NMGRL and UGS, 2006
R5	BING-18	Tiqlp	quartz latite porphyry	Bingham Canyon	Oquirrh Mtns	402630.764E	4486640.554N	UTM27-12	37.66 ± 0.08	sanidine	BERK	$^{40}Ar/^{39}Ar$	single-crystal laser fusion	Deino and Keith, 1997
R5	BING-18	Tiqlp	quartz latite porphyry	Bingham Canyon	Oquirrh Mtns	402630.764E	4486640.554N	UTM27-12	37.72 ± 0.09	sanidine	BERK	$^{40}Ar/^{39}Ar$	plateau age	Deino and Keith, 1997
R6	BING-38		minette dike in Tiqmp	Bingham Canyon	Oquirrh Mtns	401681.219E	4485914.359N	UTM27-12	37.74 ± 0.11	biotite	BERK	$^{40}Ar/^{39}Ar$	plateau age	Deino and Keith, 1997
R4	LARK-6	Tvfou	latite cobble	Copperton (Lark)	Oquirrh Mtns	40°36'54"	112°07'00"	NAD27?	38.17 ± 0.09	sanidine	BERK	$^{40}Ar/^{39}Ar$	single-crystal laser fusion	Deino and Keith, 1997
-	674-1	Tim	monzonite	Bingham Canyon	Oquirrh Mtns	nd	nd	nd	38.40 ± 0.16	biotite	NMGRL	$^{40}Ar/^{39}Ar$	plateau age	Parry and others, 2001
-	TICK-113	Tvlo	volcaniclastic sand	Tickville Spring	W Traverse Mtns	40°26'42.500"	112°06'4.051"	NAD27?	38.68 ± 0.13	sanidine	BERK	$^{40}Ar/^{39}Ar$	single-crystal laser fusion	Deino in Maughan, 2001
-	BING-6	Tilp	latite	Tickville Spring	Oquirrh Mtns	40°29'42"	112°07'24"	NAD27?	38.84 ± 0.19	plagioclase	BERK	$^{40}Ar/^{39}Ar$	plateau age	Deino and Keith, 1997
-	TICK-23	Tvlo	latite cobble	Tickville Spring	W Traverse Mtns	40°28'47"	112°07'11"	NAD27?	39.18 ± 0.11	biotite	BERK	$^{40}Ar/^{39}Ar$	plateau age	Deino and Keith, 1997
-	DH	Tiqlp	nd	Stockton	Oquirrh Mtns	40°27'15"	112°20'39"	NAD83	39.4 ± 0.34	K-feldspar	nd	$^{40}Ar/^{39}Ar$	from drill hole	Krahulec, 2005
T24	T24	Tvs	dacite	North Willow Canyon	Stansbury Mtns	40.55543°	112.59221°	WGS84	39.68 ± 0.50	biotite	NIGL	$^{40}Ar/^{39}Ar$	plateau age	UGS and NIGL, 2017
T30	T30	Tvs	rhyolite	North Willow Canyon	Stansbury Mtns	40.54427°	112.57715°	WGS84	41.30 ± 0.60	biotite	NIGL	$^{40}Ar/^{39}Ar$	plateau age	UGS and NIGL, 2017
-	74-KA-4	Tb	alkali olivine basalt	-	Stansbury Mtns	40°37'35"	112°38'50"	NAD27?	12.1 ± 0.3	whole rock	USGS	K-Ar	-	Moore and McKee, 1983
-	74-KA-3	Tsh	alkali olivine basalt	-	Stansbury Mtns	40°37'35"	112°35'15"	NAD27?	12.7 ± 0.2	whole rock	USGS	K-Ar	-	Moore and McKee, 1983
-	74-KA-9	Tb	augite basalt	-	Cedar Mtns	40°42'10"	112°55'15"	NAD27?	13.8 ± 0.4	whole rock	USGS	K-Ar	-	Moore and McKee, 1983
-	4	Tiqlp	latite porphyry	-	Oquirrh Mtns	40°35'00"	112°12'00"	NAD27?	36.5 ± 1.1	biotite	USGS	K-Ar	Pass Canyon area	Moore, 1973
-	12B	Tipqm	quartz latite	-	Oquirrh Mtns	nd	nd	nd	36.9 ± 0.9	hornblende	USGS	K-Ar	Bingham tunnel portal	Moore and others, 1968
-	12A	Tipqm	quartz latite	-	Oquirrh Mtns	nd	nd	nd	36.9 ± 1.0	biotite	USGS	K-Ar	Bingham tunnel portal	Moore and others, 1968
R3	AITW-0930	Tnf	volcanic clast	Antelope Island	Antelope Island	40°52'48"	112°10'22"	NAD27	38.8 ± 1.5	phlogopite	KE	K-Ar	-	Doelling and others, 1990
-	70-KA-1	Tirs	biotite-augite granodiorite	-	Stansbury Mtns	40°31'40"	112°36'00"	NAD27?	39.0 ± 0.6	biotite	USGS	K-Ar	-	Moore and McKee, 1983
-	74-KA-6	Tvs	hornblende-biotite latite	-	Stansbury Mtns	40°33'25"	112°35'25"	NAD27?	39.4 ± 0.5	biotite	USGS	K-Ar	-	Moore and McKee, 1983
-	70-KA-2A	Tirs	hornblende latite	-	Stansbury Mtns	40°31'00"	112°35'45"	NAD27?	40.3 ± 0.5	biotite	USGS	K-Ar	-	Moore and McKee, 1983
-	74-KA-7	Tvs	hornblende-augite dacite	-	Stansbury Mtns	40°33'15"	112°41'50"	NAD27?	40.6 ± 1.7	hornblende	USGS	K-Ar	-	Moore and McKee, 1983
-	74-KA-5	Tvs	biotite-hornblende latite	-	Stansbury Mtns	40°30'05"	112°34'45"	NAD27?	41.8 ± 0.5	biotite	USGS	K-Ar	-	Moore and McKee, 1983
R1	AIGW-0102	Tnf	claystone/bentonite	Antelope Island	Antelope Island	40°52'52"	112°10'25"	NAD27	42.9 ± 1.7	biotite	KE	K-Ar	-	Doelling and others, 1990
R2	AIMJ-0101	Tnf	volcanic clast	Antelope Island	Antelope Island	40°52'51"	112°10'28"	NAD27	49.2 ± 1.9	biotite	KE	K-Ar	-	Doelling and others, 1990

Notes:

Map number and map unit corresponds to plate 1.
Approximate locations for BING-18 and BING-38.
Laboratory: NIGL is Nevada Isotope Geochronology Laboratory, Las Vegas, NV; NMGRL is New Mexico Geochronology Research Laboratory, Socorro, NM; BERK is Berkely Geochronology Center, Berkeley, CA; USGS is U.S. Geological Survey Lab, Menlo Park CA; KE is Krueger Enterprises, Cambridge, MA.
nd is no data.

Table A6. *Summary of U-Pb zircon age analyses for the Tooele 30' x 60' quadrangle.*

Map Number	Sample Number	Map Unit	Rock Name	7.5' Quadrangle	Location	Original Location	Original Location	Original Location Coordinate System	Age (Ma)	Laboratory	Analysis Type	Comments	Reference
-	5091-400	Tiqmp	quartz monzonite porphyry	Bingham Canyon?	Oquirrh Mtns	nd	nd	nd	37.94 ± 0.08	nd	Crystallization age		von Quadt and others, 2011
-	KM5	Tilp	latite porphyry	Bingham Canyon?	Oquirrh Mtns	700E	neg 250N	mine coordinates	37.94 ± 0.13	nd	Crystallization age		von Quadt and others, 2011
-	D310	Tiqlp	quartz latite porphyry	Bingham Canyon?	Oquirrh Mtns	nd	nd	nd	37.97 ± 0.11	nd	Crystallization age		von Quadt and others, 2011
Zr2	760-1	Tim	monzonite	Bingham Canyon	Oquirrh Mtns	40°30'26" N	112°09'40" W	nd	38.55 ± 0.19	Ontario	Crystallization age	Last Chance Stock	Parry and others, 2001
T3	T3	Tso	sandstone	Farnsworth Peak	Oquirrh Mtns	40.63223° N	112.14668° W	UTM WGS84	39.38 ± 1.91	GeoSep	DZ max depositional age		UGS and O'Sullivan, 2017
T46	T46	Ks	sandstone	Quincy Spring	N Cedar Mtns	40.5847° N	112.99034° W	UTM WGS84	116.52 ± 4.78	GeoSep	DZ max depositional age		UGS and O'Sullivan, 2017
Zr1	01FCC8	Xfcl	biotite orthogneiss	Antelope Island South	Antelope Island	0400950E	4523250N	UTM 27-12	1691 ± 26	ANU	Crystallization age		Nelson and others, 2011

Notes:

Map number and map unit corresponds to plate 1.
Approximate locations for samples 760-1 and 01FCC8.
Laboratory: Ontario is Royal Ontario Museum geochronology laboratories, Toronto, Canada; GeoSep is GeoSep Services, Moscow, ID; ANU is Australian National University, Canberra, Australia.
nd is no data.
DZ is detrital zircon.

Table A7. *Selected major- and trace-element whole-rock geochemical analyses for the Tooele 30' x 60' quadrangle.*

									%	%	%	%	%	%	%	%	%	%	%	%	%	%	%
Map Number	**Sample Number**	**Map Unit**	**Rock Name**	**7.5' Quadrangle**	**Location**	**Location Data Latitude (°N) WGS84**	**Location Data Longitude (°W) WGS84**	**Source**	**SiO2**	**Al_2O_3**	**Fe_2O_3**	**CaO**	**MgO**	**Na_2O**	**K_2O**	**Cr_2O_3**	**TiO_2**	**MnO**	**P_2O_5**	**SrO**	**BaO**	**LOI**	**Total**
T2	T2	Tiqlp	rhyolite	Tooele	Oquirrh Mountains	40.51161	112.30016	This study	67.47	14.16	3.11	2.33	1.57	3.15	4.58	<0.01	0.41	0.04	0.18	0.06	0.18	2.58	99.81
T4	T4	Tvu	latite	Farnsworth Peak	Oquirrh Mountains	40.63232	112.15107	This study	60.09	14.98	5.31	5.36	3.48	3.22	3.46	0.01	0.75	0.08	0.288	0.09	0.21	2.25	99.59
T17	T17	Tb	trachybasalt	Timpie	Stansbury Mountains	40.62585	112.64719	This study	48.35	13.52	11.38	8.61	6.49	2.54	3.56	0.03	2.24	0.15	1.223	0.14	0.29	1.3	99.82
T20	T20	Tsh	shoshonite	North Willow Canyon	Stansbury Mountains	40.62468	112.58983	This study	50.66	15.04	9.43	8.22	6.68	2.65	3.83	0.03	1.5	0.13	0.745	0.2	0.35	0.25	99.72
T21	T21	Tirs	quartz monzonite	North Willow Canyon	Stansbury Mountains	40.62154	112.58545	This study	65.31	15.13	3.74	3.3	1.91	3.94	3.97	<0.01	0.47	0.04	0.192	0.13	0.24	0.56	98.94
T22	T22	Tirs	rhyolite	North Willow Canyon	Stansbury Mountains	40.51831	112.59584	This study	67.67	14.06	3.11	2.68	1.75	2.68	4.46	<0.01	0.34	0.04	0.139	0.04	0.14	2.66	99.77
T24	T24	Tvs	dacite	North Willow Canyon	Stansbury Mountains	40.55543	112.59221	This study	65.67	13.87	2.9	4.06	1.08	2.86	4.03	<0.01	0.34	0.08	0.139	0.05	0.13	4.04	99.24
T25	T25	Tvs	rhyolite	North Willow Canyon	Stansbury Mountains	40.55497	112.58975	This study	70.42	13.13	2.87	2.77	1.2	3.09	3.89	<0.01	0.32	0.04	0.133	0.05	0.13	0.92	98.96
T27	T27	Tvs	trachydacite	North Willow Canyon	Stansbury Mountains	40.55291	112.58781	This study	61.47	15.43	6.05	3.67	1.19	3.28	4.36	<0.01	0.65	0.02	0.352	0.07	0.15	3.09	99.79
T28	T28	Tvs	trachydacite	North Willow Canyon	Stansbury Mountains	40.55359	112.58328	This study	61.60	15.14	6.1	3.97	1.11	3.29	4.29	0.01	0.67	0.09	0.356	0.07	0.16	2.48	99.33
T29	T29	Tvs	trachydacite	North Willow Canyon	Stansbury Mountains	40.55361	112.57475	This study	65.99	15.71	3.85	3.29	0.44	3.49	4.33	<0.01	0.43	0.07	0.18	0.07	0.16	1.56	99.56
T30	T30	Tvs	rhyolite	North Willow Canyon	Stansbury Mountains	40.54427	112.57715	This study	68.05	14.43	3.25	2.77	1.27	3.15	4.32	<0.01	0.34	0.05	0.14	0.05	0.14	1.74	99.7
T31	T31	Tvs	andesite	North Willow Canyon	Stansbury Mountains	40.50167	112.57036	This study	56.61	12.65	9.18	7.78	5.75	2.44	2.83	0.03	0.9	0.12	0.29	0.05	0.11	0.87	99.62
T34	T34	Tb	trachybasalt	Salt Mountain	Salt Mountain	40.54509	112.68285	This study	49.28	13.95	11.56	8.02	6.66	2.63	3.54	0.04	2.3	0.16	1.181	0.13	0.28	0.43	100.15
T35	T35	Tvs	dacite	Salt Mountain	Salt Mountain	40.55613	112.69231	This study	63.14	14.51	4.08	4.14	2.07	3.14	3.92	<0.01	0.46	0.08	0.188	0.06	0.16	3.02	98.98
T37	T37	Tvs	trachydacite	Salt Mountain	Salt Mountain	40.56504	112.68190	This study	66.74	14.11	3.74	3.18	1.34	3.57	5.44	0.02	0.36	0.09	0.237	0.05	0.19	0.77	99.83
T39	T39	Tvs	andesite	Salt Mountain	Salt Mountain	40.54210	112.69051	This study	57.73	14.01	7.26	6.43	3.92	2.48	2.9	0.02	0.79	0.1	0.308	0.05	0.11	3.15	99.25
T42	T42	Tb	basalt	Hastings Pass NE	Cedar Mountains	40.70218	112.86610	This study	50.25	14.4	11.29	8.69	7.98	2.37	2.23	0.06	1.45	0.16	0.518	0.08	0.15	0.13	99.76
T44	T44	Tb	basalt	Hastings Pass	Cedar Mountains	40.70142	112.92234	This study	50.24	15.12	11.68	9.27	7.37	2.53	1.31	0.06	1.41	0.17	0.4	0.05	0.1	0.21	99.92
T45	T45	Tb	basalt	Hastings Pass	Cedar Mountains	40.65475	112.98005	This study	50.20	14.17	11.15	8.64	8.31	2.34	2.41	0.07	1.43	0.16	0.534	0.08	0.17	0.3	99.96
T57	T57	Tm	olivine melanephelinite	Low	Cedar Mountains	40.80950	112.87752	This study	40.97	10.5	9.64	12.44	15.81	2.86	2.34	0.13	0.84	0.17	0.656	0.25	0.2	3.54	100.35

						Location Data Latitude (N) NAD83	**Location Data Longitude (W) NAD83**		**SiO2**	**Al_2O_3**	**Fe_2O_3**	**CaO**	**MgO**	**Na_2O**	**K_2O**	**Cr_2O_3**	**TiO_2**	**MnO**	**P_2O_5**	**SrO**	**BaO**	**LOI**	**Total**
CG1	C41504-2	Tilp	dacite	Copperton	Oquirrh Mountains	40° 30' 09.6"	112° 07' 25.3"	Biek and others, 2007	61.33	14.78	5.55	3.72	3.55	3.07	3.52	0.01	0.64	0.06	0.27	0.07	0.24	2.29	99.10
CG2	C41504-3	Tilp	dacite	Copperton	Oquirrh Mountains	40° 30' 29.4"	112° 06' 57.3"	Biek and others, 2007	61.99	14.69	5.12	3.79	3.25	2.80	3.46	0.01	0.58	0.05	0.23	0.07	0.24	2.30	98.58
CG3	C42704-1	Tipqm	dacite	Copperton	Oquirrh Mountains	40° 31' 08.2"	112° 06' 00.5"	Biek and others, 2007	64.59	15.60	4.63	3.45	1.82	3.22	3.46	<0.01	0.56	0.04	0.28	0.08	0.16	1.33	99.22
CG4	C42704-2	Tipqm	dacite	Copperton	Oquirrh Mountains	40° 31' 36.1"	112° 05' 57.9"	Biek and others, 2007	66.00	15.09	3.50	2.65	1.31	3.17	3.52	<0.01	0.44	0.04	0.22	0.07	0.16	2.10	98.28
CG5	C43004-3	Tipqm	dacite	Copperton	Oquirrh Mountains	40° 32' 27.7"	112° 06' 22.9"	Biek and others, 2007	57.15	15.28	5.45	3.19	3.30	1.87	3.90	0.02	0.60	0.03	0.26	0.07	0.21	7.07	98.40
CG6	C50404-2	Tvu	trachydacite	Copperton	Oquirrh Mountains	40° 34' 18.8"	112° 06' 52.1"	Biek and others, 2007	61.33	15.47	5.05	3.24	1.87	2.93	4.38	0.01	0.66	0.04	0.34	0.10	0.29	2.64	98.36
CG7	C50504-1	Tvfou	dacite	Copperton	Oquirrh Mountains	40° 35' 38.4"	112° 07' 15.4"	Biek and others, 2007	61.25	15.56	5.59	3.56	1.99	3.07	3.57	0.02	0.62	0.02	0.26	0.07	0.22	3.22	99.02

Notes:

Map number and map unit corresponds to plate 1.
Rock names from total alkali-silica diagram of LeBas and others (1986) or Middlemost (1994).
Analytical procedures: ME-XRF06 (whole-rock package by XRF); LOI for ME-XRF06 by WST-SIM, ME-4ACD81 (base metals 4-acid digestion by ICP-AES), ME-MS81 (lithium borate fusion by ICP-MS).
Major oxides reported in weight percent (%); < indicates value below detection limit.
LOI is loss on ignition.
Minor and trace elements reported in parts per million (ppm); < indicates value below detection limit.
Analyses performed by ALS Minerals and ALS Chemex.
Data from Copperton 7.5' quadrangle are also included here, as it was inadvertently omitted from the UGS website, see Biek and others (2007). Also see Clark and Biek (2017).
Only new and unpublished data are presented here. We did not compile the prior voluminous geochemical data available for the Bingham mining district, or older data from the Stansbury Mountains.

Table A7. *Continued.*

Ag	As	Ba	Cd	Ce	Co	Cr	Cs	Cu	Dy	Er	Eu	Ga	Gd	Hf	Ho	La	Lu	Mo	Nb	Nd	Ni	Pb	Pr	Rb	Sc	Sm	Sn	Sr	Ta	Tb	Th	Tl	Tm	U	V	W	Y	Yb	Zn	Zr
ppm	ppm	ppm	ppm	ppm	ppm	ppm	ppm	ppm	ppm	ppm	ppm	ppm	ppm	ppm	ppm	ppm	ppm	ppm	ppm	ppm	ppm	ppm	ppm	ppm	ppm	ppm	ppm	ppm	ppm	ppm	ppm	ppm	ppm	ppm	ppm	ppm	ppm	ppm	ppm	ppm
<0.5	6	1665	<0.5	197.5	7	60	5.84	28	2.98	1.49	1.39	22	4.57	10.6	0.56	116.5	0.25	<1	25.2	57.1	19	48	18.45	254	5	7.73	2	573	2.1	0.66	80	<10	0.23	7.69	62	2	16.2	1.52	40	396
<0.5	7	2000	<0.5	135	20	110	2.46	42	3.28	1.82	1.88	21.8	5.31	6.1	0.58	75.7	0.23	1	11.9	50.4	59	34	14.6	128	12	7.99	1	881	0.7	0.73	20.2	<10	0.23	3.33	123	1	17.6	1.71	79	233
<0.5	<5	2740	<0.5	155.5	37	240	0.5	33	6.39	3.2	3.25	20.4	8.9	11.5	1.22	77.4	0.41	<1	22	71.6	148	16	17.95	65.3	20	11.9	2	1065	1	1.23	8.68	10	0.45	1.83	224	1	30	2.85	124	461
<0.5	<5	3220	<0.5	192	34	230	0.47	44	5.25	2.42	2.98	19.5	7.74	11.3	0.91	100	0.29	<1	18.5	77.3	137	25	21.4	69.6	19	11.4	2	1470	0.9	0.98	14.2	<10	0.34	2.15	183	1	23.1	2.07	99	436
<0.5	5	2420	<0.5	116.5	9	40	1.17	14	2.26	1.11	1.58	21.9	3.76	4.7	0.44	65.2	0.15	<1	9.6	43.8	22	34	12.45	97.8	6	6.71	1	1070	0.6	0.48	21.7	<10	0.18	2.69	67	1	11.1	1.16	63	169
<0.5	<5	1355	<0.5	67	6	40	3.18	12	2.46	1.41	0.95	17.3	2.72	5	0.43	40.2	0.24	<1	10.4	23.1	7	25	6.73	138	5	3.65	1	323	0.7	0.36	16.85	<10	0.21	4.86	53	2	12.6	1.55	43	182
<0.5	<5	1260	<0.5	73.5	5	40	4.01	15	3.59	1.93	1.02	17.4	4.2	4.5	0.64	43.3	0.29	<1	10.3	28.2	8	30	7.71	125.5	5	5.06	1	431	0.8	0.61	16	<10	0.31	4.96	51	1	19.9	1.85	42	170
<0.5	<5	1250	<0.5	60.3	6	40	4.95	10	2.16	1.38	0.78	16.2	2.62	4.2	0.43	35	0.22	<1	9.7	21	6	24	6.16	124.5	5	3.53	1	454	0.7	0.39	15.3	<10	0.21	3.18	49	1	11.4	1.38	39	148
<0.5	<5	1410	<0.5	84.5	7	50	3.63	27	4.54	2.66	1.59	19.5	5.26	5.4	0.88	48	0.39	<1	13.1	37.1	6	21	9.99	135.5	10	6.55	1	552	0.8	0.78	15.55	10	0.4	3.3	111	1	22.9	2.66	71	213
<0.5	<5	1540	<0.5	87.8	12	60	3.01	24	4.73	2.54	1.61	19.8	5.3	5.7	0.91	46	0.38	<1	13	36.7	8	23	9.56	135	11	6.62	2	567	0.8	0.75	15.9	<10	0.37	4.11	97	2	22.7	2.45	74	220
<0.5	<5	1540	<0.5	84.7	5	20	3.2	9	2.87	1.69	1.19	17.9	3.47	5.4	0.56	47.8	0.26	<1	13.1	31.1	2	23	8.95	125.5	4	5.12	1	616	0.8	0.5	16.05	<10	0.24	3.63	60	2	15.2	1.81	57	208
<0.5	<5	1375	<0.5	68.5	7	40	4.38	15	2.54	1.52	0.95	18.3	3.12	5.1	0.49	41.2	0.23	<1	11.3	24.2	7	26	7.44	133.5	5	4.52	1	463	0.8	0.4	17.1	<10	0.25	2.58	60	1	13.3	1.45	44	192
<0.5	<5	966	<0.5	59.5	31	240	2.01	70	4.35	2.44	1.46	16.7	4.7	4.1	0.88	31.5	0.38	<1	9.6	27.4	49	10	7.16	70.2	24	5.66	1	379	0.6	0.71	9.01	<10	0.35	2.32	216	1	23	2.4	80	148
<0.5	<5	2580	<0.5	148	39	230	0.62	32	5.99	3.19	3.28	21.2	9.15	11.4	1.11	78.6	0.36	<1	20.3	69.9	156	15	18.2	64.7	21	12.55	2	1055	0.9	1.22	8.65	10	0.44	1.69	221	1	31.7	2.55	125	460
<0.5	<5	1490	<0.5	73	13	50	4.29	17	2.73	1.85	1.12	19.3	3.37	4.7	0.58	45.6	0.26	<1	10.4	28.4	13	30	7.89	118	7	4.69	1	548	0.6	0.48	16.65	<10	0.23	4.67	74	2	16.7	1.66	52	189
<0.5	<5	1745	<0.5	61.4	11	140	4.06	24	3.06	2.16	1.12	19.6	4.83	4.3	0.67	34.6	0.28	<1	10.4	28	21	37	7.3	161.5	8	5.36	1	408	0.7	0.57	14.85	10	0.3	4.69	37	2	20.1	1.9	48	152
<0.5	<5	954	<0.5	59.6	21	110	2.55	44	3.83	2.13	1.41	18.8	5.07	4.1	0.75	33.3	0.32	<1	8.1	27.8	27	13	7.08	110	18	5.34	1	408	0.4	0.69	9.88	<10	0.32	2.7	162	1	21.1	2.13	69	161
0.5	5	1255	0.5	99.1	44	450	0.52	28	5.73	3.15	2.17	19.3	7.09	8.4	1.2	49.7	0.46	<1	20.9	44.8	153	12	12.25	48	26	8.11	1	646	1.1	1.06	6.83	<10	0.49	1.4	231	1	30	3.01	116	325
<0.5	<5	710	0.5	68.2	41	360	0.5	27	6.1	3.57	1.84	18.8	6.62	5.3	1.29	34.4	0.47	<1	16.6	34	108	7	8.69	29.7	27	6.51	1	423	1	1	5.36	10	0.51	1.07	228	1	32.4	3.32	115	214
<0.5	<5	1395	0.6	107	43	470	0.56	35	5.75	3.15	2.07	18.8	7.06	8.8	1.15	52.6	0.44	<1	21.3	47.6	164	8	12.9	52.6	26	8.44	2	711	1.1	0.98	7.58	<10	0.44	1.5	214	1	29.1	2.79	115	345
<0.5	<5	1855	<0.5	190	53	970	1.45	110	3.33	1.37	2.35	14.2	6.03	2.5	0.6	94.1	0.16	<1	33.5	85.3	400	14	23	78.7	21	10.4	1	2080	1.1	0.65	10.65	<10	0.17	2.5	155	<1	14.6	1.32	77	90

Ag	As	Ba	Cd	Ce	Co	Cr	Cs	Cu	Dy	Er	Eu	Ga	Gd	Hf	Ho	La	Lu	Mo	Nb	Nd	Ni	Pb	Pr	Rb	Sc	Sm	Sn	Sr	Ta	Tb	Th	Tl	Tm	U	V	W	Y	Yb	Zn	Zr
<1	nd	2170	nd	113.5	20.1	200	1.7	35	3.3	1.7	1.7	20	6.1	6	0.6	63.8	0.2	<2	13	42.0	48	46	12.2	107.5	nd	7.0	1	721	0.7	0.7	17	<0.5	0.2	2.9	112	1	16.8	1.5	75	191.0
<1	nd	2320	nd	114.0	17.0	210	0.9	28	3.0	1.7	1.6	20	5.9	6	0.6	64.2	0.2	<2	13	41.2	48	30	12.2	106.0	nd	6.7	1	736	0.8	0.7	16	<0.5	0.2	3.0	96	1	17.4	1.6	62	185.5
<1	nd	1535	nd	96.8	12.0	70	1.8	12	3.3	1.8	1.5	22	5.6	5	0.6	53.5	0.2	<2	10	41.7	15	23	11.5	112.5	nd	6.2	1	792	0.7	0.7	11	<0.5	0.2	3.6	93	2	17.3	1.7	65	185.5
<1	nd	1660	nd	103.5	8.7	120	4.1	11	3.3	1.9	1.5	21	5.2	5	0.6	51.8	0.2	2	12	38.6	11	24	11.0	134.5	nd	6.4	1	702	0.7	0.7	12	<0.5	0.2	2.7	65	2	19.7	1.8	58	182.5
<1	nd	2050	nd	118.5	16.6	180	2.0	21	2.8	1.5	1.4	22	5.1	6	0.5	63.3	0.1	<2	13	42.2	41	25	12.4	131.5	nd	6.5	1	766	0.8	0.6	18	<0.5	0.1	3.0	92	2	15.5	1.4	69	201.0
<1	nd	2980	nd	174.0	15.1	210	2.8	46	4.6	2.2	2.4	22	9.5	8	0.8	106.5	0.2	3	18	73.0	52	46	21.0	159.5	nd	10.8	1	1090	1.0	1.1	34	<0.5	0.2	6.1	117	3	23.8	1.7	81	278.0
<1	nd	2040	nd	97.9	19.2	330	2.2	31	3.0	1.5	1.5	21	5.6	5	0.5	58.9	0.2	2	12	39.8	71	29	11.4	120.0	nd	6.1	1	771	0.8	0.7	17	<0.5	0.2	3.1	100	1	15.6	1.4	77	193.5

Notes:

Map number and map unit corresponds to plate 1.
Rock names from total alkali-silica diagram of LeBas and others (1986) or Middlemost (1994).
Analytical procedures: ME-XRF06 (whole-rock package by XRF); LOI for ME-XRF06 by WST-SIM, ME-4ACD81 (base metals 4-acid digestion by ICP-AES), ME-MS81 (lithium borate fusion by ICP-MS).
Major oxides reported in weight percent (%); < indicates value below detection limit.
LOI is loss on ignition.
Minor and trace elements reported in parts per million (ppm); < indicates value below detection limit.
Analyses performed by ALS Minerals and ALS Chemex.
Data from Copperton 7.5' quadrangle are also included here, as it was inadvertently omitted from the UGS website, see Biek and others (2007). Also see Clark and Biek (2017).
Only new and unpublished data are presented here. We did not compile the prior voluminous geochemical data available for the Bingham mining district, or older data from the Stansbury Mountains.

Table A8. *Selected microfossil identifications and ages for the Tooele 30' x 60' quadrangle.*

Map Number	Sample Number	Map Unit	Stratigraphic Position	7.5' Quadrangle	Location Data	Location Data	Fossil Type	Fauna	Age
Data from Clark (this study)					**Latitude (°N) WGS84**	**Longitude (°W) WGS84**			
T5	T5	Ppp	Phosphoria Fm, Meade Peak Mbr	Farnsworth Peak	40.65240	112.15651	conodont	*Neostreptognathodus sulcoplicatus*	Kungurian (Late Leonardian)
T6	T6	Ppp	Park City Fm, Grandeur Mbr (basal limestone)	Farnsworth Peak	40.65188	112.15372	conodont	*Neostreptognathodus* sp.	Leonardian
T53	T53	Posc?		Puddle Valley Knolls	40.88189	112.97398	fusulinid	*Schwagerina* sp.	Wolfcampian
T50	T50	IPobm		Hastings Pass	40.70199	112.94318	conodont	*Idiognathodid* sp.	Pennsylvanian
T7	T7	IPobm		Farnsworth Peak	40.69135	112.15923	conodont	*Streptognathodus pawhuskaensis*	Gzhelian (Virgilian)
T48	T48	IPobm		Delle	40.81500	112.79136	fusulinid	*Triticites* sp.	Missourian to early Wolfcampian
T55	T55	IPobm		Low	40.80735	112.92489	fusulinid	*Triticites* sp.	Virgilian
T41	T41	IPobp		Delle	40.83999	112.81898	conodont	*Idiognathodid* sp.	Pennsylvanian
T13	T13	IPobp		Farnsworth Peak	40.72060	112.18958	fusulinid	*Fusulinella* sp., *Beedeina* sp.?	Middle Pennsylvanian
Note: Fossils identified by Scott Ritter (Brigham Young University).									
Data from Tooker and Roberts (1970)					**UTM27-12 E Approx**	**UTM27-12 N Approx**			
F17	f23432	IPobmu		Bingham Canyon	400971	4488591	fusulinid	*Triticites* sp., *Pseudofusulinella* sp.	nd
F14	f23111	IPobmu		Bingham Canyon	395888	4487299	fusulinid	*Triticities* sp.	nd
F13	f23112	IPobmu		Bingham Canyon	396876	4486046	fusulinid	*Triticities* sp.	nd
F12	f22604	IPobmu		Bingham Canyon	396742	4485409	fusulinid	*Triticites* sp., *?Kansanella* sp., *Millerella* sp.	nd
F11	f22603	IPobml		Bingham Canyon	396737	4485373	fusulinid	*Triticites* sp.	Missourian or early Virgilian
F10	f22602	IPobml		Bingham Canyon	396637	4485256	fusulinid	*Triticites* sp.	Missourian or Virgilian
F9	f22600	IPobml		Bingham Canyon	396592	4485057	fusulinid	*Bradyina* sp., *Triticities* sp.	Missourian
F8	f22598	IPobml		Bingham Canyon	396457	4484478	fusulinid	*Triticites* sp.,	Missourian
F7	22597	IPobml		Bingham Canyon	396261	4484186	fusulinid	*Triticities* sp.	Missourian
F16	f22431	IPobml		Bingham Canyon	400216	4486457	fusulinid	*Triticites* sp.	nd
F15	f23105	IPobml		Bingham Canyon	394442	4485151	fusulinid	*Triticites* sp.	nd
F1	f21018	IPobm		Farnsworth Peak	403209	4504815	fusulinid	*Triticites* sp.	Late Pennsylvanian
F2	f20479	IPobm		Farnsworth Peak	402271	4507671	fusulinid	*Triticites* sp., *Pseudofusulinella*?	Late Penn. or Early Permian
F3	f22569	IPobp		Farnsworth Peak	396547	4501765	fusulinid	*Fusulina* sp.	Desmoinesian
F4	f22568	IPobp		Farnsworth Peak	398100	4505429	fusulinid	*Climacammina* sp., *Bradyina* sp., *Fusulina* sp., *Wedekindellina*?	Desmoinesian
F5	f22570	IPobp		Farnsworth Peak	396519	4504962	fusulinid	*Fusulina* sp.	Desmoinesian
F6	f20486	IPobp		Farnsworth Peak	396430	4504795	fusulinid	*Profusulinella*	early Atokan
Note: Fossils identified by R.C. Douglass (USGS)									
Unpublished data from John Welsh (Bear Creek Mining Company)					**UTM27-12 E Approx**	**UTM27-12 N Approx**			
F18	-	IPobm		Farnsworth Peak	396858	4506483	fusulinid	nd	Missourian?
F19	-	IPobm		Farnsworth Peak	398800	4499604	fusulinid	nd	Missourian?
F20	-	IPobp		Farnsworth Peak	396571	4505276	fusulinid	nd	Desmoinesian?
F21	-	IPobp		Bingham Canyon	399183	4496885	fusulinid	nd	Desmoinesian?
F22	-	IPobp		Bingham Canyon	400734	4493186	fusulinid	nd	Desmoinesian?

Notes:
Map number and map unit corresponds to plate 1.
nd is no data.
Data in the quadrangle from Maurer (1970), Davis and others (1989, 1994), and other data from Tooker and Roberts (1970) are not included here.
Kowalewska and Cohen (1998) reported on ostracodes, mollusks, and brine shrimp fecal pellets from the Amoco Sandbar well.
Peterson, in Bortz and others (1985), reported on palynology data in the Amoco-Antelope Island well.

Table A9. *Comparison of stratigraphic nomenclature for Mesozoic, Paleozoic and Proterozoic geologic units of the western thrust system in the Tooele 30' x 60' quadrangle.*

			Grassy Mtns	**Cedar thrust sheet**	**Grassy Mtns, S. Lakeside Mtns**	**S. Lakeside Mtns**	**S. Lakeside Mtns**	**S. Lakeside Mtns**
		This Map	This Map	This Map	Doelling (1964)	Young (1953)	Nichols and others (1992); Silberling and Nichols (1992a)	Poole and Sandberg (1991)
Mesozoic	Cretaceous	Cretaceous strata						
Mesozoic	Triassic	Dinwoody Fm?						
Paleozoic	Permian	Gerster Fm, Plympton Fm						
Paleozoic	Permian	Phosphoria Fm, Meade Peak Mbr						
Paleozoic	Permian	Park City Fm, Grandeur Mbr						
Paleozoic	Permian	sandstone, limestone and dolomite	sandstone, limestone and dolomite		"Unnamed" Fm			
Paleozoic	Permian	Oquirrh Group-Freeman Peak Fm, Curry Peak Fm	Oquirrh Group-sandstone and limestone unit	Oquirrh Group-sandstone and limestone unit	Oquirrh Fm, units 2, 3, 4, 5, 6	Oquirrh Fm		
Paleozoic	Pennsylvanian	Oquirrh Group-Bingham Mine Fm	Oquirrh Group-sandstone and siltstone unit	Oquirrh Group-sandstone and siltstone unit	Oquirrh Fm, unit 2	Oquirrh Fm		
Paleozoic	Pennsylvanian	Oquirrh Group-Butterfield Peaks Fm, West Canyon Ls	Oquirrh Group-limestone unit	Oquirrh Group-limestone unit	Oquirrh Fm, unit 1	Oquirrh Fm		
Paleozoic	Mississippian	Manning Canyon Fm			Manning Canyon Fm	Manning Canyon Fm		Manning Canyon Shale
Paleozoic	Mississippian	Great Blue Ls			Great Blue Fm	Great Blue Ls		Great Blue Ls
Paleozoic	Mississippian	Humbug Fm			Humbug Fm	Humbug Fm	Humbug Fm	Humbug Fm
Paleozoic	Mississippian	Woodman Fm/ Deseret Ls			Deseret Ls	Humbug Fm, Deseret Ls	Woodman Fm	Woodman Fm
Paleozoic	Mississippian	Gardison Ls, Fitchville Fm, Pinyon Peak Ls			Madison Ls	Deseret Ls, Madison Ls	Gardison Ls, Fitchville Fm, Pinyon Peak Ls	Lodgepole Ls, Pinyon Peak Ls
Paleozoic	Devonian	Stansbury Fm						
Paleozoic	Devonian	Guilmette Fm, Simonson Dol			Guilmette Fm, Simonson Dol	Jefferson Dol		
Paleozoic	Devonian	Sevy Dol			Water Canyon Dol	Water Canyon Fm		
Paleozoic	Silurian-Ordovician	Laketown Dol, Ely Springs Dol, Eureka Quartzite			Laketown Dol, Fish Haven Dol, Swan Peak Fm	Laketown Dol, Fish Haven Dol, Swan Peak Fm		
Paleozoic	Ordovician	Pogonip Group			Swan Peak Fm, Garden City Fm	Swan Peak Fm, Garden City Ls		
Paleozoic	Cambrian	Upper and Middle Cambrian strata						
Paleozoic	Cambrian	Notch Peak Fm			St. Charles Fm, Nounan Fm	Lynch Dol		
Paleozoic	Cambrian	Orr Fm			St. Charles Fm, Nounan Fm	Lynch Dol		
Paleozoic	Cambrian	Lamb Dol			Nounan Fm	Lynch Dol		
Paleozoic	Cambrian	Trippe Ls			Marjum Fm	Bowman Ls, Hartmann Ls		
Paleozoic	Cambrian	Pierson Cove Fm			Marjum Fm	Hartmann Ls		
Paleozoic	Cambrian	Wheeler Fm			Wheeler Fm	Hartmann Ls		
Paleozoic	Cambrian	Swasey Ls			Swasey Ls	Hartmann Ls		
Paleozoic	Cambrian	Whirlwind Fm			Whirlwind Fm	Hartmann Ls		
Paleozoic	Cambrian	Dome Ls, Chisholm Fm, Howell Ls			Dome Fm, Chisholm Fm, Howell Ls	Hartmann Ls, Ophir Shale		
Paleozoic	Cambrian	Pioche Fm			Pioche Shale	Tintic Quartzite		
Paleozoic	Cambrian	Prospect Mtn Quartzite			Tintic Quartzite	Tintic Quartzite		
Neoproterozoic		Mutual Fm						
Neoproterozoic		Inkom Fm						
Neoproterozoic		Caddy Canyon Quartzite						
Neoproterozoic		Perry Canyon Fm						

Note: In this table some age boundaries and correlations are somewhat generalized. Also see map explanation for detailed correlation charts and lithologic columns.

Table A9. *Continued.*

Era	Period	Cedar Mtns Maurer (1970)	Cedar Mtns Wardlaw and others (1979)	Stansbury Mtns Rigby (1958)	Stansbury Island Chapusa (1969)	Stansbury Island Palmer (1970)	Stansbury Island, Stansbury Mtns Trexler (1992)	Stansbury Mtns Nichols and others (1992)	Stansbury Mtns Sandberg and Gutschick (1979)	Stansbury Island Sandberg and Gutschick (1979)
Mesozoic	Cretaceous	North Horn? Fm								
Mesozoic	Triassic	*not mapped*								
Paleozoic	Permian	Gerster Fm	Park City Group-Gerster Ls, Plympton Fm							
Paleozoic	Permian	Phosphoria Fm, Meade Peak Mbr	Phosphoria Fm, Meade Peak Mbr							
Paleozoic	Permian	Park City Fm, Grandeur Mbr	Park City Group, Grandeur Fm							
Paleozoic	Permian	"Permian unnamed fm"								
Paleozoic	Permian	Oquirrh Fm, units 4, 5								
Paleozoic	Pennsylvanian	Oquirrh Fm, units 3, 4								
Paleozoic	Pennsylvanian	Oquirrh Fm, units 1, 2, 3		Oquirrh Fm						
Paleozoic	Mississippian			Manning Canyon Fm						
Paleozoic	Mississippian			Great Blue Ls	Great Blue Ls			Great Blue Ls		
Paleozoic	Mississippian			Humbug Fm	Humbug Fm	Humbug Fm		Humbug Fm		
Paleozoic	Mississippian			Pine Canyon Fm	Deseret Ls	Deseret Ls		Deseret Ls	Deseret Ls	Deseret Ls
Paleozoic	Mississippian			Pine Canyon Fm, Gardner Dol, Pinyon Peak Ls	Madison Ls, Fitchville? Fm	Gardison Ls, Fitchville Fm	Fitchville Fm	Gardison Ls, Fitchville Fm	Gardison Ls, Fitchville Fm	Lodgepole Ls, Leatham Fm
Paleozoic	Devonian			Pinyon Peak Ls, Stansbury Fm	Stansbury Fm	Stansbury Fm	Stansbury Fm	Stansbury Fm	Pinyon Peak Ls, Stansbury Fm	Pinyon Peak Ls, Stansbury Fm
Paleozoic	Devonian			Simonson? Dol						
Paleozoic	Devonian			Sevy Dol						
Paleozoic	Silurian-Ordovician			Laketown Dol, Fish Haven Dol	Laketown Dol	Fish Haven Dol				
Paleozoic	Ordovician			Kanosh Shale, Garden City Fm	Garden City Fm	Garden City Fm				
Paleozoic	Cambrian				Upper-Middle Cambrian					
Paleozoic	Cambrian			Ajax Dol		Ajax Dol				
Paleozoic	Cambrian			Dunderberg Shale, Opex Fm		Dunderberg Shale, Opex Fm				
Paleozoic	Cambrian			Cole Canyon Dol, Bluebird Dol		Cole Canyon Dol				
Paleozoic	Cambrian			Bowman Ls, Herkimer Ls		Herkimer Ls				
Paleozoic	Cambrian			Dagmar Dol, Teutonic Ls		Dagmar Dol, Teutonic Ls				
Paleozoic	Cambrian			Teutonic Ls		Teutonic Ls				
Paleozoic	Cambrian			Teutonic Ls		Teutonic Ls				
Paleozoic	Cambrian			Ophir Group-Condor Fm		Ophir Fm				
Paleozoic	Cambrian			Ophir Group-Dome, Burnt Canyon, Burrows equivalents, Millard Ls, Busby Quartzite		Ophir Fm				
Paleozoic	Cambrian			Ophir Group-Busby Quartzite and Pioche Shale	Pioche "Shale"	Ophir Fm				
Paleozoic	Cambrian			Tintic Quartzite	Prospect Mountain Quartzite	Tintic Quartzite				
Neoproterozoic					Big Cottonwood Series	Big Cottonwood Fm				
Neoproterozoic					Big Cottonwood Series	Big Cottonwood Fm				
Neoproterozoic					Big Cottonwood Series	Big Cottonwood Fm				

Note: In this table some age boundaries and correlations are somewhat generalized. Also see map explanation for detailed correlation charts and lithologic columns.
Maurer assigned a Tertiary (Paleocene to Eocene) age to the North Horn? Fm.

Table A10. *Comparison of stratigraphic nomenclature for Paleozoic and Proterozoic geologic units of the eastern thrust system in the Tooele 30' x 60' quadrangle.*

Era	Period	**Oquirrh Mtns & Antelope Island** This Map	**Oquirrh Mtns - Bingham Sequence** Tooker and Roberts (1970), Swenson and others (1991), Laes and others (1997)	**Oquirrh Mtns - Rogers Canyon Sequence** Tooker and Roberts (1970, 1971a), Laes and others (1997)	**Oquirrh Mtns** Welsh and James (1961)	**Antelope Island** Doelling and others (1990), Yonkee and others (2000a)
Paleozoic	Permian	Park City Fm, Phosphoria Fm	Park City Fm	Park City Fm, Grandeur Mbr/ Park City Fm	Park City Fm	
Paleozoic	Permian	Diamond Creek Ss, Kirkman Fm	Diamond Creek Fm, Kirkman, Fm	Oquirrh Group-Kessler Canyon Fm	Diamond Creek Fm, Kirkman Fm	
Paleozoic	Permian	Oquirrh Group-Freeman Peak Fm	Oquirrh Group-Freeman Peak Fm	Oquirrh Group-Kessler Canyon Fm	Clinker Fm	
Paleozoic	Permian	Oquirrh Group-Curry Peak Fm	Oquirrh Group-Curry Peak Fm	Oquirrh Group-Kessler Canyon Fm	Curry Fm	
Paleozoic	Pennsylvanian	Oquirrh Group-Bingham Mine Fm	Oquirrh Group-Bingham Mine Fm	Oquirrh Group-Kessler Canyon Fm	Oquirrh Group-Bingham Mine Fm	
Paleozoic	Pennsylvanian	Oquirrh Group-Butterfield Peaks Fm	Oquirrh Group-Butterfield Peaks Fm	Oquirrh Group-Erda Fm	Oquirrh Group-Butterfield Fm, "White Pine" Fm	
Paleozoic	Pennsylvanian	Oquirrh Group-West Canyon Ls	Oquirrh Group-West Canyon Ls	Oquirrh Group-Lakepoint Ls	Oquirrh Group-Maple Fm	
Paleozoic	Mississippian	Manning Canyon Fm	Manning Canyon Shale	Oquirrh Group-Lakepoint Ls		
Paleozoic	Mississippian	Great Blue Ls	Great Blue Ls	Green Ravine Fm		
Paleozoic	Cambrian	Tintic Quartzite				Tintic Quartzite
Neoproterozoic		slate and dolomite				Kelley Canyon Fm
Neoproterozoic		Mineral Fork Fm				Mineral Fork Fm
Paleoproterozoic		Farmington Canyon Complex				Farmington Canyon Complex

Note: In this table some age boundaries and correlations are somewhat generalized. Also see figure 3 and map explanation for detailed correlation charts and lithologic columns.

APPENDIX B:

PHOTO GALLERY

Photograph 1. *View to the south of southern Antelope Island with Farmington Canyon Complex rocks and the Bonneville-level shoreline, Great Salt Lake, and the northern Oquirrh Mountains. In the foreground is Farmington Canyon Complex rocks with some gravel cover. Photo by Donald Clark.*

Photograph 2. *View to the northeast of Antelope Island and the south arm of Great Salt Lake. Most of the rocks in this view are Paleoproterozoic Farmington Canyon Complex. Photo by Ken Krahulec.*

Photograph 3. View to the northeast of the northern Oquirrh Mountains and Oquirrh Group rocks, Kennecott/Rio Tinto tailings impoundment, the south arm of Great Salt Lake, and Antelope Island. Photo by Donald Clark.

Photograph 4. View to the northwest of the Nelson Peak glacial cirque in the northern Oquirrh Mountains. Hummocky deposits in lower part of cirque basin are glacial till (Qgt). Photo by Donald Clark.

Photograph 5. *View of tephra in the Salt Lake Formation in the Clay Hollow area of the eastern Oquirrh Mountains. Sample collected by Charles (Jack) Oviatt. Photo by Donald Clark.*

Photograph 6. *View to the northeast of the Bingham Canyon mine in the Oquirrh Mountains from the overlook area north of Butterfield Canyon Road. Photo by Mark Milligan.*

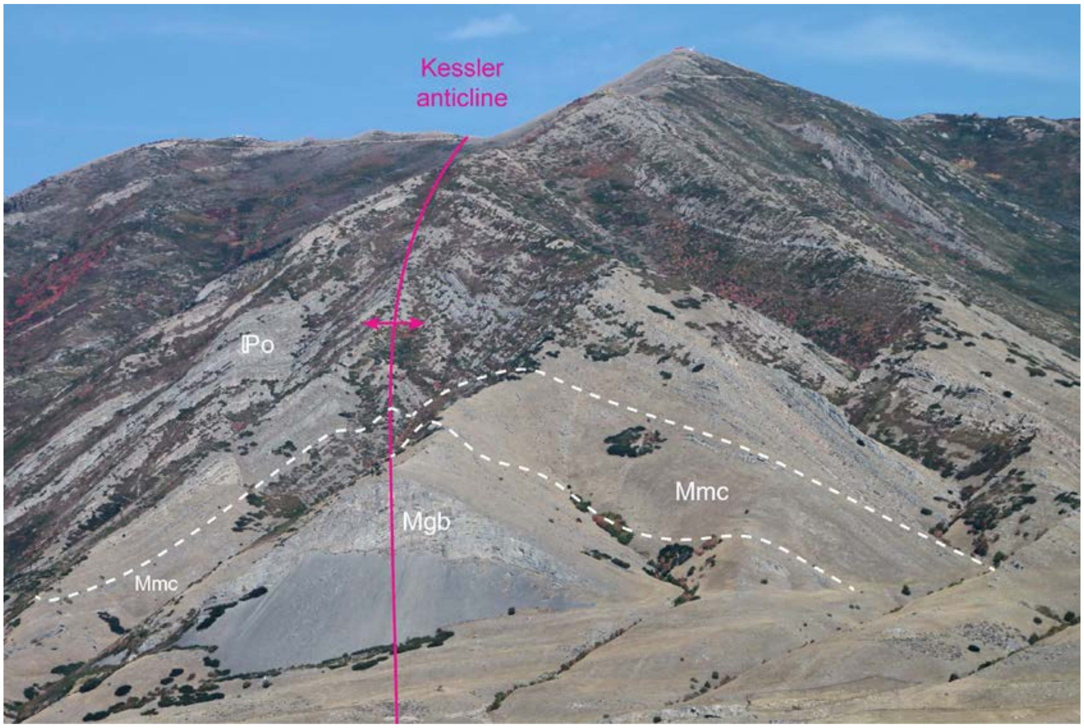

Photograph 7. *View to the east of the Kessler anticline on the west side of the northern Oquirrh Mountains. Talus-covered core is Great Blue Formation (Mgb) overlain by the Manning Canyon Formation (Mmc) and lower Oquirrh Group strata (IPo). Photo by Ken Krahulec.*

Photograph 8. *View to the north of the western Oquirrh Mountains with "the chaos" in foreground and middle distance. This area includes the highly deformed Diamond Creek Sandstone and Kirkman Formation located between the North Oquirrh and Midas thrust faults near the Uinta trend. Photo by Donald Clark.*

Photograph 9. *View to the west of Tooele Valley and the northern Stansbury Mountains. Photo by Donald Clark.*

Photograph 10. *View to the southeast of northern Stansbury Island and U.S. Magnesium evaporation pond and dike (*Qhe*). The three main Lake Bonneville shorelines are present (descending) Bonneville (B), Provo (P), and Stansbury (S). A steep fault (F) separates Neoproterozoic rocks (*Z*) (left) from Cambrian rocks (*Ꞓ*) (right). Photo by Donald Clark.*

Photograph 11. *View to the north of southern Stansbury Island showing Mississippian through Cambrian rocks. Lighter-colored beds are quartzite of the Devonian Stansbury Formation (Dst) on the flanks of the Stansbury anticline. Prominent shorelines of Lake Bonneville include Provo (P) and Stansbury (S). Salt evaporation ponds (Qhe) in the foreground. Photo by Donald Clark.*

Photograph 12. *Close up view of the Devonian Stansbury Formation conglomeratic lithofacies in the northern Stansbury Mountains near Flux. Clasts are largely dolomite in a dolomitic matrix. Photo by Donald Clark.*

Photograph 13. *View to the north of Oquirrh Group strata on the east flank of the northern Stansbury Mountains near West Canyon. Lines define bedding that are folded into an eroded synclinal structure. Photo by Donald Clark.*

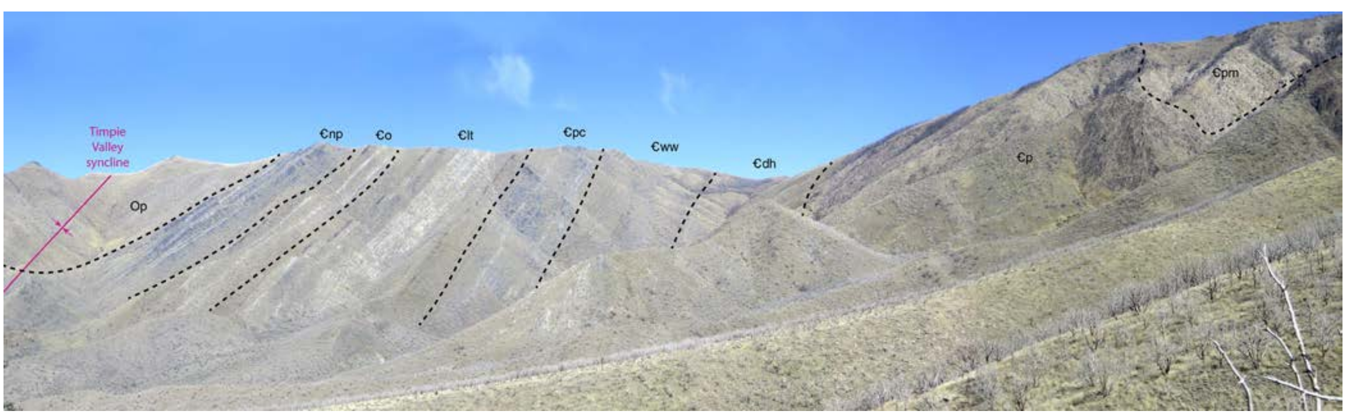

Photograph 14. *View to the north of the Cambrian section in the Muskrat Canyon area of the northern Stansbury Mountains. The Timpie Valley syncline is cored by Pogonip Group rocks (*Op*) at left and Cambrian strata (see explanation for geologic units) on the west flank of the Deseret anticline. Photo by Donald Clark.*

Photograph 15. *View to the northeast of the Tertiary basin between Salt Mountain and the northern Stansbury Mountains. The basin contains Salt Lake Formation conglomerate (*Tslc*) overlain by older fan alluvium (*Qafo*). Salt Mountain (foreground) has volcanic rocks of the Stanbury Mountains (*Tvs*) and Ordovician and Cambrian rocks (*O-€*). Simplified trace of the Stansbury fault zone is at the foot of the Stansbury Mountains with largely Cambrian (*€*) rocks in view. Photo by Donald Clark.*

Photograph 16. *View to the southeast in the southern Lakeside Mountains of the Mississippian section including (left to right) the Gardison Limestone, Fitchville Formation, Pinyon Peak Limestone, undivided (*MDgp*), Woodman Formation (*Mw*) with Delle Phosphatic Member in lower part, Humbug Formation (*Mh*), and Great Blue Limestone (*Mgb*). Photo by Donald Clark.*

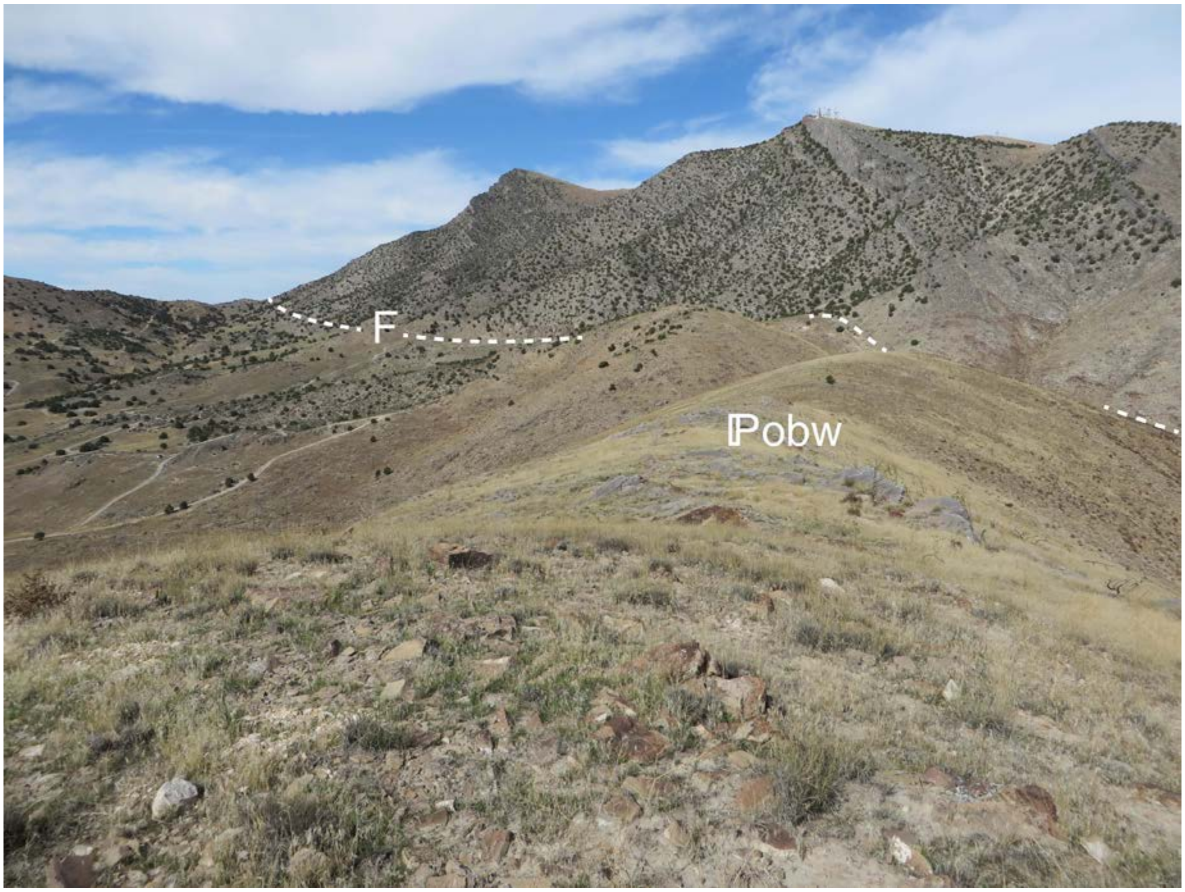

Photograph 17. *View to the northwest of the Lakeside fault (F) in the southern Lakeside Mountains. Oquirrh Group rocks (IPobw) in foreground are faulted against Mississippian through Ordovician rocks in background. Photo by Donald Clark.*

Photograph 18. *View to the south of northern Cedar Mountains and Bonneville-level shoreline (notch) etched into lower Permian Oquirrh Group strata. Photo by Donald Clark.*

Photograph 19. *View to the south along the east side of the northern Cedar Mountains, Hastings Canyon area. Includes Miocene basalt outcrops overlying Tertiary strata and Oquirrh Group strata. Bonneville level-shoreline notch is etched into basaltic rocks (left center). Photo by Donald Clark.*

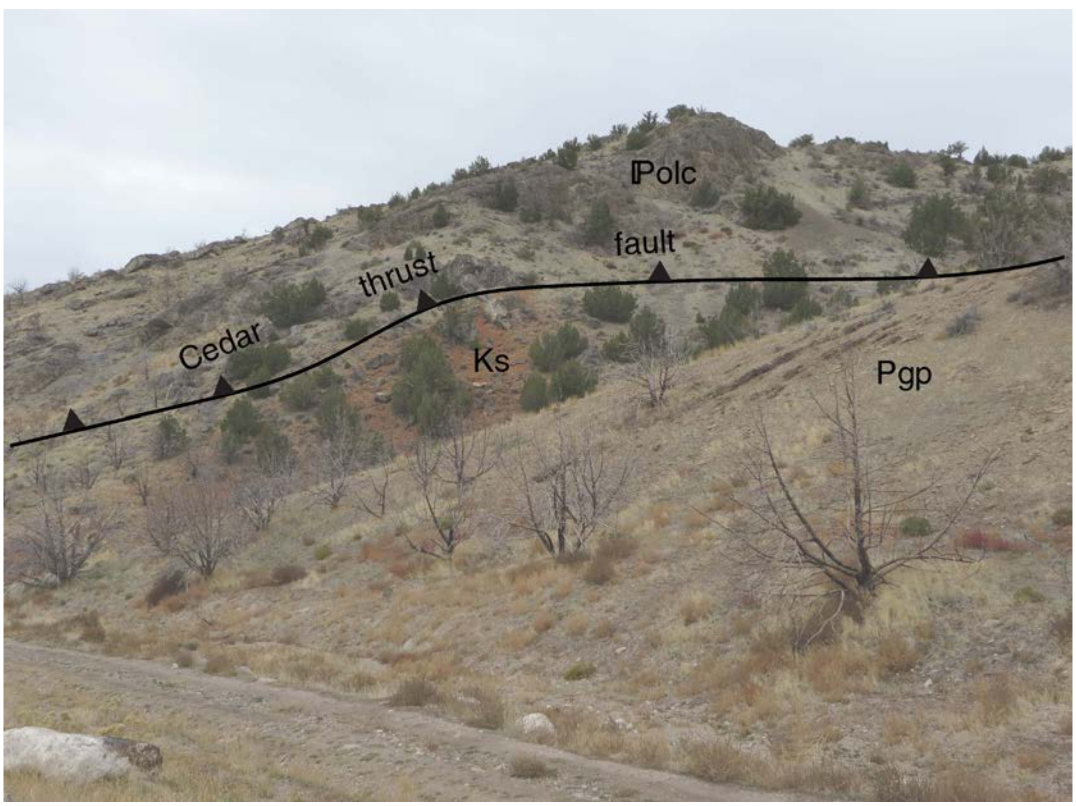

Photograph 20. *View to the west of Oquirrh Group rocks (IPolc) at top in thrust contact with Cretaceous strata (Ks) and Permian strata (Pgp) in foreground at the western Cedar Mountains. Photo by Donald Clark.*

Photograph 21. *View to the north of west-dipping synorogenic Cretaceous strata (red beds) in the western Cedar Mountains. Photo by Donald Clark.*